PATENT

IN THE UNITED STATES PATENT AND TRADEMARK OFFICE

In re Application of: Donald W. Kufe, *et al.*	Group Art Unit: 1635
Serial No.: 10/778,859	Examiner: Vivlemore, Tracy Ann
Filed: February 13, 2004	Atty. Dkt. No.: DFCI:004US
For: MUC1 Interference RNA Compositions and Methods Derived Therefrom	

SECOND DECLARATION OF DONALD W. KUFE UNDER 37 C.F.R. § 1.132

Commissioner for Patents
P. O. Box 1450
Alexandria, VA 22313-1450

I, Donald W. Kufe, do declare that:

1. I am a United States citizen residing at 179 Grove St., Wellesley, MA, 02482.

2. I am the first named inventor of the above-referenced U.S. patent application.

3. I have reviewed the Office Action dated April 18, 2007, that is related to the above-referenced application.

4. I understand that the Examiner has rejected the pending claims as being obvious in view of papers by Dobie, Hammond, and Elbashir, alone or in combination with papers by Parrish or Kennerdell.

5. As set forth in my previous declaration submitted with the response to the Office Action dated July 26, 2007, I disagree with the Examiner's position.

6. To counter the Examiner's assertion that my invention is obvious in view of these papers, I am submitting a copy of a paper by Ren *et al.* reporting studies from my laboratory, entitled "Human MUC1 carcinoma-associated protein confers resistance to genotoxic anticancer agents" (Cancer Cell, 5:163-175, 2005; "Ren"; Exhibit A). This paper examined the effects of endogenous MUC1 expression on sensitivity of human carcinoma cells to genotoxic agents by knocking down MUC1 with small interfering RNA (siRNA). The results demonstrate that exposure of A549 lung carcinoma cells to MUC1siRNA effectively downregulated MUC1 expression. Ren, page 168 and figure 6A. As a control, there was no detectable downregulation of MUC1 in A549 cells exposed to a control siRNA. Ren, page 168 and figure 6A. Importantly, A549 cells exposed to MUC1 siRNA responded to CDDP with an increase in apoptosis compared to that obtained with cells exposed to mock conditions or control siRNA. Ren, page 168 and figure 6B. These findings indicate that siRNA of my invention can be applied to effectively knock down MUC1 expression in A549 cells, and that knocking down MUC1 expression increases sensitivity to genotoxic agents such as CDDP. Ren, page 168-169, and figures 6-7.

7. As further support of the highly effective ability of siRNA to silence MUC1 expression, I also present results from studies in my laboratory (Exhibit B) which show the ability of two siRNAs to downregulate MUC1. In these studies, we generated siRNAS to two MUC1 sequences, as set forth on page 8. We demonstrated that the two siRNAs, referred to as MUC1 siRNA#1 and MUC1 siRNA#2, both effectively downregulate MUC1 expression. Page 13, and figure 3A. Once again, these data support the finding that siRNA of my invention can effectively downregulate MUC1 expression.

8. I hereby declare that all statements made herein of my knowledge are true and that all statements made on information and belief are believed to be true; and further that these statements were made with the knowledge that willful false statements and the like so made are punishable by fine or imprisonment, or both, under Section 1001 of Title 18 of the United States Code and that such willful false statements may jeopardize the validity of the application or any patent issued thereon.

9/10/07
Date

Donald W. Kufe
Donald W. Kufe

EXHIBIT A

ARTICLE

Human MUC1 carcinoma-associated protein confers resistance to genotoxic anticancer agents

Jian Ren,[1] Naoki Agata,[2] Dongshu Chen,[2] Yongqing Li,[2] Wei-hsuan Yu,[1] Lei Huang,[1] Deepak Raina,[1] Wen Chen,[1] Surender Kharbanda,[2] and Donald Kufe[1,*]

[1]Dana-Farber Cancer Institute, Harvard Medical School, Boston, Massachusetts 02115
[2]ILEX Products, Inc., Boston, Massachusetts 02215
*Correspondence: donald_kufe@dfci.harvard.edu

Summary

The MUC1 transforming protein is overexpressed by most human carcinomas. The present studies demonstrate that the MUC1 C-terminal subunit (MUC1 C-ter) localizes to mitochondria in HCT116/MUC1 colon carcinoma cells and that heregulin stimulates mitochondrial targeting of MUC1 C-ter. We also show that MUC1 attenuates cisplatin-induced (1) release of mitochondrial apoptogenic factors, (2) activation of caspase-3, and (3) induction of apoptosis. Moreover, knockdown of MUC1 expression in A549 lung and ZR-75-1 breast carcinoma cells by MUC1siRNA was associated with increased sensitivity to genotoxic drugs in vitro and in vivo. These findings indicate that MUC1 attenuates the apoptotic response to DNA damage and that this oncoprotein confers resistance to genotoxic anticancer agents.

Introduction

The apoptotic response of cells is induced by extrinsic and intrinsic pathways that activate the caspase family of cysteine proteases. The extrinsic apoptotic pathway is activated by ligand stimulation of the tumor necrosis factor (TNF) family of death receptors. Activation of caspase-8 by death receptor signaling results in cleavage of procaspase-3 (Boldin et al., 1996; Muzio et al., 1996; Stennicke et al., 1998). Caspase-8 also cleaves Bid, a proapoptotic member of the Bcl-2 family, and thereby stimulates release of mitochondrial cytochrome c to the cytosol (Li et al., 1998a; Luo et al., 1998). Activation of the intrinsic pathway by diverse Bid-independent stress signals is also associated with the release of mitochondrial cytochrome c (Kluck et al., 1997; Liu et al., 1996; Yang et al., 1997). In the cytosol, cytochrome c forms a complex with Apaf-1 and activates caspase-9 (Li et al., 1997; Srinivasula et al., 1998). Like caspase-8, caspase-9 can directly activate caspase-3 (Li et al., 1997). In turn, caspase-3 cleaves multiple proteins, which, when inactivated or activated by cleavage, contribute to the induction of apoptosis. Protein kinase Cδ (PKCδ) is one such caspase-3 substrate that is cleaved to a catalytically active fragment, the expression of which is sufficient to induce apoptosis (Emoto et al., 1995). Many genotoxic anticancer drugs induce apoptosis by activation of the intrinsic pathway (Herr and Debatin, 2001; Kroemer and Reed, 2000). Moreover, resistance to cytotoxic anticancer agents is often associated with defects in the intrinsic pathway (Bunz, 2001; Datta et al., 1995).

The human DF3/MUC1 transmembrane glycoprotein is expressed on the apical borders of normal secretory epithelial cells (Kufe et al., 1984). By contrast, transformation of epithelia to carcinomas is associated with marked overexpression of MUC1 throughout the entire cell membrane (Kufe et al., 1984). MUC1 is expressed as a cell surface heterodimer that consists of N-terminal (N-ter) and C-terminal (C-ter) subunits, which form a stable complex following cleavage of a single MUC1 polypeptide in the endoplasmic reticulum (ER) (Ligtenberg et al., 1992). The >250 kDa N-ter ectodomain contains variable numbers of 20 amino acid tandem repeats that are extensively modified by O-linked glycans (Gendler et al., 1988; Siddiqui et al., 1988). The ~20–25 kDa C-ter, which anchors the N-ter to the cell surface, consists of a 58 amino acid extracellular region, a 28 amino acid transmembrane domain, and a 72 amino acid cytoplasmic domain (CD) (Merlo et al., 1989). The MUC1-CD is phosphorylated on Y-46 by the epidermal growth factor receptor (EGFR), c-Src (Li et al., 2001a, 2001b), and Lyn (Li et al., 2003a). Other studies have shown that MUC1-CD is phosphorylated on S-44 by glycogen synthase kinase 3β (GSK3β) (Li et al., 1998b) and on T-41 by PKCδ (Ren et al., 2002). Phosphorylation on Y-46 and T-41 induces binding of MUC1-CD with the Wnt effector β-catenin (Li et al., 2001a, 2001b; Ren et al., 2002). Conversely, GSK3β-mediated phosphorylation of S-44 decreases the interaction of MUC1-CD and β-catenin (Li et al., 1998b). These findings have indicated that MUC1-CD functions in integrating signals from the EGFR and Wnt pathways.

SIGNIFICANCE

The human MUC1 transmembrane glycoprotein is aberrantly overexpressed in about 800,000 of the 1.3 million tumors diagnosed in the U.S. each year. MUC1 interacts with the ErbB and Wnt signaling pathways and induces transformation. The present studies demonstrate that MUC1 localizes to mitochondria and that MUC1 blocks activation of the intrinsic apoptotic pathway by genotoxic agents. The results also demonstrate that MUC1 confers resistance to treatment in animal tumor models. These findings indicate that overexpression of MUC1 in human tumors could be of importance to the effectiveness of anticancer therapy.

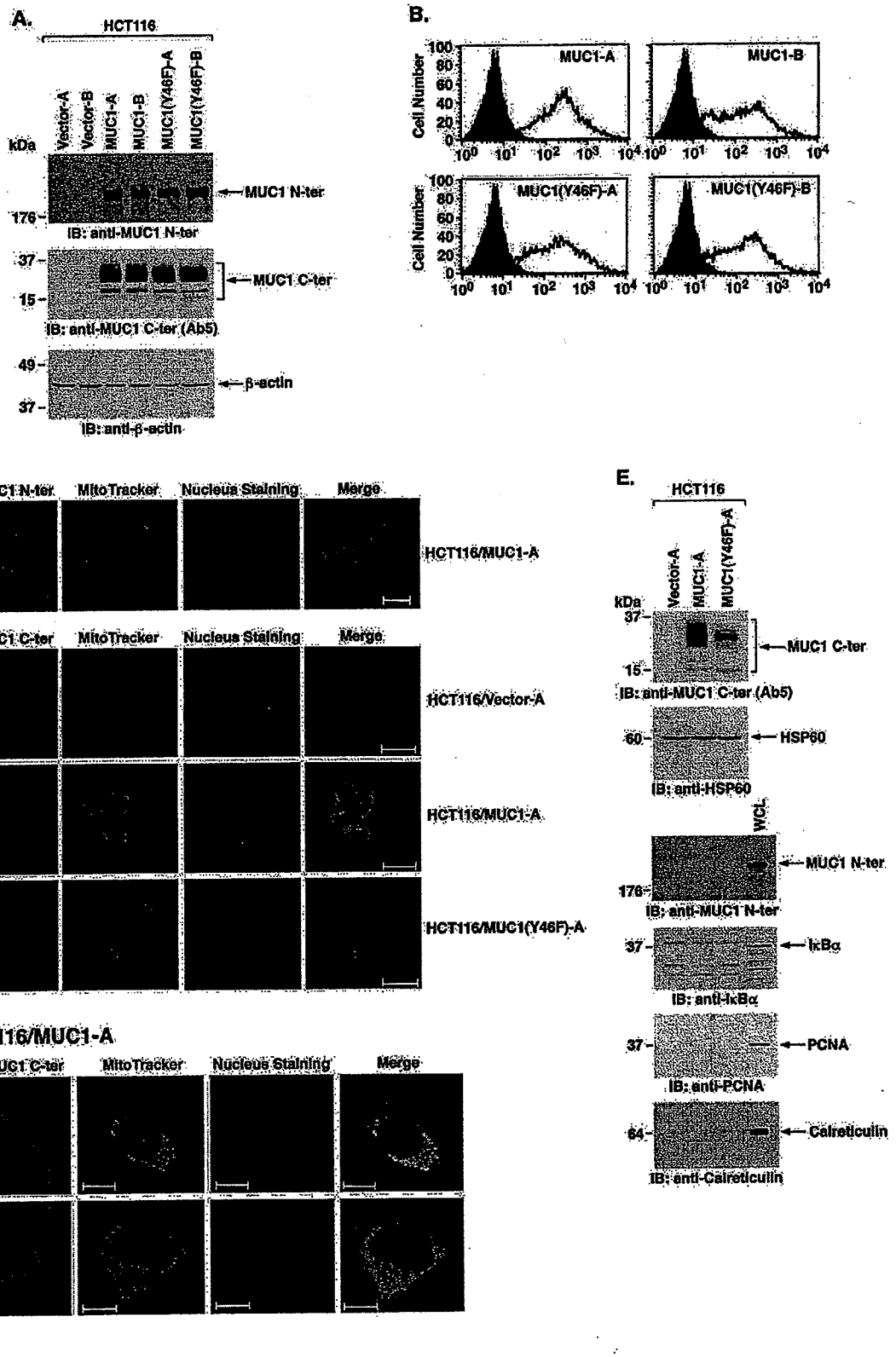
A.
HCT116
Vector-A
Vector-B
MUC1-A
MUC1-B
MUC1(Y46F)-A
MUC1(Y46F)-B
kDa
MUC1 N-ter
176
IB: anti-MUC1 N-ter
37
15
MUC1 C-ter
IB: anti-MUC1 C-ter (Ab5)
49
37
β-actin
IB: anti-β-actin
B.
MUC1-A
MUC1-B
MUC1(Y46F)-A
MUC1(Y46F)-B
Cell Number
C.
Anti-MUC1 N-ter
MitoTracker
Nucleus Staining
Merge
HCT116/MUC1-A
Anti-MUC1 C-ter
HCT116/Vector-A
HCT116/MUC1-A
HCT116/MUC1(Y46F)-A
D. HCT116/MUC1-A
Anti-MUC1 C-ter
MitoTracker
Nucleus Staining
Merge
E.
HCT116
Vector-A
MUC1-A
MUC1(Y46F)-A
kDa
37
15
MUC1 C-ter
IB: anti-MUC1 C-ter (Ab5)
60
HSP60
IB: anti-HSP60
WCL
MUC1 N-ter
176
IB: anti-MUC1 N-ter
37
IκBα
IB: anti-IκBα
37
PCNA
IB: anti-PCNA
64
Calreticulin
IB: anti-Calreticulin

Overexpression of MUC1 confers anchorage-independent growth and tumorigenicity of rodent fibroblasts and human epithelial cells (Li et al., 2003c; Ren et al., 2002). Other work has shown that, in addition to localization at the cell membrane, the MUC1 C-ter is expressed in nuclear complexes with β-catenin (Li et al., 2003a, 2003b, 2003c; Wen et al., 2003). Moreover, treatment of cells with heregulin (HRG), which activates ErbB2-4, is associated with targeting of MUC1 C-ter to the nucleus in a complex with γ-catenin (Li et al., 2003c). These observations have indicated that the function of MUC1 as a transforming protein may be mediated by regulating gene expression. In the present studies, we show that the MUC1 C-ter localizes to mitochondria. Significantly, the results demonstrate that MUC1 blocks activation of the intrinsic apoptotic pathway by DNA damaging agents. Our findings indicate that overexpression of MUC1 by human carcinomas contributes to the resistance of these cells to genotoxic agents.

Results

MUC1 C-ter localizes to mitochondria

MUC1-negative HCT116 cells were transfected to stably express the empty vector, MUC1, or the MUC1(Y46F) mutant. Two clones (A and B) of each were selected from independent transfections. Immunoblot analysis with anti-MUC1 demonstrated no detectable expression of the MUC1 N-ter or C-ter subunits in the vector transfectants (Figure 1A). By contrast, MUC1 N-ter expression was similar in cells transfected with MUC1 or MUC1(Y46F) (Figure 1A). Similar levels of MUC1 C-ter were also found in the MUC1 and MUC1(Y46F) transfectants (Figure 1A). To assess whether MUC1 is expressed at the cell membrane, the transfectants were analyzed by flow cytometry with the anti-MUC1 N-ter antibody. In contrast to HCT116/vector cells, MUC1 was detectable on the surface of HCT116 cells expressing MUC1 or MUC1(Y46F) (Figure 1B). To further define the distribution of MUC1, confocal microscopy was performed with antibodies against the MUC1 N-ter and C-ter. Both subunits were detectable at the cell membrane of the MUC1 transfectants (Figure 1C). Unexpectedly, however, the MUC1 C-ter, and not the N-ter, was also expressed in a pattern that suggested mitochondrial localization (Figure 1C). Indeed, colocalization of the MUC1 C-ter and MitoTracker supported targeting of MUC1 C-ter to mitochondria (Figure 1C). By contrast, there was substantially less mitochondrial localization of the MUC1(Y46F) C-ter (Figure 1C). Higher magnification and focusing of the images within a single HCT116/MUC1 cell showed clear localization of MUC1 C-ter at the cell membrane (Figure 1D, upper panels) and with MitoTracker throughout the mitochondrial network (Figure 1D, lower panels). Of note, detection of MUC1 C-ter at the cell membrane is obscured when focusing the confocal images on mitochondria (Figure 1D, lower panels). Moreover, within the cell, MUC1 C-ter expression is not restricted to mitochondria and, in addition to colocalization with MitoTracker, is detectable in the ER and cytosol (Figure 1D). To confirm these findings, mitochondrial lysates from the transfectants were subjected to immunoblot analysis with anti-MUC1 C-ter. The results demonstrate that the C-ter is detectable in the mitochondrial fraction from HCT116/MUC1, but not from HCT116/vector, cells (Figure 1E). Moreover, in concert with the confocal data, mitochondrial localization of the MUC1(Y46F) C-ter was considerably less than that found for the MUC1 C-ter (Figure 1E). Equal loading of mitochondrial lysates was confirmed by immunoblotting for the mitochondrial HSP60 protein (Figure 1E). Absence of the MUC1 N-ter indicated that the mitochondrial fraction was not contaminated with cell membranes (Figure 1E). Immunoblot analysis of the mitochondrial lysates with antibodies against the cytosolic IκBα, nuclear PCNA, and ER-associated calreticulin proteins further indicated that the mitochondria are not significantly contaminated with these subcellular fractions (Figure 1E).

Targeting of MUC1 C-ter to mitochondria is associated with HRG treatment

To compare MUC1 C-ter expression at the cell membrane with that in mitochondria, lysates from these fractions were subjected to immunoblot analysis with antibodies directed against the extracellular domain (ECD) and cytoplasmic domain (CD) (Figure 2A, upper panel). The results obtained with the Ab5 antibody, which reacts with the C-terminal 17 amino acids of MUC1 CD, demonstrated similar patterns for MUC1 C-ter expressed at the cell membrane and in mitochondria (Figure 2A). Reactivity with Ab5 was observed predominantly at 20–25 kDa (Figure 2A). Reactive bands were also observed at ~17 and 15 kDa (Figure 2A). Immunoblotting with the DF3E antibody, which was generated against the VETQFNQYKTEAAS motif in the MUC1 ECD (Li et al., 2001a), demonstrated reactivity with lysates from both the cell membrane and mitochondria (Figure 2A). Notably, reactivity of the DF3E antibody with the 20–25 kDa MUC1 C-ter and the 17 kDa fragment indicates that the 15 kDa fragment, as detected with Ab5, does not contain the DF3E epitope (Figure 2A). Another antibody generated against the MUC1 ECD, designated ECD1, reacted predominantly with

Figure 1. MUC1 C-ter localizes to mitochondria

HCT116 cells were transfected to stably express the empty vector, MUC1, or MUC1(Y46F). Clones (A and B) were selected from two independent transfections.

A: Lysates were subjected to immunoblot analysis with anti-MUC1 N-ter (DF3), anti-MUC1 C-ter (Ab5), and anti-β-actin.

B: Cells were incubated with anti-MUC1 N-ter (open patterns) or control mouse IgG (closed patterns) and analyzed for immunofluorescence by flow cytometry.

C: Confocal microscopy of HCT116/Vector-A, HCT116/MUC1-A, and HCT116/MUC1(Y46F)-A cells stained with anti-MUC1 N-ter (DF3) or C-ter (Ab5). Mitochondria were stained with MitoTracker Red. Nuclei were stained with TO-PRO-3. Scale bars represent 20 μm in the upper three panels and 10 μm in the lower panel.

D: Higher magnification of an HCT116/MUC1-A cell stained with anti-MUC1 C-ter (Ab5), Mitotracker Red CMXRos, and TO-PRO-3. Confocal images were focused on cell membrane (upper panels) and mitochondrial (lower panels) staining with anti-MUC1 C-ter. Scale bars represent 10 μm.

E: Mitochondrial fractions from HCT116/vector-A, HCT116/MUC1-A, and HCT116/MUC1(Y46F)-A cells were subjected to SDS-PAGE and immunoblotting with the indicated antibodies. Whole-cell lysate (WCL) was included as a control for detection of the membrane-associated MUC1 N-ter, cytoplasmic IκBα, nuclear PCNA, and endoplasmic reticulum-associated calreticulin proteins.

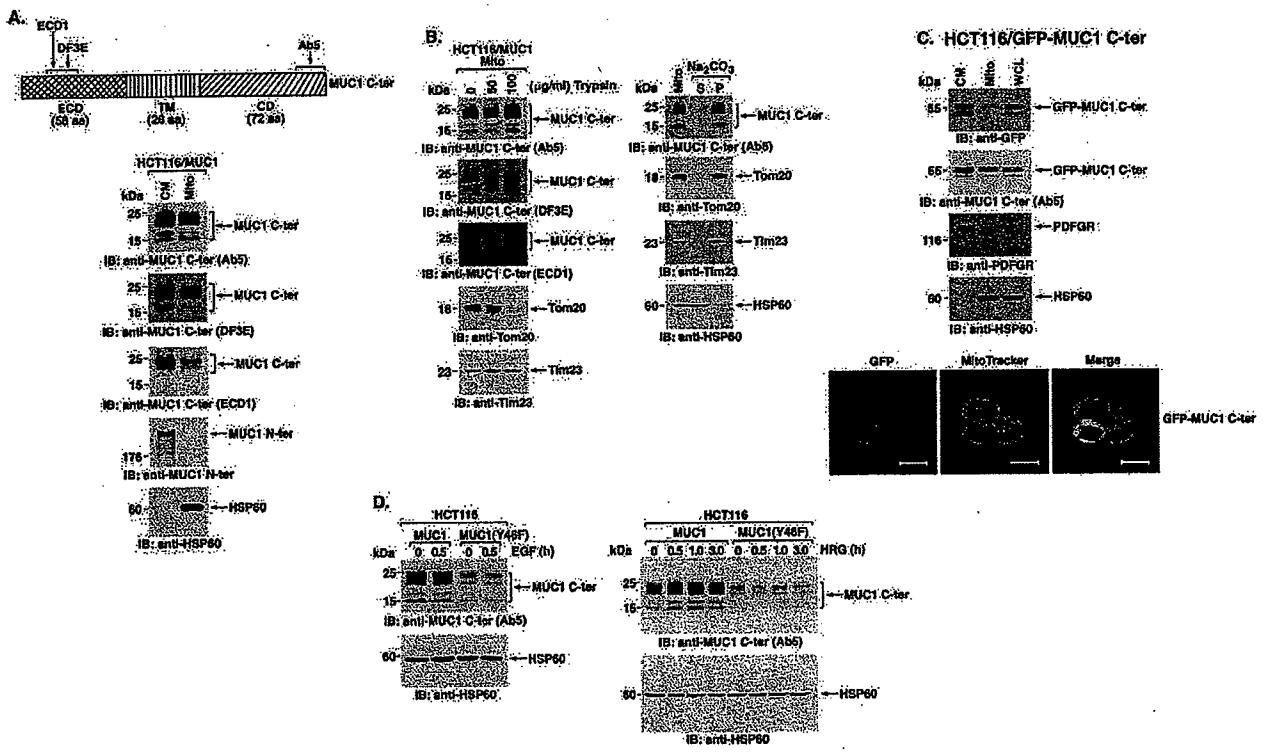

Figure 2. HRG stimulation targets MUC1 C-ter to mitochondria

A: Schematic representation of MUC1 C-ter with sites recognized by the indicated antibodies (upper panel). Lysates from the cell membrane (CM) and mitochondrial (Mito) fractions of HCT116/MUC1-A cells were subjected to SDS-PAGE and immunoblot analysis with the indicated antibodies (lower panels).

B: Purified mitochondria (0.4 mg protein/ml) were treated with 0, 50, or 100 μg/ml trypsin for 20 min at 4°C (left). The samples were subjected to immunoblot analysis with the indicated antibodies. Purified mitochondria (0.4 mg protein/ml) were resuspended in 0.1 M Na_2CO_3 (pH 11.5), incubated for 30 min at 0°C, and then centrifuged at 100,000 × g for 30 min at 4°C (right). The supernatant (S) and pellet (P) were analyzed by immunoblotting with the indicated antibodies.

C: HCT116 cells were transiently transfected with MUC1 C-ter tagged at the N terminus with GFP (GFP-MUC1 C-ter) and harvested at 36 hr. Lysates from cell membrane (CM) and mitochondrial (Mito) fractions were subjected to immunoblot analysis with the indicated antibodies (left). Whole-cell lysate (WCL) was included as a control. Confocal microscopy was performed on the transfected HCT116 cells after staining with MitoTracker Red and TO-PRO-3. Scale bars represent 10 μm.

D: HCT116/MUC1 and HCT116/MUC1(Y46F) cells were stimulated with EGF for 30 min (left) or HRG for the indicated times (right). Mitochondrial lysates were subjected to immunoblot analysis with anti-MUC1 C-ter and anti-HSP60. Intensity of the signals was determined by densitometric scanning.

the 20–25 kDa MUC1 C-ter in both the cell membrane and mitochondria. The DF3E and ECD1 antibodies react selectively with the HCT116/MUC1 and not the HCT116/vector cells (data not shown). These results suggest that the 17 and 15 kDa fragments represent MUC1 C-ter cleavage products without certain ECD sequences (Figure 2A). As controls, MUC1 N-ter expression was detectable only in the cell membrane fraction, and HSP60 expression was restricted to the mitochondrial fraction (Figure 2A). Moreover, as shown in Figure 1D, there was no detectable contamination of the mitochondrial fraction with IκBα, PCNA, or calreticulin (data not shown). To further assess localization of MUC1 C-ter in mitochondria, we digested purified mitochondria with trypsin. Treatment with trypsin at concentrations of 50 and 100 μg/ml had little if any effect on MUC1 C-ter as analyzed by immunoblotting with the Ab5, DF3E, and ECD1 antibodies (Figure 2B, left). As a marker protein of the mitochondrial outer membrane, the control and trypsin-treated mitochondria were immunoblotted with an antibody against Tom20, a component of the translocase of the outer membrane of mitochondria (TOM) (Iwahashi et al., 1997). As shown previously (Gotow et al., 2000), Tom20 levels were substantially decreased by trypsin treatment (Figure 2B, left). By contrast, trypsin had no effect on expression of the mitochondrial inner membrane protein Tim23 (Figure 2B, left). To determine whether MUC1 C-ter is integrated into mitochondrial membrane, the purified mitochondria were incubated in alkaline sodium carbonate. The extract was centrifuged, and the supernatant (luminal and peripheral proteins) and the pellet (integral membrane proteins) were analyzed by immunoblotting. The results show that MUC1 C-ter is detectable in the pellet fraction and not the supernatant (Figure 2B, right). Similar results were obtained for Tom20 and Tim23 (Figure 2B, right). As a control, the matrix HSP60 protein was readily solubilized by alkaline sodium carbonate treatment (Figure 2B, right). These results indicate that mitochondrial MUC1 C-ter is an integral membrane protein. To extend these findings, we expressed MUC1 C-ter with a GFP tag at the N

terminus and assessed mitochondrial localization. Immunoblot analysis of mitochondrial lysates with anti-GFP and anti-MUC1 C-ter confirmed mitochondrial targeting of the GFP-tagged MUC1 C-ter fusion protein (Figure 2C, upper panels). As controls, expression of the platelet-derived growth factor receptor (PDGFR) and HSP60 was restricted to the cell membrane and mitochondrial fractions, respectively (Figure 2C, upper panels). The results of confocal studies also demonstrate colocalization of GFP-MUC1 C-ter with MitoTracker (Figure 2C, lower panels). The transfection efficiency of HCT116 cells is ~25% under these experimental conditions (Ren et al., 2002). Shown is one HCT116 cell transfected with GFP-MUC1 C-ter surrounded by three cells not expressing the vector (Figure 2C, lower panels). Of note, the GFP-MUC1 C-ter is devoid of a signal sequence and was not detectable at the cell membrane (Figure 2C). As a control, the prominent pattern of mitochondrial localization was not apparent when expressing GFP alone (data not shown). These findings collectively demonstrate that MUC1 C-ter localizes to mitochondria. MUC1 C-ter is targeted to the nucleus with β-catenin in cells stimulated with EGF (Li et al., 2001b, 2003c). Stimulation of HCT116/MUC1 or HCT116/MUC1(Y46F) cells with EGF, however, had little effect on mitochondrial targeting of MUC1 C-ter (Figure 2D, left). In contrast to EGF, HRG activates ErbB2 in the response of epithelial cells to stress (Vermeer et al., 2003) and targets MUC1 C-ter to the nucleolus (Li et al., 2003c). Significantly, HRG treatment for 0.5 hr was associated with a 2.3-fold increase in localization of MUC1 C-ter to mitochondria, and this response persisted through 3 hr (Figure 2D, right). Moreover, HRG had little effect on mitochondrial localization of MUC1(Y46F) C-ter (Figure 2D, right). Similar results were obtained in three separate experiments. In addition, there was no detectable β-catenin or γ-catenin in the mitochondrial fractions from control or HRG-stimulated cells (data not shown). These findings indicate that targeting of MUC1 to mitochondria is regulated, at least in part, by HRG-induced signaling and that the Y46F mutation attenuates this response.

MUC1 attenuates cytochrome c release and caspase-3 activation

Treatment of cells with DNA-damaging agents is associated with release of mitochondrial cytochrome c and activation of the intrinsic apoptotic pathway. To determine if MUC1 C-ter affects cytochrome c release, the HCT116 transfectants were treated with cisplatin (CDDP). Treatment of HCT116/vector cells with CDDP was associated with increased levels of cytosolic cytochrome c (Figure 3A). Notably, expression of MUC1 significantly attenuated the release of cytochrome c (Figure 3A). By contrast, expression of MUC1(Y46F) was ineffective in blocking CDDP-induced cytochrome c release (Figure 3A). Similar results were obtained in the other separately isolated B clones (data not shown). Release of cytochrome c in the response to genotoxic stress is associated with activation of caspase-3 and cleavage of PKCδ (Emoto et al., 1995). To assess the effects of MUC1 on caspase-3 activation, CDDP-treated cells were analyzed for cleavage of pro-caspase-3. The results demonstrate that, compared to HCT116/vector cells, MUC1 attenuates CDDP-induced activation of caspase-3 (Figure 3B). Cleavage of pro-caspase-3 in CDDP-treated HCT116/MUC1(Y46F) cells was similar to that in HCT116/vector cells (Figure 3B). In concert with these results, caspase-3-mediated cleavage of PKCδ was attenuated in CDDP-treated HCT116/MUC1, as compared to HCT116/vector and HCT116/MUC1(Y46F), cells (Figure 3C). Smac/DIABLO is a mitochondrial protein that induces caspase-dependent cell death by interacting with inhibitor of apoptosis proteins (IAPs) and blocking their caspase inhibitory activity (Du et al., 2000; Verhagen et al., 2000). To determine if MUC1 attenuates release of Smac/DIABLO, HCT116/vector, HCT116/MUC1, and HCT116/MUC1(Y46F) cells were treated with CDDP for 24, 48, and 72 hr, and cytosolic lysates were subjected to immunoblot analysis. The results demonstrate that, like cytochrome c, release of Smac/DIABLO is attenuated in HCT116/MUC1, as compared to HCT116/vector and HCT116/MUC1(Y46F) cells (Figure 3D). In addition, MUC1 attenuated release of the mitochondrial caspase-independent death effector apoptosis-inducing factor (AIF) (Susin et al., 1999) as compared to that in cells expressing the vector or MUC1(Y46F) (Figure 3D). CDDP treatment of HCT116/vector and HCT116/MUC1(Y46F) cells for 72 hr was associated with >90% cell death and decreases in the β-actin signals used as a control for loading (Figure 3D). By contrast, treatment of HCT116/MUC1 cells with CDDP for 72 hr was associated with cessation of cell growth and <30% cell death. These findings indicate that MUC1 C-ter attenuates DNA damage-induced activation of the intrinsic apoptotic pathway.

MUC1 blocks DNA damage- and TRAIL-induced apoptosis

To determine if MUC1 affects the induction of apoptosis by CDDP, cells were analyzed for sub-G1 DNA content. Treatment of HCT116/vector cells with CDDP for 24 hr was associated with approximately 40% apoptosis (Figure 4A). Significantly, CDDP-induced apoptosis was attenuated in HCT116/MUC1 but not in HCT116/MUC1(Y46F) cells (Figure 4A). The attenuation of apoptosis by MUC1 as determined from cells with sub-G1 DNA content was confirmed when using TUNEL staining as an alternative method (data not shown). In addition, similar results were obtained in multiple experiments with the separately isolated HCT116 cell clones (Figure 4B). Expression of wild-type MUC1 but not the MUC1(Y46F) mutant also blocked apoptosis induced by the genotoxic agent etoposide (Figure 4C). Stimulation of cell surface death receptors with TNF-α or the TNF-related apoptosis-inducing factor TRAIL is associated with activation of the extrinsic apoptotic pathway. To determine if MUC1 affects death receptor-induced apoptosis, HCT116 cells were treated with TNF-α. In concert with previous work (Tsuchida et al., 1995), TNF-α alone failed to induce apoptosis of HCT116/vector cells (data not shown). However, treatment with TNF-α in the presence of cycloheximide (CHX) was associated with induction of HCT116/vector cell apoptosis (Figure 4D). Similar results were obtained when HCT116/MUC1 and HCT116/MUC1(Y46F) cells were treated with TNF-α and CHX (Figure 4D), indicating that MUC1 has no effect on TNF-α+CHX-induced apoptosis. By contrast, TRAIL was effective in inducing apoptosis of HCT116/vector cells without adding CHX and, importantly, MUC1 but not MUC1(Y46F) attenuated this response (Figure 4E). Moreover, when HCT116/MUC1 cells were treated with TRAIL+CHX, MUC1 was ineffective in attenuating TRAIL-induced apoptosis (Figure 4E). Of note, CHX had no apparent effect on expression of MUC1 C-ter (data not shown). These findings indicate that (1) MUC1 attenuates apoptosis induced by activation of the intrinsic pathway, and (2) MUC1 attenuates TRAIL-induced apoptosis by a mechanism that may be mediated by a short-lived protein.

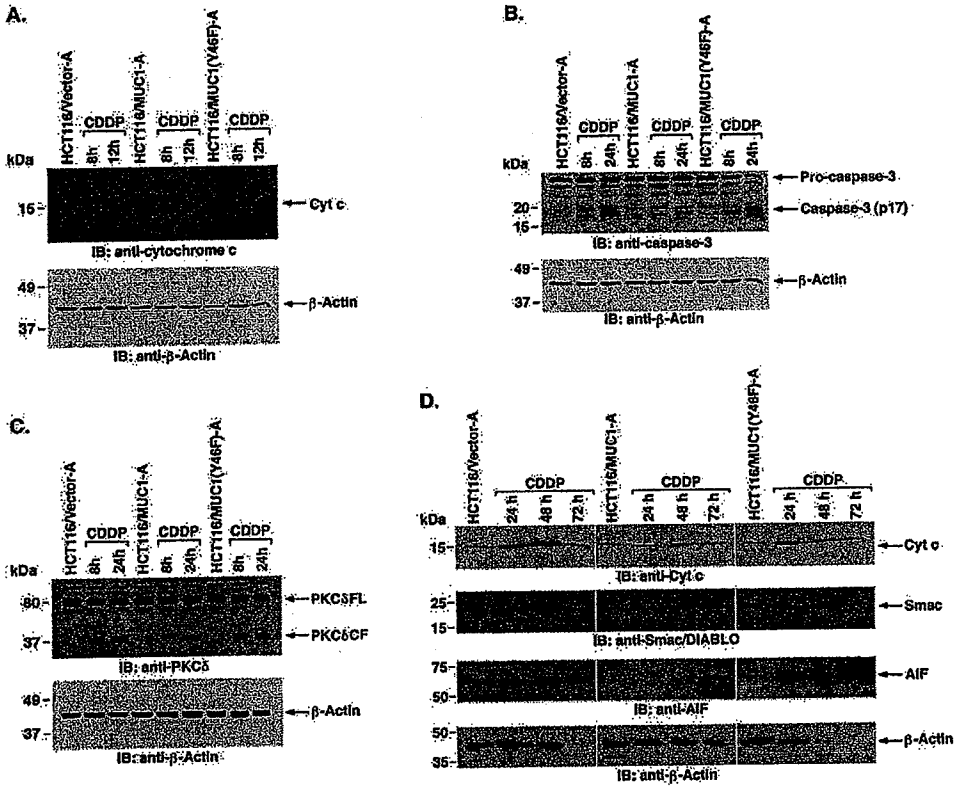

Figure 3. MUC1 attenuates CDDP-induced activation of the intrinsic mitochondrial apoptotic pathway

A: The indicated cells were treated with 100 μM CDDP for 8 and 12 hr. Cytosolic lysates were analyzed by immunoblotting with anti-cytochrome c and anti-β-actin.

B and C: The indicated cells were treated with 100 μM CDDP for 8 and 24 hr. Cell lysates were analyzed by immunoblotting with anti-caspase-3 (B) or anti-PKCδ (C) and anti-β-actin.

D: The indicated cells were treated with 100 μM CDDP for 24, 48, and 72 hr. Cytosolic lysates were analyzed by immunoblotting with the indicated antibodies.

Diverse carcinomas express the MUC1 C-ter in mitochondria

To determine if other carcinomas exhibit mitochondrial localization of the MUC1 C-ter, we first performed confocal immunofluorescence studies on human SW480 colon carcinoma cells stably transfected to express an empty vector or MUC1. SW480 cells transfected with the empty vector expressed a low level of MUC1 and exhibited little if any MUC1 C-ter in mitochondria (Figure 5A). By comparison, SW480/MUC1 cells exhibited substantially higher levels of MUC1 expression and clear colocalization of MUC1 C-ter with MitoTracker (Figure 5A). To extend these observations to carcinomas that endogenously express MUC1, we performed similar studies on human lung and breast cancer cells. There was no detectable MUC1 N-ter in mitochondria of A549 lung carcinoma cells (data not shown). However, as shown for the MUC1 transfectants, the MUC1 C-ter was detectable in mitochondria (Figure 5B). Similar results were obtained with T-47D (Figure 5C) and ZR-75-1 (Figure 5D) breast carcinoma cells. These findings indicate that the MUC1 C-ter localizes to mitochondria in both MUC1 transfectants and carcinomas that endogenously express MUC1.

Downregulation of MUC1 sensitizes carcinoma cells to apoptosis induced by genotoxic agents

To assess the effects of endogenous MUC1 expression on sensitivity of human carcinoma cells to genotoxic agents, we knocked down MUC1 with small interfering RNA (siRNA) duplexes. Exposure of A549 lung carcinoma cells to MUC1siRNA was associated with downregulation of MUC1 expression (Figure 6A). As a control, there was no detectable downregulation of MUC1 in A549 cells exposed to a control siRNA (CsiRNA) (Figure 6A). A549 cells exposed to mock conditions, MUC1-siRNA or CsiRNA, were then analyzed for annexin V staining and sub-G1 DNA. As determined by annexin V staining, A549 cells exposed to CsiRNA or MUC1siRNA exhibited no significant increase in apoptosis compared to mock conditions (Figure 6B). Importantly, the A549 cells exposed to MUC1siRNA responded to CDDP with an increase in apoptosis compared to that obtained with cells exposed to mock conditions or CsiRNA (Figure 6B). Similar results were obtained in multiple experiments and by analysis for sub-G1 DNA (Figure 6C and data not shown).

To extend these observations to another cell type, we generated a retrovirus expressing MUC1siRNA. Infection of ZR-75-1

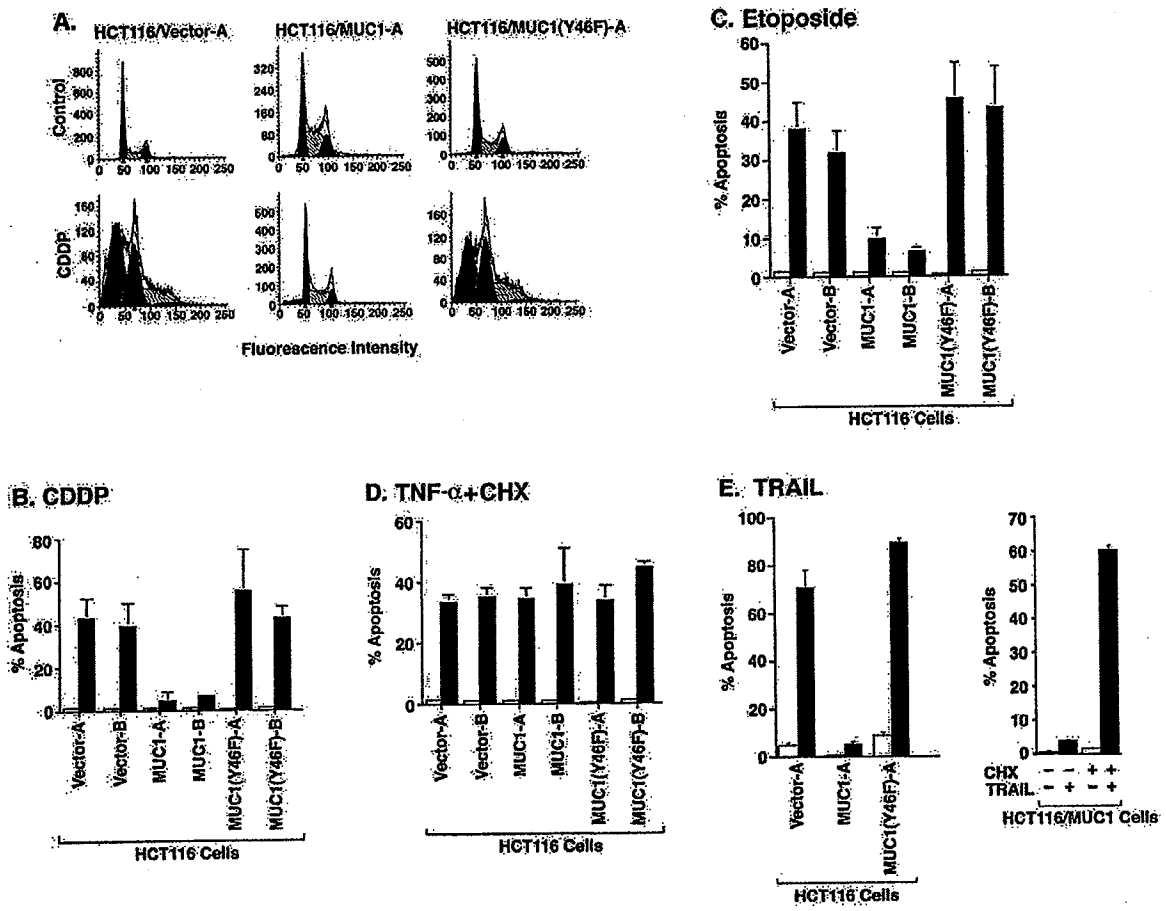

Figure 4. MUC1 attenuates DNA damage- and TRAIL-induced apoptosis

A: The indicated cells were treated with 100 μM CDDP for 24 hr and then analyzed for sub-G1 DNA.
B: Clones A and B of the indicated cells were left untreated (open bars) or treated with 100 μM CDDP for 24 hr (solid bars).
C: Clones A and B of the indicated cells were left untreated (open bars) or treated with 70 μM etoposide for 48 hr (solid bars).
D: Clones A and B of the indicated cells were left untreated (open bars) or treated with 20 ng/ml TNF-α and 10 μg/ml CHX for 12 hr (closed bars). The results are presented as the percentage apoptosis (mean ± SD of three independent experiments) as determined by analysis of sub-G1 DNA.
E: The indicated cells were left untreated (open bars) or treated with 100 ng/ml TRAIL for 14 hr (closed bars) (left). HCT116/MUC1 cells were treated with 100 ng/ml TRAIL and/or 10 μg/ml CHX as indicated for 14 hr (right). The results are presented as the percentage apoptosis (mean ± SD of three experiments) as determined by analysis of sub-G1 DNA.

breast carcinoma cells with the MUC1siRNA retrovirus and selection in G418 was associated with stable downregulation of MUC1 expression (Figure 7A). As a control, stable transduction of ZR-75-1 cells with the empty retrovirus had no effect on MUC1 expression (Figure 7A). Release of mitochondrial apoptogenic factors is associated with loss of the mitochondrial transmembrane potential ($\Delta\Psi m$) (Arnoult et al., 2003). CDDP-treated ZR-75-1/vector cells exhibited little if any decrease in $\Delta\Psi m$ (Figure 7B). By contrast, CDDP treatment of ZR-75-1/MUC1siRNA cells was associated with a clear loss of $\Delta\Psi m$ (Figure 7B). In concert with these findings, cytochrome c release was attenuated in CDDP-treated ZR-75-1/vector, as compared to ZR-75-1/MUC1siRNA, cells (Figure 7B). In the absence of exposure to a cytotoxic agent, ZR-75-1 cells expressing the empty retroviral vector or MUC1siRNA exhibited less than 5% apoptosis (Figure 7C). Treatment of ZR-75-1/vector cells with CDDP was associated with the induction of ~25% apoptosis (Figure 7C). Significantly, treatment of ZR-75-1/MUC1siRNA cells with CDDP resulted in over 60% apoptosis (Figure 7C). The ZR-75-1 cells were also treated with different concentrations of etoposide. The results show that sensitivity to 10 and 50 μM etoposide was increased substantially by knocking down MUC1 expression (Figure 7D). These findings and those in A549 cells indicate that knocking down MUC1 expression increases sensitivity to genotoxic agents.

MUC1 confers resistance to genotoxic agents in vivo

To determine if MUC1 expression affects chemosensitivity in vivo, HCT116/vector and HCT116/MUC1 cells were injected

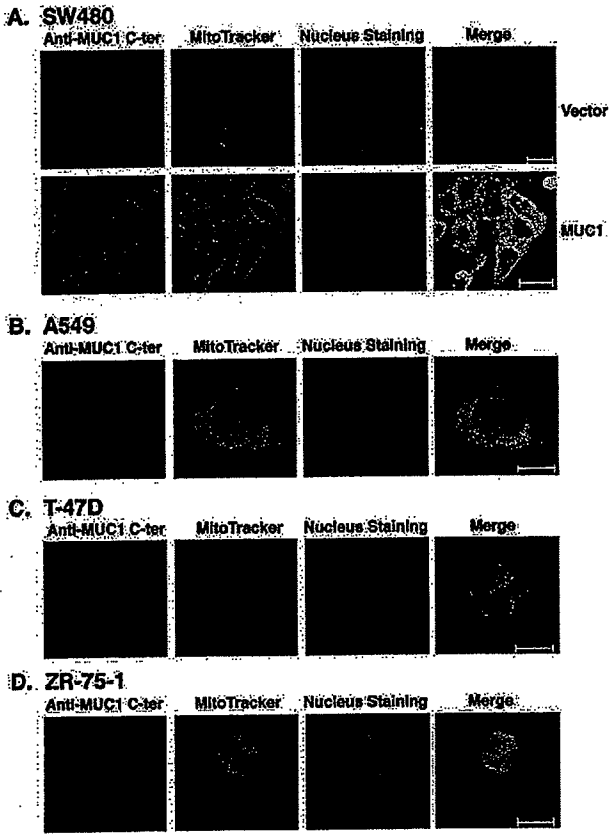

Figure 5. MUC1 C-ter localizes to mitochondria of diverse carcinoma cells

A: SW480 carcinoma cells stably transfected to express an empty vector or MUC1 were incubated with anti-MUC1 C-ter and then a FITC-conjugated secondary antibody. Mitochondria were stained with MitoTracker Red. Nuclei were stained with TO-PRO-3. Scale bars represent 20 μm.

B–D: A549 lung (**B**), T-47D breast (**C**), and ZR-75-1 breast (**D**) carcinoma cells were analyzed by staining with anti-MUC1 C-ter, MitoTracker Red, and TO-PRO-3. Scale bars represent 10 μm (**B**) or 20 μm (**C** and **D**).

subcutaneously into the flanks of nude mice. Growth of the HCT116/MUC1 cells was similar to that found for the HCT116/vector cells (Figure 8A). CDDP treatment of mice injected with the HCT116/vector cells was associated with a significant inhibition of tumor growth (Figure 8A). Notably, however, treatment of the HCT116/MUC1 tumors with CDDP resulted in little if any effect (Figure 8A). To determine if knocking down MUC1 affects chemosensitivity, we injected mice with ZR-75-1 cells stably expressing the empty retroviral vector or MUC1siRNA. Growth of the ZR-75-1/MUC1siRNA tumors was somewhat slowed compared to that found for ZR-75-1/vector cells (Figure 8B). Treatment with CDDP was associated with a partial slowing of ZR-75-1/vector tumor growth (Figure 8B). In contrast, the ZR-75-1/MUC1siRNA tumors were considerably more sensitive to CDDP treatment (Figure 8B). These findings indicate that MUC1 expression contributes to CDDP resistance of carcinoma cells in in vivo tumor models.

Discussion

MUC1 localizes to mitochondria

Recent work has indicated that MUC1 C-ter functions as a transducer of signals from activated ErbB receptor tyrosine kinases and the Wnt pathway to the nucleus (Li et al., 2003c). In the present studies, confocal microscopy showed that MUC1 C-ter also localizes to mitochondria. Subcellular fractionation studies confirmed mitochondrial targeting of MUC1 C-ter and not MUC1 N-ter. Immunoblot analysis of subcellular fractions showed that mitochondrial MUC1 C-ter is similar to MUC1 C-ter at the cell membrane. The results indicate that mitochondrial MUC1 C-ter (20–25 kDa) includes both ECD and CD sequences and that the 17/15 kDa fragments may represent MUC1 C-ter cleavage products. Cell fractionation and confocal microscopy studies of GFP-tagged MUC1 C-ter further confirmed localization of MUC1 C-ter to mitochondria. Our results also indicate that MUC1 C-ter is expressed in mitochondria as an integral membrane protein. MUC1 C-ter most likely localizes to the mitochondrial outer membrane (MOM) based on the lack of a readily identifiable mitochondrial targeting sequence and a functional role in attenuating activation of the intrinsic apoptotic pathway. Little is known, however, about how proteins are targeted to the MOM and then integrated in mitochondrial membranes (Mihara, 2000; Rapaport, 2003). The N terminus of Tom20 is anchored in the mitochondrial outer membrane and, as such, the C terminus is susceptible to protease digestion. Other proteins, such as Bcl-2 and Bcl-x_L, are anchored to the MOM by their C termini. Conversely, Tom40 is tightly embedded in the MOM and is not accessible to proteases (Suzuki et al., 2000). The demonstration that MUC1 C-ter is also not susceptible to trypsin digestion indicates that MUC1 C-ter may be embedded in the MOM. Our data, however, do not exclude the possibility that MUC1 C-ter may associate with the mitochondrial inner membrane. In this context, Bcl-2 has been detected in both the mitochondrial outer and inner membranes (Gotow et al., 2000).

The present studies further demonstrate that treatment of cells with HRG but not EGF is associated with increased targeting of MUC1 C-ter to mitochondria. Previous work using ZR-75-1 and HCT116/MUC1 cells has shown that HRG stimulates binding of MUC1 C-ter to γ-catenin and that MUC1 C-ter functions as a shuttle for nuclear targeting of γ-catenin (Li et al., 2003c). The present results indicate that MUC1 C-ter is not complexed with γ-catenin when targeted into mitochondria. In this regard, we have not found γ-catenin in mitochondria of HRG-stimulated ZR-75-1 or HCT116/MUC1 cells (data not shown). These results support a model in which the discrimination between nuclear or mitochondrial localization of MUC1 C-ter is determined by HRG-induced activation of distinct signaling pathways. The results also demonstrate that constitutive and HRG-induced mitochondrial targeting of MUC1 C-ter are attenuated by the Y46F mutation. This finding is consistent, at least in part, with the involvement of a tyrosine kinase that is activated and phosphorylates Y-46 in the HRG response. c-Src is activated by HRG (Belsches-Jablonski et al., 2001; Vadlamudi et al., 2003) and phosphorylates MUC1 on Y-46 (Li et al., 2001a). Thus, c-Src or other tyrosine kinases that are activated by HRG may contribute to mitochondrial targeting of MUC1 C-ter. Additional work has shown that MUC1 C-ter forms a complex with the cytosolic chaperones HSP70 and HSP90 and that these interactions are attenuated by the Y46F mutation (unpublished

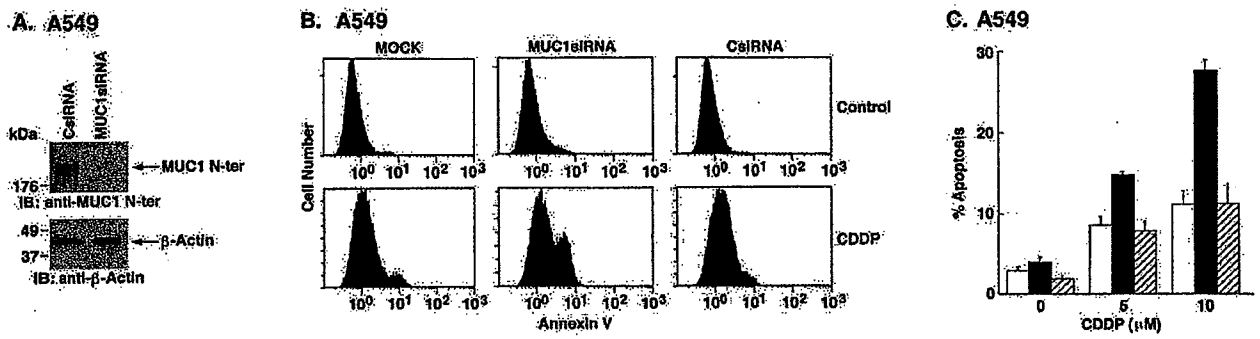

Figure 6. Transient downregulation of MUC1 expression sensitizes A549 carcinoma cells to CDDP-induced apoptosis

A: A549 cells were treated with CsiRNA or MUC1siRNA and harvested 72 hr after transfection. Lysates were analyzed by immunoblotting with anti-MUC1 N-ter and anti-β-actin.

B: A549 cells were left untransfected (MOCK) or transfected with MUC1siRNA or CsiRNA, incubated for 72 hr, and then treated with 10 μM of CDDP for 48 hr. Cells were stained with FITC-conjugated annexin V and analyzed by flow cytometry.

C: The results for MOCK (open bars), MUC1siRNA transfected (solid bars), or CsiRNA transfected (hatched bars) cells are expressed as the percentage apoptosis (mean ± SD of three independent experiments).

data). HSP70 and HSP90 function in the delivery of proteins to the mitochondrial import receptor Tom70 and thus may be responsible for targeting MUC1 C-ter to the MOM (Truscott et al., 2003; Young et al., 2003). The GFP-MUC1 C-ter used in our studies was generated without a signal sequence and was not detectable at the cell surface. Thus, the detection of GFP-MUC1 C-ter in mitochondria indicates that MUC1 C-ter can be targeted into mitochondria without prior localization to the cell

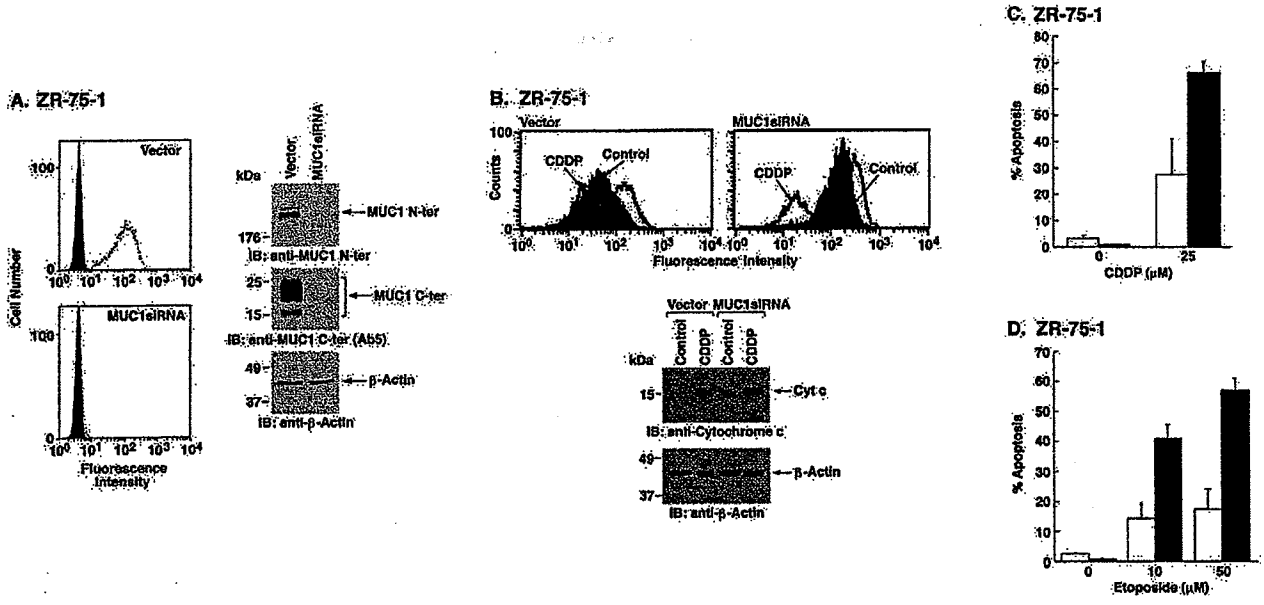

Figure 7. Stable downregulation of MUC1 sensitizes ZR-75-1 cells to CDDP- and etoposide-induced apoptosis

A: ZR-75-1 cells were infected with a control retroviral vector or one expressing MUC1siRNA. Stable transfectants were selected in the presence of G418. Cells were incubated with anti-MUC1 N-ter (open patterns) or control mouse IgG (closed patterns) and analyzed for immunofluorescence by flow cytometry (left). Lysates were analyzed by immunoblotting with the indicated antibodies (right panels).

B: ZR-75-1/vector and ZR-75-1/MUC1siRNA cells were incubated with $DiOC_6[3]$ and then left untreated (Control) or exposed to 25 μM CDDP for 48 hr. Mitochondrial transmembrane potential was assessed by flow cytometry (upper panels). Cytosolic lysates were analyzed by immunoblotting with the indicated antibodies (lower panels).

C and D: ZR-75-1/vector (open bars) and ZR-75-1/MUC1siRNA (solid bars) cells were treated with 25 μM CDDP for 72 hr (**C**) or with 10 and 50 μM etoposide for 72 hr (**D**). Cells were analyzed for sub-G1 DNA. The results are presented as the percentage apoptosis (mean ± SD of three independent experiments).

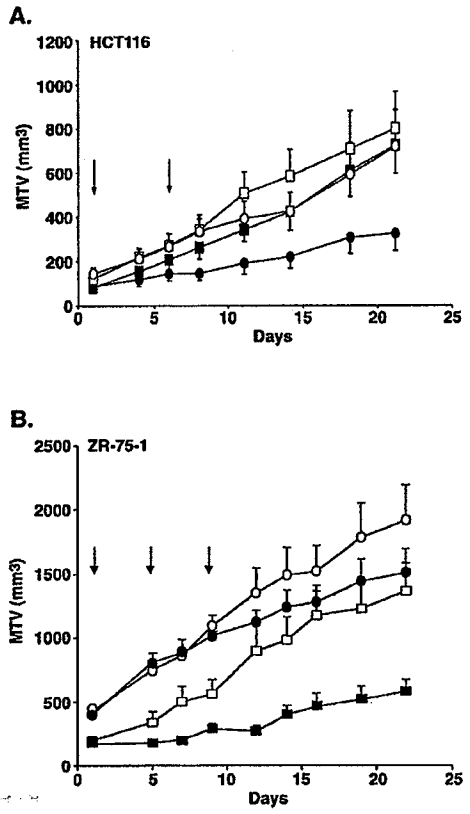

Figure 8. MUC1 confers resistance to CDDP treatment in vivo

A: HCT116/vector (○, ●) or HCT116/MUC1 (□, ■) cells (1×10^6) were injected subcutaneously into the posterior flanks of nude mice.

B: ZR-75-1/vector (○, ●) or ZR-75-1/MUC1siRNA (□, ■) cells (1×10^7) were injected into nude mice that had been pretreated with β-estradiol. The mice were treated as indicated (arrows) with intraperitoneal injections of PBS (□, ○) or 7 mg/kg CDDP (■, ●). Tumor volumes were calculated from bidimensional measurements at the indicated times. The results are expressed as the tumor volume (mean ± SD) of 4–8 mice per group.

membrane. MUC1 C-ter (no signal sequence) may be expressed by alternate splicing of MUC1 transcripts and thereby targeted directly to mitochondria. Alternatively, the results obtained with GFP-MUC1 C-ter may reflect a physiologic or stress-induced mechanism in which, after processing in the ER, MUC1 C-ter is released into the cytosol and transported to mitochondria. In support of such mechanisms, the c-Abl kinase localizes to the ER and is trafficked to mitochondria in the response to stress (Ito et al., 2001). Additional studies are ongoing to more precisely define the signals responsible for both the targeting and insertion of MUC1 C-ter as an integral mitochondrial membrane protein.

MUC1 attenuates the intrinsic apoptotic pathway

Genotoxic agents that are used in cancer treatment often induce apoptosis by activation of the mitochondrial pathway (Herr and Debatin, 2001; Kroemer and Reed, 2000). Thus, the identification of antiapoptotic proteins that confer resistance to anticancer agents is of potential importance. The present results further demonstrate that MUC1 expression is associated with attenuation of CDDP-induced release of mitochondrial cytochrome c, Smac/DIABLO, and AIF. In addition, the MUC1(Y46F) mutant was less effective than MUC1 in attenuating CDDP-induced release of these apoptogenic proteins. In concert with these findings, MUC1 but not MUC1(Y46F) was also effective in attenuating CDDP-induced activation of caspase-3 and cleavage of PKCδ. These findings were not restricted to CDDP, since MUC1 also attenuated activation of the intrinsic mitochondrial pathway by etoposide (data not shown). Moreover, the results are not attributable to clonal variation, because independently selected HCT116/MUC1 clones exhibited the same resistant phenotype. Overexpression of MUC1 in rat 3Y1 cells is associated with increases in phospho-Bad and Bcl-x_L levels (unpublished data). The finding, however, that HCT116/MUC1 cells do not express increased levels of phospho-Bad or of the Bcl-x_L/Bcl-2 proteins (data not shown) indicates that MUC1 C-ter attenuates DNA damage-induced release of apoptogenic mitochondrial effectors by other mechanisms. In this regard, the present results indicate that MUC1 attenuates loss of $\Delta\Psi m$ in the response to DNA damage. Release of mitochondrial apoptogenic factors can occur in part without changes in $\Delta\Psi m$; however, complete release of cytochrome c and Smac/DIABLO has been associated with loss of $\Delta\Psi m$ (Arnoult et al., 2003). Thus, MUC1 C-ter may attenuate mitochondrial release of apoptogenic factors by stabilizing the $\Delta\Psi m$ in response to stress. Nuclear MUC1 C-ter may also contribute to attenuation of proapoptotic signals that are activated by DNA damage. To further define the mechanistic effects of MUC1 C-ter on the intrinsic pathway, studies are underway to determine whether MUC1 C-ter regulates proapoptotic proteins that induce loss of $\Delta\Psi m$.

Stimulation of TNF-receptor-1 (TNF-R1) or the TRAIL receptors (R1 and R2) activates caspase-8 and thereby the extrinsic apoptotic pathway. Caspase-8-mediated cleavage of Bid also links death receptor signaling to the mitochondrial pathway by inducing the release of cytochrome c and Smac/DIABLO (Du et al., 2000; Li et al., 1998a; Luo et al., 1998; Verhagen et al., 2000). In this context, death receptor-induced apoptosis of type II cells is dependent on the mitochondrial pathway (Scaffidi et al., 1998). Based on the finding that MUC1 attenuates DNA damage-induced apoptosis by downregulating mitochondrial signaling, we asked if MUC1 also affects stimulation of the extrinsic pathway. Treatment of HCT116/vector cells with TNF-α alone resulted in no detectable apoptosis. However, in concert with reports in other cell types (Tsuchida et al., 1995), HCT116/vector cells exhibited an apoptotic response when treated with TNF-α and CHX. The results show that MUC1 has no apparent effect on TNF-α+CHX-induced apoptosis. By contrast, apoptosis of HCT116/vector cells was induced by TRAIL in the absence of CHX. Moreover, MUC1 and not MUC1(Y46F) attenuated TRAIL-induced apoptosis, indicating that MUC1 C-ter downregulates mitochondrial amplification of TRAIL death signaling. Importantly, the attenuation of TRAIL-induced apoptosis by MUC1 was reversed by adding CHX. These results indicate that MUC1-mediated downregulation of TRAIL-induced apoptosis is conferred by the synthesis of a short-lived protein (Munshi et al., 2001; Thakkar et al., 2001; Wajant et al., 2000). The use of CHX with TNF-α may also explain why MUC1 had no effect on TNF-α +CHX-induced apoptosis. These findings indicate that attenuation of the intrinsic pathway by mitochondrial localization of

MUC1 C-ter may affect death receptor-induced apoptosis. However, the results do not exclude the possibility that MUC1 may downregulate death receptor signaling by other mechanisms.

Have human tumors exploited MUC1 as an otherwise physiologic mechanism to attenuate stress-induced apoptosis?

Stable expression of MUC1 in the MUC1-negative HCT116 cells represents one approach to assess the effects of MUC1 on chemosensitivity. We reasoned, however, that downregulating MUC1 in carcinoma cells that endogenously overexpress this oncoprotein might be equally informative. MUC1 siRNA was thus used to knock down MUC1 expression in A549 lung and ZR-75-1 breast cancer cells. The results demonstrate that transient downregulation of MUC1 expression in A549 cells is associated with increased sensitivity to CDDP-induced apoptosis. Stable downregulation of MUC1 in ZR-75-1 cells also resulted in an increased apoptotic response to CDDP treatment in vitro. Moreover, the demonstration that MUC1 downregulation potentiates apoptosis induced by etoposide indicates that MUC1 expression attenuates the apoptotic response to diverse genotoxic agents in vitro. Importantly, stable downregulation of MUC1 increased the sensitivity of ZR-75-1 tumors to CDDP treatment. Conversely, MUC1 expression in HCT116 cells conferred in vivo resistance to CDDP treatment. These findings suggest that MUC1 may contribute to resistance of human tumors to genotoxic anticancer agents.

Mucins represent a defensive physical barrier to environmental stress and may function in transducing signals that protect the epithelium from damage. Mechanical or toxic damage to epithelial cells is associated with disruption of tight junctions between neighboring cells, loss of polarity, and activation of a repair program (Vermeer et al., 2003). Stimulation of ErbB2 by HRG contributes to this repair by promoting cell division and thereby replacement of damaged cells (Vermeer et al., 2003). Our findings that HRG stimulation also induces both nuclear (Li et al., 2003c) and mitochondrial targeting of MUC1 C-ter suggest that MUC1 may play a role in the repair of epithelial integrity. The epithelial stress response is transiently associated with loss of polarity (Vermeer et al., 2003). With transformation and transition to a mesenchymal phenotype, epithelial cells lose the capability to reverse loss of polarity. Thus, in the HRG-induced stress response of normal epithelial cells, nuclear and/or mitochondrial MUC1 could transiently protect against apoptosis following injury. Conversely, irreversible nuclear and/or mitochondrial targeting of MUC1 in carcinoma cells could confer a phenotype that is stably resistant to stress-induced apoptosis. In this regard, our previous studies showed that MUC1 overexpression protects cells against oxidative stress-induced apoptosis (Yin and Kufe, 2003). Moreover, the present finding that MUC1 attenuates the apoptotic response to DNA damaging agents is of potential importance to cancer treatment. Thus, what appears to be a physiologic mechanism to protect normal epithelial cells against apoptosis during stress-induced repair may have been exploited by human tumors to survive under adverse conditions and in response to anticancer agents.

Experimental procedures

Cell culture

Human HCT116 and SW480 colon carcinoma cells (ATCC, Manassas, VA) were cultured in Dulbecco's modified Eagle's medium/F12 with 10% heat-inactivated fetal bovine serum, 100 units/ml penicillin, 100 μg/ml streptomycin, and 2 mM L-glutamine. Human A549 lung, T-47D breast, and ZR-75-1 breast carcinoma cells (ATCC) were grown in RPMI 1640 medium containing 10% heat-inactivated fetal bovine serum, antibiotics, and L-glutamine. Insulin (10 ng/ml; Life Technologies, Rockville, MD) was also added to cultures of the T-47D cells. Cells were treated with EGF (10 ng/ml; Calbiochem-Novabiochem, San Diego, CA), HRG (20 ng/ml; Calbiochem-Novabiochem), cisplatin (CDDP; Sigma), etoposide (Sigma), rhTNF-α (Promega, Madison, WI), CHX (Sigma), or rhTRAIL (100 ng/ml; Calbiochem-Novabiochem).

Cell transfections

HCT116 cells were transfected with pIRES-puro2, pIRESpuro2-MUC1, or pIRES-puro2-MUC1(Y46F), as described (Li et al., 2001b). SW480 cells were transfected with pIRES-puro2 or pIRES-puro2-MUC1. Stable transfectants were selected in the presence of 0.4 μg/ml puromycin (Calbiochem-Novabiochem, San Diego, CA). Two independent transfections were performed for each vector. Single cell clones were isolated by limiting dilution and expanded for analysis. In other studies, HCT116 cells were transiently transfected with the pEGFP-C1 vector (Clontech) in which MUC1 C-ter was cloned downstream to sequences encoding the green fluorescence protein (GFP).

Immunoblot analysis

Lysates were prepared from subconfluent cells as described (Li et al., 2001a). Equal amounts of protein were separated by SDS-PAGE and transferred to nitrocellulose membranes. The immunoblots were probed with anti-MUC1 N-ter (DF3) (Kufe et al., 1984), anti-MUC1 C-ter (Ab5; Neomarkers, Fremont, CA), anti-MUC1 C-ter (rabbit polyclonal DF3E) (Li et al., 2001a), anti-MUC1 C-ter (monoclonal ECD1; generated against the MUC1 ECD), anti-β-actin (Sigma), anti-HSP60 (Stressgen Biotechnologies, Victoria, BC, Canada), anti-PCNA (Calbiochem-Novabiochem, San Diego, CA), anti-IκBα (Santa Cruz Biotechnology, Santa Cruz, CA), anti-calreticulin (Stressgen Biotechnologies, Victoria, BC, Canada), anti-PDGFR (Santa Cruz Biotechnology), anti-Tom20 (BD PharMingen, San Diego, CA), anti-Tim23 (BD PharMingen), anti-cytochrome c (BD PharMingen), anti-caspase-3 (BD PharMingen), anti-PKCδ (Santa Cruz Biotechnology), anti-Smac/DIABLO (Medical & Biological Laboratories, Ltd., Japan), or anti-AIP (Santa Cruz Biotechnology). The immunocomplexes were detected with horseradish peroxidase-conjugated secondary antibodies and enhanced chemiluminescence (ECL, Amersham Biosciences, Piscataway, NJ). Intensity of the signals was determined by densitometric scanning.

Flow cytometry

Cells were incubated with anti-MUC1 N-ter or control mouse IgG for 1 hr at 4°C, washed, incubated with goat anti-mouse Ig fluorescein-conjugated antibody (Jackson Immunoresearch Laboratories, West Grove, PA), and then fixed in 2% formaldehyde/PBS. Reactivity was detected by FACScan.

Confocal microscopy

Cells cultured on coverslips were incubated in Dulbecco's modified Eagle's/F12 medium containing 100 nM MitoTracker Red CMXRos (Molecular Probes, Eugene, OR) for 20 min at 37°C. After staining, the cells were washed with fresh growth medium, prefixed in 3.7% formaldehyde/growth medium for 15 min at 37°C, washed with PBS, permeabilized in PBS containing 0.2% Triton X-100 for 5 min at 25°C, washed with PBS, then postfixed in 3.7% formaldehyde/PBS for 5 min at 25°C. After several washes with PBS, the cells were blocked with 10% goat serum for 1 hr at 25°C, stained with anti-MUC1 C-ter antibody for 1.5 hr at 25°C, washed with PBS, incubated with FITC-conjugated secondary antibody (Jackson ImmunoResearch Laboratories, West Grove, PA) for 40 min at 25°C, washed with PBS, and incubated with 2 μM TO-PRO3 (Molecular Probes) for 10 min at 25°C. After mounting the coverslips, images were captured with a LSM510 confocal microscope (ZEISS) at 1024 × 1024 pixel resolution. The excitation wavelength for FITC, MitoTracker Red, and TO-PRO3 were 488 nm, 543 nm, and 633 nm, respectively. Fluorescein fluorescence was captured through a 505–530 nm band-pass filter. MitoTracker Red CMXRos fluorescence was collected through a 560–615 nm band-pass filter. TO-PRO3 staining was visualized through a 650 nm long-pass filter.

Subcellular fractionation

Purified mitochondria and cytoplasmic lysates were prepared as described (Kumar et al., 2003). Cell membranes were purified from supernatants after

sedimentation of nuclei and mitochondria as described (Kharbanda et al., 1996). Purified mitochondria (0.4 mg protein/ml) were resuspended in 5 mM HEPES (pH 7.4), 210 mM mannitol, 70 mM sucrose, and 1 mM EGTA before treatment with trypsin (Sigma) at concentrations of 50 and 100 μg/ml for 20 min at 4°C. The samples were then subjected to SDS-PAGE and immunoblotting. Purified mitochondria (0.4 mg protein/ml) were also resuspended in 0.1 M Na_2CO_3 (pH 11.5), incubated for 30 min at 0°C, and then centrifuged at 100,000 × g for 30 min at 4°C. The supernatant was neutralized with HCl. The supernatant and pellet were then subjected to immunoblot analysis.

Generation of siRNA for transfection

siRNAs were synthesized to target the MUC1 sequence 5′-AAGTTCAGTGC CCAGCTCTAC-3′. The sense and antisense MUC1siRNAs were 5′-GUUCA GUGCCCAGCUCUACdTdT-3′ (sense) and 5′-GUAGAGCUGGGCACUGA ACdTdT-3′ (antisense) (Dharmacon Research, Inc.). A nonspecific control siRNA (CsiRNA) was also synthesized (5′-GCGCGCUUUGUAGGAUUCG dTdT-3′and 3′-dTdTCGCGCGAAACAUCCUAAGC-5′) (Dharmacon Research, Inc.). Cells were plated in 6-well plates at 1–3 × 10^5 cells/well, grown in antibiotic-free medium overnight, and then transfected with MUC1siRNA or CsiRNA using Oligofectamine reagent and Opti-MEM I reduced serum medium (Invitrogen Life Technology, Inc.) according to the manufacturer's instructions. At 72 or 96 hr after transfection, cells were trypsinized, replated, and incubated overnight before treatment.

Generation of retroviral vectors expressing MUC1siRNA

Oligonucleotides of siRNA were designed that contained a sense strand of 19 nucleotide sequences of MUC1 followed by a short spacer (GAGTACTG), the reverse complement of the sense strand, and five thymidines as an RNA polymerase III transcriptional stop signal. Forward oligonucleotides for MUC1 were TCGAG-GGTACCATCAATGTCCACGGAGTACTGCGTGGAC ATTGATGGTACCTTTTT including a XhoI cleavage site and the reverse CTA GAAAAAGGTACCATCAATGTC-CACGCAGTACTCCGTGGACATTGATGG TACCC including a XbaI site. Oligos were annealed and cloned into the XhoI-XbaI site of the pSuppressorRetro vector (Imgenex Co., San Diego, CA). 293T cells were cotransfected with a plasmid expressing MUC1siRNA and pCL-Ampho virus DNA using Fugene (Roche, Indianapolis). The supernatant was collected after 48 hr for infection of target cells.

Analysis of mitochondrial transmembrane potential

Cells were incubated with 0.5 nM 3,3-dihexyloxacarbocyanine iodide ($DiOC_6$[3]; Molecular Probes) for 30 min and analyzed by flow cytometry as described (Shapiro, 2000).

Apoptosis assays

Apoptotic cells were quantified by analysis of sub-G1 DNA, TUNEL staining, and annexin-V staining. At least two methods were used in each experiment. To assess sub-G1 DNA content, cells were harvested, washed with PBS, fixed with 80% ethanol, and incubated in PBS containing 20 ng/ml RNase (Roche) for 60 min at 37°C. Cells were then stained with 40 μg/ml propidium iodide (Sigma) for 30 min at room temperature in the dark. DNA content was analyzed by flow cytometry (EPICS XL-MCL, Coulter Corp.). Apoptotic cells with DNA fragmentation were detected by staining with the In Situ cell death detection kit (TUNEL; Roche Applied Science) and visualized by confocal microscopy (ZEISS LSM510). Apoptosis was also detected by staining cells with annexin V-FITC (BD Biosciences) in annexin V binding buffer (10 mM HEPES, 140 mM NaCl, 2.5 mM $CaCl_2$ [pH 7.4]). After staining, cells were analyzed by flow cytometry.

In vivo treatment models

HCT116/vector or HCT116/MUC1 cells (1 × 10^6) were injected subcutaneously in the flanks of 4- to 6-week-old female nude (nu/nu) mice. For studies of ZR-75-1 tumors, β-estradiol (1.7 mg, 60 day release; Innovative Research, Toledo, OH) was implanted subcutaneously 3 days prior to subcutaneous injection of 1 × 10^7 ZR-75-1/control or ZR-75-1/MUC1siRNA cells. Mice were treated intraperitoneally with 7 mg/kg CDDP or, as a control, PBS.

Acknowledgments

This work was supported by grants CA29431 and CA97098 awarded by the National Cancer Institute. The authors acknowledge Kamal Chauhan for excellent technical support. D.K. has a financial interest in ILEX.

Received: August 7, 2003
Revised: December 12, 2003
Accepted: December 22, 2003
Published: February 23, 2004

References

Arnoult, D., Gaume, B., Karbowski, M., Sharpe, J.C., Cecconi, F., and Youle, R.J. (2003). Mitochondrial release of AIF and EndoG requires caspase activation downstream of Bax/Bak-mediated permeabilization. EMBO J. *22*, 4385–4399.

Belsches-Jablonski, A.P., Biscardi, J.S., Peavy, D.R., Tice, D.A., Romney, D.A., and Parsons, S.J. (2001). Src family kinases and HER2 interactions in human breast cancer cell growth and survival. Oncogene *20*, 1465–1475.

Boldin, M., Goncharov, T., Goltsev, Y., and Wallach, D. (1996). Involvement of MACH, a novel MORT1/FADD-interacting protease, in Fas/APO-1- and TNF receptor-induced cell-death. Cell *85*, 803–815.

Bunz, F. (2001). Cell death and cancer therapy. Curr. Opin. Pharmacol. *1*, 337–341.

Datta, R., Manome, Y., Taneja, N., Boise, L.H., Weichselbaum, R.R., Thompson, C.B., Slapak, C.A., and Kufe, D.W. (1995). Overexpression of Bcl-x_L by cytotoxic drug exposure confers resistance to ionizing radiation-induced internucleosomal DNA fragmentation. Cell Growth Differ. *6*, 363–370.

Du, C., Fang, M., Li, Y., Li, L., and Wang, X. (2000). Smac, a mitochondrial protein that promotes cytochrome c-dependent caspase activation by eliminating IAP inhibition. Cell *102*, 33–42.

Emoto, Y., Manome, G., Meinhardt, G., Kisaki, H., Kharbanda, S., Robertson, M., Ghayur, T., Wong, W.W., Kamen, R., Weichselbaum, R., and Kufe, D. (1995). Proteolytic activation of protein kinase C δ by an ICE-like protease in apoptotic cells. EMBO J. *14*, 6148–6156.

Gendler, S., Taylor-Papadimitriou, J., Duhig, T., Rothbard, J., and Burchell, J.A. (1988). A highly immunogenic region of a human polymorphic epithelial mucin expressed by carcinomas is made up of tandem repeats. J. Biol. Chem. *263*, 12820–12823.

Gotow, T., Shibata, M., Kanamori, S., Tokuno, O., Ohsawa, Y., Sato, N., Isahara, K., Yayoi, Y., Watanabe, T., Leterrier, J.F., et al. (2000). Selective localization of Bcl-2 to the inner mitochondrial and smooth endoplasmic reticulum membranes in mammalian cells. Cell Death Differ. *7*, 666–674.

Herr, I., and Debatin, K.M. (2001). Cellular stress response and apoptosis in cancer therapy. Blood *98*, 2603–2614.

Ito, Y., Pandey, P., Mishra, N., Kumar, S., Narula, N., Kharbanda, S., Saxena, S., and Kufe, D. (2001). Targeting of the c-Abl tyrosine kinase to mitochondria in endoplasmic reticulum stress-induced apoptosis. Mol. Cell. Biol. *21*, 6233–6242.

Iwahashi, J., Yamazaki, S., Komiya, T., Nomura, N., Nishikawa, S., Endo, T., and Mihara, K. (1997). Analysis of the functional domain of the rat liver mitochondrial import receptor Tom20. J. Biol. Chem. *272*, 18467–18472.

Kharbanda, S., Saleem, A., Yuan, Z.-M., Kraeft, S., Weichselbaum, R., Chen, L.B., and Kufe, D. (1996). Nuclear signaling induced by ionizing radiation involves colocalization of the activated p56/p53^{lyn} tyrosine kinase with p34^{cdc2}. Cancer Res. *56*, 3617–3621.

Kluck, R.M., Bossy-Wetzel, E., Green, D.R., and Newmeyer, D.D. (1997). The release of cytochrome c from mitochondria: a primary site for Bcl-2 regulation of apoptosis. Science *275*, 1132–1136.

Kroemer, G., and Reed, J.C. (2000). Mitochondrial control of cell death. Nat. Med. *6*, 513–519.

Kufe, D., Inghirami, G., Abe, M., Hayes, D., Justi-Wheeler, H., and Schlom, J. (1984). Differential reactivity of a novel monoclonal antibody (DF3) with human malignant versus benign breast tumors. Hybridoma *3*, 223–232.

Kumar, S., Mishra, N., Raina, D., Kharbanda, S., Saxena, S., and Kufe, D. (2003). Abrogation of the apoptotic response to oxidative stress by the c-Abl tyrosine kinase inhibitor STI571. Mol. Pharmacol. *63*, 276–282.

Li, P., Nijhawan, D., Budihardjo, I., Srinivasula, S.M., Ahmad, M., Alnemri, E.S., and Wang, X. (1997). Cytochrome c and dATP-dependent formation of Apaf-1/caspase-9 complex initiates an apoptotic protease cascade. Cell *91*, 479–489.

Li, H., Zhu, H., Xu, C.-J., and Yuan, J. (1998a). Cleavage of BID by caspase 8 mediates the mitochondrial damage in the fas pathway of apotosis. Cell *94*, 491–501.

Li, Y., Bharti, A., Chen, D., Gong, J., and Kufe, D. (1998b). Interaction of glycogen synthase kinase 3β with the DF3/MUC1 carcinoma-associated antigen and β-catenin. Mol. Cell. Biol. *18*, 7216–7224.

Li, Y., Kuwahara, H., Ren, J., Wen, G., and Kufe, D. (2001a). The c-Src tyrosine kinase regulates signaling of the human DF3/MUC1 carcinoma-associated antigen with GSK3β and β-catenin. J. Biol. Chem. *276*, 6061–6064.

Li, Y., Ren, J., Yu, W.-H., Li, G., Kuwahara, H., Yin, L., Carraway, K.L., and Kufe, D. (2001b). The EGF receptor regulates interaction of the human DF3/MUC1 carcinoma antigen with c-Src and β-catenin. J. Biol. Chem. *276*, 35239–35242.

Li, Y., Chen, W., Ren, J., Yu, W., Li, Q., Yoshida, K., and Kufe, D. (2003a). DF3/MUC1 signaling in multiple myeloma cells is regulated by interleukin-7. Cancer Biol. Ther. *2*, 187–193.

Li, Y., Liu, D., Chen, D., Kharbanda, S., and Kufe, D. (2003b). Human DF3/MUC1 carcinoma-associated protein functions as an oncogene. Oncogene *22*, 6107–6110.

Li, Y., Yu, W.-H., Ren, J., Huang, L., Kharbanda, S., Loda, M., and Kufe, D. (2003c). Heregulin targets γ-catenin to the nucleolus by a mechanism dependent on the DF3/MUC1 protein. Mol. Cancer Res. *1*, 765–775.

Ligtenberg, M.J., Kruijshaar, L., Buijs, F., van Meijer, M., Litvinov, S.V., and Hilkens, J. (1992). Cell-associated episialin is a complex containing two proteins derived from a common precursor. J. Biol. Chem. *267*, 6171–6177.

Liu, X., Kim, C., Yang, J., Jemmerson, R., and Wang, X. (1996). Induction of apoptotic program in cell-free extracts: requirement for dATP and cytochrome c. Cell *86*, 147–157.

Luo, X., Budihardjo, H., Zou, H., Slaughter, C., and Wang, X. (1998). Bid, a Bcl2 interacting protein, mediates cytochrome c release from mitochondria in response to activation of cell surface death receptors. Cell *94*, 481–490.

Merlo, G., Siddiqui, J., Cropp, C., Liscia, D.S., Lidereau, R., Callahan, R., and Kufe, D. (1989). DF3 tumor-associated antigen gene is located in a region on chromosome 1q frequently altered in primary human breast cancer. Cancer Res. *49*, 6966–6971.

Mihara, K. (2000). Targeting and insertion of nuclear-encoded preproteins into the mitochondrial outer membrane. Bioessays *22*, 364–371.

Munshi, A., Pappas, G., Honda, T., McDonnell, T.J., Younes, A., Li, Y., and Meyn, R.E. (2001). TRAIL (APO-2L) induces apoptosis in human prostate cancer cells that is inhibitable by Bcl-2. Oncogene *20*, 3757–3765.

Muzio, M., Chinnaiyan, A.M., Kischkel, F.C., O"Rourke, K., Shevchenko, A., Ni, J., Scaffidi, C., Bretz, J.D., Zhang, M., Gentz, R., et al. (1996). FLICE, a novel FADD-homologous ICE/CED-3-like protease, is recruited to the CD95 (Fas/APO-1) death-inducing signaling complex. Cell *85*, 817–827.

Rapaport, D. (2003). Finding the right organelle. Targeting signals in mitochondrial outer-membrane proteins. EMBO Rep. *4*, 948–952.

Ren, J., Li, Y., and Kufe, D. (2002). Protein kinase C δ regulates function of the DF3/MUC1 carcinoma antigen in β-catenin signaling. J. Biol. Chem. *277*, 17616–17622.

Scaffidi, C., Fulda, S., Srinivasan, A., Friesen, C., Li, F., Tomaselli, K.J., Debatin, K.M., Krammer, P.H., and Peter, M.E. (1998). Two CD95 (APO-1/Fas) signaling pathways. EMBO J. *17*, 1675–1687.

Shapiro, H.M. (2000). Membrane potential estimation by flow cytometry. Methods *21*, 271–279.

Siddiqui, J., Abe, M., Hayes, D., Shani, E., Yunis, E., and Kufe, D. (1988). Isolation and sequencing of a cDNA coding for the human DF3 breast carcinoma-associated antigen. Proc. Natl. Acad. Sci. USA *85*, 2320–2323.

Srinivasula, S., Ahmad, M., Alnemri, T., and Alnemri, E. (1998). Autoactivation of procaspase-9 by Apaf-1-mediated oligomerization. Mol. Cell *1*, 949–957.

Stennicke, H., Jurgensmeier, J., Shin, H., Deveraux, Q., Wolf, B.B., Yang, X., Zhou, Q., Ellerby, H., Ellerby, L., Bredesen, D., et al. (1998). Pro-caspase-3 is a major physiologic target of caspase-8. J. Biol. Chem. *273*, 27084–27090.

Susin, S.A., Lorenzo, H.K., Zamzami, N., Marzo, I., Snow, B.E., Brothers, G.M., Mangion, J., Jacotot, E., Costantini, P., Loeffler, M., et al. (1999). Molecular characterization of mitochondrial apoptosis-inducing factor. Nature *397*, 441–446.

Suzuki, H., Okazawa, Y., Komiya, T., Saeki, K., Mekada, E., Kitada, S., Ito, A., and Mihara, K. (2000). Characterization of rat TOM40, a central component of the preprotein translocase of the mitochondrial outer membrane. J. Biol. Chem. *275*, 37930–37936.

Thakkar, H., Chen, X., Tyan, F., Gim, S., Robinson, H., Lee, C., Pandey, S.K., Nwokorie, C., Onwudiwe, N., and Srivastava, R.K. (2001). Pro-survival function of Akt/protein kinase B in prostate cancer cells. Relationship with TRAIL resistance. J. Biol. Chem. *276*, 38361–38369.

Truscott, K.N., Brandner, K., and Pfanner, N. (2003). Mechanisms of protein import into mitochondria. Curr. Biol. *13*, R326–R337.

Tsuchida, H., Takeda, Y., Takei, H., Shinzawa, H., Takahashi, T., and Sendo, F. (1995). In vivo regulation of rat neutrophil apoptosis occurring spontaneously or induced with TNF-alpha or cycloheximide. J. Immunol. *154*, 2403–2412.

Vadlamudi, R.K., Sahin, A.A., Adam, L., Wang, R.A., and Kumar, R. (2003). Heregulin and HER2 signaling selectively activates c-Src phosphorylation at tyrosine 215. FEBS Lett. *543*, 76–80.

Verhagen, A.M., Ekert, P.G., Pakusch, M., Silke, J., Connolly, L.M., Reid, G.E., Moritz, R.L., Simpson, R.J., and Vaux, D.L. (2000). Identification of DIABLO, a mammalian protein that promotes apoptosis by binding to and antagonizing IAP proteins. Cell *102*, 43–53.

Vermeer, P.D., Einwalter, L.A., Moninger, T.O., Rokhlina, T., Kern, J.A., Zabner, J., and Welsh, M.J. (2003). Segregation of receptor and ligand regulates activation of epithelial growth factor receptor. Nature *422*, 322–326.

Wajant, H., Haas, E., Schwenzer, R., Muhlenbeck, F., Kreuz, S., Schubert, G., Grell, M., Smith, C., and Scheurich, P. (2000). Inhibition of death receptor-mediated gene induction by a cycloheximide-sensitive factor occurs at the level of or upstream of Fas-associated death domain protein (FADD). J. Biol. Chem. *275*, 24357–24366.

Wen, Y., Caffrey, T., Wheelock, M., Johnson, K., and Hollingsworth, M. (2003). Nuclear association of the cytoplasmic tail of MUC1 and β-catenin. J. Biol. Chem. *278*, 38029–38039.

Yang, J., Liu, X., Bhalla, K., Kaekyung Kim, C., Ibrado, A.M., Cai, J., Peng, T.I., Jones, D.P., and Wang, X. (1997). Prevention of apoptosis by Bcl-2: release of cytochrome c from mitochondria blocked. Science *275*, 1129–1132.

Yin, L., and Kufe, D. (2003). Human MUC1 carcinoma antigen regulates intracellular oxidant levels and the apoptotic response to oxidative stress. J. Biol. Chem. *278*, 35458–35464.

Young, J.C., Hoogenraad, N.J., and Hartl, F.U. (2003). Molecular chaperones Hsp90 and Hsp70 deliver preproteins to the mitochondrial import receptor Tom70. Cell *112*, 41–50.

EXHIBIT B

Materials and Methods

Cell culture. Human K562 and KU812 CML and BC-1 lymphoma cells were cultured in RPMI1640 medium (Cellgro) supplemented with 10% heat-inactivated fetal bovine serum (FBS; Cellgro), 100 units/ml penicillin, 100 μg/ml streptomycin (ATCC) and 2 mM L-glutamine (ATCC). Bone marrow mononuclear cells isolated from two patients with CML in blast crisis were cultured for 7 d in RPMI1640 medium with 15% FBS and antibiotics. Cells were treated with imatinib (Novartis).

Immunoprecipitation and immunoblotting. Cells were lysed by sonication in the presence of 10 mM Tris-HCl, pH 7.5, 150 mM NaCl, 5 mM EDTA, 0.5% NP-40, 100 μg/ml phenylmethylsulphonyl fluoride and protease inhibitor mixture. Soluble proteins were incubated with anti-MUC1-C (Ab5; Labvision), anti-Bcr (G6, N-20, C-20; Santa Cruz Biotechnology; SCB) or anti-Abl (SCB) for 2 h at 4°C, followed by precipitation with protein A/G beads (Pierce). Immune complexes and lysates were subjected to immunoblot analysis with anti-MUC1-N (MAb DF3) (10), anti-MUC1-C, anti-β-actin (Sigma), anti-GST (Oncogene Biosciences), anti-IκBα (SCB) and anti-lamin B (Oncogene Biosciences). Reactivity was detected with horseradish peroxidase-conjugated second antibodies and chemiluminescence (Amersham Biosciences).

In vitro binding assays. Purified GST, GST-MUC1-CD(1-72), GST-MUC1-CD(1-45), GST-MUC1-CD(46-72), GST-Bcr(1-197), GST-Bcr(1-385) or GST-Bcr(1-426) were immobilized on glutathione beads

(Pierce). The beads were incubated with cell lysates, His-MUC1-CD(1-72) or His-Bcr(1-426) for 2 h at 4°C, washed and the adsorbates analyzed by immunoblotting.

Silencing of MUC1 in CML cells. The BLOCK-iT Target Screening System (Invitrogen) was used to generate siRNAs that target two MUC1 sequences (#1, AAGGTACCATCAATGTCCACG; or #2, AAGTTCAGTGCCCAGCTCTAC) and a control sequence (CGCTTACCGATTCAGAATGG). The siRNA cassettes were transferred to pHAGE-fullEF1α-MCS-IZsGreen-W for the generation of lentiviral vectors. The K562 and KU812 cells were infected with the lentiviruses at a multiplicity of infection of 5 in the presence of 8 μg/ml polybrene (Sigma). Cell clones were selected in methylcellulose semi-solid medium for expression of EGFP and assayed for downregulation of MUC1 by immunoblotting. For construction of adenoviruses, the siRNAs that target MUC1 sequences #1 or #2 and a control sequence targeting the luciferase gene were ligated into the pSIREN-DNR vector (Clontech). The siRNA cassettes were transferred to pLP-Adeno-X-PRLS by Cre/LoxP-mediated recombination. The vectors were then packaged into adenoviruses by transfection into HEK293 cells. Cells were infected with the adenoviruses at a multiplicity of infection of 5.

Subcellular fractionation. Nuclear and cytoplasmic fractions were prepared using the Nuclear Extraction Kit (Active Motif).

RT-PCR. Total cellular RNA was extracted with TRIZOL (Roche). Bcr-Abl-specific (Bcr-forward, 5′-TCAGACCCTGAGGCTCAAAGTC-3′ and Abl-reverse, 5′-GGAGCTGCAGATGCTGACCACC-3′), MUC1-specific (forward, 5′-GGTACCATCAATGTCCACG-3′ and reverse, 5′-CTACAAGTTGGCAGAAGTGG-3′ -3′) and β-actin-specific (forward, 5′-ATCATGTTTGAGACCTTCAA-3′ and reverse, 5′-CATCTCTTGCTCGAAGTCCA-3′) primers (Invitrogen) were used for reverse transcription and amplification (GeneAmp PCR System; Perkin Elmer Applied Systems). Amplified fragments were analyzed by electrophoresis in 2% agarose gels.

Pulse-chase analysis. Cells were cultured in methionine-free medium containing 250 μCi/ml [^{35}S]-labeled methionine (EasyTag Protein Labeling Mix; Perkin Elmer) for 2 h, washed and then chased in the presence of complete medium. Anti-Bcr precipitates were subjected to SDS-PAGE and autoradiography as described (25). Intensity of the signals was determined by densitometric scanning.

Analysis of self-renewal capacity. Cells were seeded at 2000/well of a 6-well plate containing 0.4% methylcellulose in RPMI 1640 medium supplemented with 10% or 2% FBS. At 4 weeks, colonies were counted under a stereomicroscope.

Apoptosis assays. Cells were fixed in 70% ethanol and incubated in PBS containing 50 μg/ml RNase and 2.5 μg/ml propidium iodide. DNA content was analyzed by flow cytometry. The

percentage of cells with sub-G1 DNA was determined by the MODFIT LT Program (Verity Software). Primary CML blasts were stained with Hoechst dye (Sigma) as described (33), and visualized under a fluorescence microscope for condensed and fragmented nuclei. Five hundred cells were scored for apoptosis in each of three independent experiments.

Fluorescence in situ hybridization (FISH). Cytospin preparations of mononuclear cells isolated from the bone marrow of a patient with CML in blast crisis were stained with anti-MUC1-N using the Vectastain ABC Kit (Vector Laboratories). Destaining was performed according to the manufacturer's recommendations (BioView, Inc.). The slides were then dehydrated in ethanol. Denaturation of the sample and probes (LSI Bcr-Abl Dual Color, Dual Fusion Translocation Probe; Vysis) was completed at 73°C for 2 min and the samples were hybridized with the probes at 37°C for 48 h. The samples were washed, counterstained with Blue View Drop (BioView) and visualized under a fluorescence microscope.

Results

MUC1-C associates with Bcr-Abl in CML cells. MUC1 is expressed in epithelial cells as a heterodimer of the MUC1-N and MUC1-C subunits. To assess expression of MUC1 in K562 CML cells, lysates were immunoblotted with antibodies against MUC1-N and MUC1-C. The results demonstrate that MUC1-N is expressed as the high molecular weight (>250 kDa) glycosylated form as detected by MAb DF3 (Fig. 1A). The transmembrane MUC1-C subunit was detectable as ~25-15 kDa species (Fig. 1A), consistent with that found in carcinoma cells (19). Similar patterns of MUC1 expression were found by probing lysates of KU812 CML cells (Fig. 1A). Recent studies have demonstrated that MUC1-C associates with c-Abl and blocks nuclear targeting of c-Abl in the response to DNA damage (27). Immunoblot analysis of anti-MUC1-C precipitates with anti-Bcr demonstrated that MUC1-C associates with the p210 Bcr-Abl fusion protein in both K562 and KU812 cells (Fig. 1B). In the reciprocal experiment, immunoblot analysis of anti-Bcr and anti-c-Abl precipitates with anti-MUC1-C supported the association of Bcr-Abl and MUC1-C (Fig. 1C). To determine whether the 72 amino acid MUC1 cytoplasmic domain (CD) confers the association with Bcr-Abl, we incubated K562 and KU812 cell lysates with GST or GST-MUC1-CD. Immunoblot analysis of the adsorbates with anti-Bcr demonstrated binding to MUC1-CD (Fig. 1D). The immunoblots also demonstrated binding of MUC1-CD to a protein with an apparent molecular weight of 130 kDa, consistent with one of the endogenous forms of Bcr (Fig. 1D). These findings indicated that MUC1-C associates with Bcr-Abl in the K562 and KU812 cell lines and that

this interaction may be mediated by binding of MUC1-CD to Bcr sequences in Bcr-Abl.

MUC1-CD binds directly to Bcr. To determine if MUC1-C associates with Bcr, we studied human BC-1 lymphoma cells that express endogenous MUC1 and Bcr, but not Bcr-Abl. Immunoprecipitation of Bcr from BC-1 lysates with two different anti-Bcr antibodies demonstrated that Bcr associates with endogenous MUC1-C (Fig. 2A). To determine if MUC1-CD associates with Bcr, BC-1 lysates were incubated with GST or GST-MUC1-CD. Analysis of the adsorbates by immunoblotting with anti-Bcr demonstrated binding of MUC1-CD to the 160 and 130 kDa forms of Bcr (Fig. 2B). The human Bcr protein contains 1271 amino acids, of which the N-terminal 902-927 amino acids are expressed in the p210 Bcr-Abl protein (34). To determine whether MUC1-CD binds to the N-terminal region of Bcr, we incubated His-MUC1-CD with GST or GST-Bcr fusion proteins generated from the N-terminal 197, 385 and 426 amino acids (Fig. 2C). The results demonstrate that MUC1-CD binds to Bcr(1-385) and Bcr(1-426), and not Bcr(1-197) (Fig. 2C). Experiments with GST fusion proteins containing fragments of MUC1-CD further demonstrated that MUC1-CD(1-45) and not MUC1-CD(46-72) confers the interaction with Bcr(1-426) (Fig. 2D). These findings indicate that MUC1-CD(1-45) binds directly to the Bcr N-terminal region (amino acids 197-426).

MUC1 stabilizes the Bcr-Abl protein. To address the significance of the MUC1-C-Bcr-Abl interaction, we infected K562

cells with a lentivirus expressing a siRNA that targets the MUC1 sequence 5'-AAGGTACCATCAATGTCCACG-3' (MUC1siRNA#1) in MUC1-C. Compared to wild-type K562 cells and those infected with a lentivirus expressing a control siRNA (CsiRNA), MUC1 expression was downregulated by MUC1siRNA#1 (Fig. 3A, left). To avoid potential off-target effects, we also infected K562 cells with a lentivirus expressing a siRNA that targets a different MUC1 sequence (5'-AAGTTCAGTGCCCAGCTCTAC-3'; MUC1siRNA#2) in MUC1-N. Downregulation of MUC1-C was similar with the two MUC1siRNAs (Fig. 3A, left). Notably, silencing MUC1 was associated with a partial decrease in Bcr-Abl levels (Fig. 3A, left). Analysis of cytoplasmic and nuclear fractions further demonstrated that the downregulation of Bcr-Abl is detectable in the cytoplasm and that silencing MUC1 is not associated with increases in nuclear Bcr-Abl (Fig. 3A, right). Immunoblotting with antibodies against the cytosolic IκBα and nuclear lamin B proteins was used to confirm equal loading of the lanes and purity of the fractions (Fig. 3A, right). Silencing of MUC1 in KU812 cells was also associated with partial downregulation of Bcr-Abl expression (Fig. 3B, left). Moreover, the decreases in Bcr-Abl were detectable in the cytosol and not related to targeting of Bcr-Abl to the nucleus (Fig. 3B, right). These results indicate that MUC1 functions in the upregulation of Bcr-Abl expression. To determine whether MUC1 affects Bcr-Abl transcription, we analyzed Bcr-Abl expression by RT-PCR. The results indicate that silencing MUC1 has little if any effect on Bcr-Abl mRNA levels in both K562 and KU812 cells (Fig. Supplemental Fig. S1). Stability of the Bcr-Abl protein was

therefore assessed by pulse-chase labeling and precipitation of Bcr-Abl with anti-Bcr. Autoradiography of the Bcr-Abl signals indicated that silencing of MUC1 decreases Bcr-Abl stability in K562 cells (Fig. 3C, left). Analysis of three separate experiments demonstrated that Bcr-Abl has a half-life of 38 h and 21 h in the presence and absence of MUC1, respectively (Fig. 3C, right). Silencing MUC1 in KU812 cells was also associated with a decrease in Bcr-Abl stability (Fig. 3D, left). The half-lives of Bcr-Abl in the KU812/CsiRNA and KU812/MUC1siRNA cells were 38 h and 17 h, respectively (Fig. 3D, right). These findings indicate that MUC1 increases Bcr-Abl expression by stabilizing the Bcr-Abl protein.

Silencing MUC1 decreases self-renewal capacity. To determine if MUC1 affects CML cell proliferation, the K562 cells were grown in medium containing 10% or 2% FBS. The results demonstrate that silencing MUC1 has little effect on K562 cell growth in 10% FBS (Supplemental Fig. S2A). In addition, K562/MUC1siRNA cell growth was modestly attenuated compared to that of K562/CsiRNA cells in 2% FBS (Supplemental Fig. S2A). By contrast, self-renewal capacity as determined by colony formation in methylcellulose was substantially decreased by silencing MUC1 in K562 cells cultured in the presence of 10% and 2% FBS (Figs. 4A-C). Silencing MUC1 also had a modest effect on growth of KU812 cells in 2% FBS (Supplemental Fig. S2B). However, as found with K562 cells, self-renewal capacity of KU812 cells was significantly decreased by silencing MUC1 (Fig. 4D).

Silencing MUC1 is associated with a differentiated phenotype. K562 cells respond to hemin and certain differentiating agents with the induction of hemoglobin synthesis (35, 36). Staining of K562 and K562/CsiRNA cells with benzidine to assess hemoglobin production demonstrated a low percentage of positive cells (Fig. 5A). By contrast, silencing MUC1 was associated with an increase in K562 cells that stain positively with benzidine (Fig. 5A). Similar results were obtained with KU812 cells silenced for MUC1 (Supplemental Fig. S3). Quantitation of benzidine staining demonstrated that silencing MUC1 significantly increases production of hemoglobin in both K562 and KU812 cells (Fig. 5B). To confirm that MUC1 is responsible for these observations, we infected K562 cells with adenoviruses expressing a control CsiRNA, MUC1siRNA#1 or MUC1siRNA#2 (Fig. 5C). The results demonstrate that downregulation of MUC1 is associated with increases in benzidine staining (Fig. 5D). These findings indicate that MUC1 suppresses differentiation of K562 and KU812 cells.

Silencing MUC1 increases sensitivity to imatinib. Previous work in carcinoma cells has demonstrated that MUC1 blocks the apoptotic response to genotoxic anti-cancer agents (19). However, the role of MUC1 in regulating apoptosis of malignant hematopoietic cells has not been studied. To explore this issue, we treated the K562 and KU812 cells with imatinib and assayed for the induction of apoptosis by sub-G1 DNA content. The results

demonstrate that silencing MUC1 is associated with imatinib-induced increases in K562 (Supplemental Fig. S4A) and KU812 (Supplemental Fig. S4B) cells with sub-G1 DNA content. These findings were confirmed in additional experiments (Supplemental Fig. S4C), indicating that MUC1 attenuates the apoptotic response to imatinib treatment.

Function of MUC1 in primary CML blasts. Mononuclear cells prepared from the bone marrow of a patient with CML in blast crisis were studied for MUC1-N expression by immunostaining and for Bcr-Abl by cytogenetics (Fig. 6A). MUC1-N was detectable in Bcr-Abl positive cells, indicating that MUC1 is expressed by CML blasts (Fig. 6A). These cells and those obtained from an additional patient with CML in blast crisis were cultured for 7 d. Infection of the cells with adenoviruses expressing MUC1siRNA#1 or MUC1siRNA#2 was associated with downregulation of MUC1-C expression (Fig. 6B). As found for K562 and KU812 cells, silencing MUC1 in the CML blasts resulted in increased hemoglobin production as detected by benzidine staining (Fig. 6C). Analysis of the CML blasts silenced for MUC1 with MUC1siRNA#1 or MUC1siRNA#2 gave similar increases in benzidine positive staining (Fig. 6D). The CML blasts were also treated with imatinib, stained with Hoechst dye and monitored for nuclear condensation and fragmentation as a measure of apoptosis (Supplemental Fig. S5A). Silencing MUC1 was associated with an increased apoptotic response to imatinib treatment as compared to that found in CML blasts infected with the control adenovirus (Supplemental Fig. S5A

and S5B). These results indicate that, as found for the CML cell lines, MUC1 suppresses differentiation and apoptosis of primary CML blasts.

not stabilization, of MUC1-C (21, 47). In contrast to Bcr-Abl, HSP90 binds to the MUC1-CD C-terminal region (amino acids 46-72) (21, 47). Thus, MUC1-CD could function in the formation of trimolecular complexes of HSP90-MUC1-C-Bcr-Abl and thereby the stabilization of Bcr-Abl.

MUC1-C promotes self-renewal and blocks differentiation of CML cells. To define the biological effects of the MUC1-C-Bcr-Abl interaction, we asked if MUC1 affects growth and self-renewal of CML cells. Silencing MUC1 had little if any effect on K562 and KU812 cell growth in 10% FBS and was associated with a modest decrease in growth rate in the presence of 2% FBS. However, more pronounced decreases in self-renewal capacity were observed in both K562 and KU812 cells silenced for MUC1. One explanation for these findings is that silencing MUC1 results in decreases in Bcr-Abl levels that in turn would be less effective in supporting self-renewal. Moreover, silencing MUC1 could have an effect independent of the MUC1-C interaction with Bcr-Abl. In this regard, recent work has demonstrated that progression of CML is supported by self-renewing leukemic granulocyte-macrophage progenitors that exhibit activation of the β-catenin pathway (9). These results indicate that β-catenin contributes to conversion of chronic phase CML to blast crisis. Other work has shown that Bcr-Abl stabilizes β-catenin by a mechanism involving its tyrosine phosphorylation (52). Notably, MUC1-C also stabilizes β-catenin by directly blocking function of the β-catenin destruction complex (25) and

therefore may play a role in activation of the β-catenin pathway in CML cells. Our results also demonstrate that silencing MUC1 in the CML cell lines and primary CML blasts is associated with the appearance of more differentiated erythroid phenotype. These findings may be also attributable to the MUC1-dependent decreases in Bcr-Abl levels and thereby release of a Bcr-Abl-mediated block in differentiation. For example, destabilization of Bcr-Abl with HSP90 inhibitors induces erythroid differentiation of K562 cells (49). In addition, treatment of K562 cells with agents, such as ara-C, that decrease self-renewal results in the irreversible induction of hemoglobin synthesis (36). Thus, the decrease in self-renewal capacity associated with MUC1 silencing may contribute in part to the increase in hemoglobin production.

MUC1-C blocks the apoptotic response of CML cells to imatinib. Overexpression of MUC1 in human carcinoma cells blocks the apoptotic response to gentoxic anti-cancer agents, oxidative stress and hypoxia (19, 53). MUC1-C is targeted to the mitochondrial outer membrane by a HSP90-dependent mechanism and attenuates activation of the intrinsic apoptotic pathway (19, 21, 47). Inhibition of Bcr-Abl with imatinib induces apoptosis of Bcr-Abl+ CML cells and is highly effective in treating patients with CML (3). The persistence of Bcr-Abl+ cells in CML patients treated with imatinib has further indicated that factors other than inhibition of the Abl kinase function may contribute to the pathogenesis of CML (34). The present results indicate that silencing MUC1 in K562 and KU812 cells increases sensitivity to

imatinib-induced apoptosis. Silencing MUC1 was also associated with an increase in ara-C-induced apoptosis (data not shown). Destabilization of Bcr-Abl with HSP90 inhibitors sensitizes CML cells to the induction of apoptosis through the intrinsic mitochondrial pathway. Thus, silencing MUC1 and thereby destabilization of Bcr-Abl could contribute to the increased sensitivity to imatinib. Moreover, based on studies in carcinoma cells, the increased sensitivity to imatinib could also be due in part to release of MUC1-C-induced stabilization of the mitochondrial permeability transition and block in release of apoptogenic factors (19). Our results further demonstrate that MUC1 blocks the apoptotic response of primary CML blasts to imatinib treatment. These findings and the demonstration that MUC1 blocks differentiation of primary CML blasts indicate that MUC1 may be of importance to the pathogenesis of CML in patients.

Acknowledgements

This work was supported by Grants CA100707, CA29431 and CA42802 awarded by the National Cancer Institute. Mr. Kamal Chauhan is acknowledged for technical support.

References

1. He Y, Wertheim JA, Xu L, et al. The coiled-coil domain and Tyr177 of bcr are required to induce a murine chronic myelogenous leukemia-like disease by bcr/abl. Blood 2002;99:2957-2968.
2. Goga A, McLaughlin J, Afar DEH, Saffran DC, Witte ON. Alternative signals to RAS for hematopoietic transformation by the BCR-ABL oncogene. Cell 1995;82:981-988.
3. Druker BJ, Tamura S, Buchdunger E, et al. Effects of a selective inhibitor of the Abl tyrosine kinase on the growth of Bcr-Abl positive cells. Nat Med 1996;2:561-566.
4. Deininger M, Buchdunger E, Druker BJ. The development of imatinib as a therapeutic agent for chronic myeloid leukemia. Blood 2005;105:2640-2653.
5. Lowenberg B. Minimal residual disease in chronic myeloid leukemia. N Engl J Med 2003;349:1399-1401.
6. Gorre ME, Sawyers CL. Molecular mechanisms of resistance to STI571 in chronic myeloid leukemia. Curr Opin Hematol 2002;9:303-307.
7. Faderl S, Talpaz M, Estrov Z, et al. The biology of chronic myeloid leukemia. N Engl J Med 1999;341:164-172.
8. Gorre ME, Mohammed M, Ellwood K, et al. Clinical resistance to STI-571 cancer therapy caused by BCR-ABL gene mutation or amplification. Science 2001;293:876-880.
9. Jamieson CH, Ailles LE, Dylla SJ, et al. Granulocyte-macrophage progenitors as candidate leukemic stem cells in blast-crisis CML. N Engl J Med 2004;351:657-667.

10. Kufe D, Inghirami G, Abe M, et al. Differential reactivity of a novel monoclonal antibody (DF3) with human malignant versus benign breast tumors. Hybridoma 1984;3:223-232.

11. Vasir B, Avigan D, Wu Z, et al. Dendritic cells induce MUC1 expression and polarization on human T cells by an IL-7-dependent mechanism. J Immunol 2005;174:2376-2386.

12. Correa I, Plunkett T, Vlad A, et al. Form and pattern of MUC1 expression on T cells activated in vivo or in vitro suggests a function in T-cell migration. Immunology 2003;108:32-41.

13. Takahashi T, Makiguchi Y, Hinoda Y, et al. Expression of MUC-1 on myeloma cells and induction of HLA-unrestricted CTL against MUC1 from a multiple myeloma patient. J Immunol 1994;153:2102-2109.

14. Dyomin VG, Palanisamy N, Lloyd KO, et al. MUC1 is activated in a B-cell lymphoma by the t(1;14)(q21;q32) translocation and is rearranged and amplified in B-cell lymphoma subsets. Blood 2000;95:2666-2671.

15. Levitin F, Stern O, Weiss M, et al. The MUC1 SEA module is a self-cleaving domain. J Biol Chem 2005;280:33374-33386.

16. Macao B, Johansson DG, Hansson GC, Hard T. Autoproteolysis coupled to protein folding in the SEA domain of the membrane-bound MUC1 mucin. Nat Struct Mol Biol 2006;13:71-76.

17. Siddiqui J, Abe M, Hayes D, et al. Isolation and sequencing of a cDNA coding for the human DF3 breast carcinoma-associated antigen. Proc Natl Acad Sci USA 1988;85:2320-2323.

18. Merlo G, Siddiqui J, Cropp C, et al. DF3 tumor-associated antigen gene is located in a region on chromosome 1q

frequently altered in primary human breast cancer. Cancer Res 1989;49:6966-6971.

19. Ren J, Agata N, Chen D, et al. Human MUC1 carcinoma-associated protein confers resistance to genotoxic anti-cancer agents. Cancer Cell 2004;5:163-175.

20. Wei X, Xu H, Kufe D. Human MUC1 oncoprotein regulates p53-responsive gene transcription in the genotoxic stress response. Cancer Cell 2005;7:167-178.

21. Ren J, Bharti A, Raina D, et al. MUC1 oncoprotein is targeted to mitochondria by heregulin-induced activation of c-Src and the molecular chaperone HSP90. Oncogene 2006;25:20-31.

22. Li Y, Kuwahara H, Ren J, Wen G, Kufe D. The c-Src tyrosine kinase regulates signaling of the human DF3/MUC1 carcinoma-associated antigen with GSK3β and β-catenin. J Biol Chem 2001;276:6061-6064.

23. Li Y, Bharti A, Chen D, Gong J, Kufe D. Interaction of glycogen synthase kinase 3β with the DF3/MUC1 carcinoma-associated antigen and β-catenin. Mol Cell Biol 1998;18:7216-7224.

24. Yamamoto M, Bharti A, Li Y, Kufe D. Interaction of the DF3/MUC1 breast carcinoma-associated antigen and β-catenin in cell adhesion. J Biol Chem 1997;272:12492-12494.

25. Huang L, Chen D, Liu D, et al. MUC1 oncoprotein blocks GSK3β-mediated phosphorylation and degradation of β-catenin. Cancer Res 2005;65:10413-10422.

26. Li Y, Liu D, Chen D, Kharbanda S, Kufe D. Human DF3/MUC1 carcinoma-associated protein functions as an oncogene.

Oncogene 2003;22:6107-6110.

27. Raina D, Ahmad R, Kumar S, et al. MUC1 oncoprotein blocks nuclear targeting of c-Abl in the apoptotic response to DNA damage. EMBO J 2006;25:3774-3783.

28. Taagepera S, McDonald D, Loeb J, et al. Nuclear-cytoplasmic shuttling of C-ABL tyrosine kinase. Proc Natl Acad Sci USA 1998;95:7457-7462.

29. Kharbanda S, Ren R, Pandey P, et al. Activation of the c-Abl tyrosine kinase in the stress response to DNA-damaging agents. Nature 1995;376:785-788.

30. Yuan Z, Huang Y, Ishiko T, et al. Regulation of DNA damage-induced apoptosis by the c-Abl tyrosine kinase. Proc Natl Acad Sci USA 1997;94:1437-1440.

31. Yoshida K, Yamaguchi T, Natsume T, Kufe D, Miki Y. JNK phosphorylation of 14-3-3 proteins regulates nuclear targeting of c-Abl in the apoptotic response to DNA damage. Nat Cell Biol 2005;7:278-285.

32. Vigneri P, Wang JY. Induction of apoptosis in chronic myelogenous leukemia cells through nuclear entrapment of BCR-ABL tyrosine kinase. Nat Med 2001;7:228-234.

33. Kawano T, Horiguchi-Yamada J, Iwase S, et al. Depsipeptide enhances imatinib mesylate-induced apoptosis of Bcr-Abl-positive cells and ectopic expression of cyclin D1, c-Myc or active MEK abrogates this effect. Anticancer Res 2004;24:2705-2712.

34. Ren R. Mechanisms of BCR-ABL in the pathogenesis of chronic myelogenous leukaemia. Nat Rev Cancer 2005;5:172-183.

35. Dean A, Erard F, Schneider AP, Schechter AN. Induction of hemoglobin accumulation in human K562 cells by hemin is reversible. Science 1981;212:459-461.

36. Luisi-DeLuca C, Mitchell T, Spriggs D, Kufe D. Induction of terminal differentiation in human K562 erythroleukemia cells by arabinofuranosyl cytosine. J Clin Invest 1984;74:821-827.

37. Maru Y, Witte ON. The BCR gene encodes a novel serine/threonine kinase activity within a single exon. Cell 1991;67:459-468.

38. Ren J, Li Y, Kufe D. Protein kinase C δ regulates function of the DF3/MUC1 carcinoma antigen in β-catenin signaling. J Biol Chem 2002;277:17616-17622.

39. Ress A, Moelling K. Bcr is a negative regulator of the Wnt signalling pathway. EMBO Rep 2005;6:1095-1100.

40. Pandey P, Kharbanda S, Kufe D. Association of the DF3/MUC1 breast cancer antigen with Grb2 and the Sos/Ras exchange protein. Cancer Res 1995;55:4000-4003.

41. Pendergast AM, Quilliam LA, Cripe LD, et al. BCR-ABL-induced oncogenesis is mediated by direct interaction with the SH2 domain of the GRB-2 adaptor protein. Cell 1993;75:175-185.

42. Puil L, Liu J, Gish G, et al. Bcr-Abl oncoproteins bind directly to activators of the Ras signalling pathway. EMBO J 1994;13:764-773.

43. Wu Y, Ma G, Lu D, et al. Bcr: a negative regulator of the Bcr-Abl oncoprotein. Oncogene 1999;18:4416-4424.

44. Arlinghaus RB. Bcr: a negative regulator of the Bcr-Abl oncoprotein in leukemia. Oncogene 2002;21:8560-8567.

45. Li Y, Ren J, Yu W-H, et al. The EGF receptor regulates interaction of the human DF3/MUC1 carcinoma antigen with c-Src and β-catenin. J Biol Chem 2001;276:35239-35242.

46. Li Y, Yu W-H, Ren J, et al. Heregulin targets γ-catenin to the nucleolus by a mechanism dependent on the DF3/MUC1 protein. Mol Cancer Res 2003;1:765-775.

47. Ren J, Raina D, Chen W, et al. MUC1 oncoprotein functions in activation of fibroblast growth factor receptor signaling. Mol Cancer Res 2006;4:873-883.

48. Wei X, Xu H, Kufe D. MUC1 oncoprotein stabilizes and activates estrogen receptor alpha. Mol Cell 2006;21:295-305.

49. Shiotsu Y, Neckers LM, Wortman I, et al. Novel oxime derivatives of radicicol induce erythroid differentiation associated with preferential G(1) phase accumulation against chronic myelogenous leukemia cells through destabilization of Bcr-Abl with Hsp90 complex. Blood 2000;96:2284-2291.

50. Gorre ME, Ellwood-Yen K, Chiosis G, Rosen N, Sawyers CL. BCR-ABL point mutants isolated from patients with imatinib mesylate-resistant chronic myeloid leukemia remain sensitive to inhibitors of the BCR-ABL chaperone heat shock protein 90. Blood 2002;100:3041-3044.

51. Guo F, Rocha K, Bali P, et al. Abrogation of heat shock protein 70 induction as a strategy to increase antileukemia activity of heat shock protein 90 inhibitor 17-allylamino-demethoxy geldanamycin. Cancer Res 2005;65:10536-10544.

52. Coluccia AM, Vacca A, Dunach M, et al. Bcr-Abl stabilizes beta-catenin in chronic myeloid leukemia through its tyrosine

phosphorylation. EMBO J 2007;26:1456-1466.

53. Yin L, Kharbanda S, Kufe D. Mucin 1 oncoprotein blocks hypoxia-inducible factor 1alpha activation in a survival response to hypoxia. J Biol Chem 2007;282:257-266.

Figure Legends

Figure 1. MUC1-C associates with Bcr-Abl in CML cells. A. Lysates from K562 and KU812 cells were immunoblotted with the indicated antibodies. **B.** Lysates were subjected to immunoprecipitation (IP) with a control hamster IgG or anti-MUC1-C. The precipitates and whole cell lysate (WCL) not subjected to immunoprecipitation were immunoblotted with the indicated antibodies. **C.** Lysates were subjected to immunoprecipitation with a control mouse IgG, anti-Bcr or anti-Abl. The precipitates and WCL were immunoblotted with the indicated antibodies. **D.** Amino acid sequence of MUC1-CD (upper panel). Phosphorylation sites and β-catenin binding site are highlighted. Lysates were incubated with GST or the indicated GST-MUC1-CD fusion proteins (lower panel). The adsorbates were immunoblotted with the indicated antibodies. WCL was included as a control.

Figure 2. MUC1-CD binds directly to Bcr. A. Lysates from BC-1 cells were precipitated with control mouse IgG, anti-Bcr(N-20) or anti-Bcr(C-20). The precipitates were immunoblotted with the indicated antibodies. **B.** Lysate from BC-1 cells was incubated with GST or GST-MUC1-CD. The adsorbates were immunoblotted with the indicated antibodies. WCL was included as a control. **C and D.** Purified His-MUC1-CD was incubated with GST or the indicated GST-Bcr fusion proteins (C). His-Bcr(1-426) was incubated with GST or the indicated GST-MUC1-CD fusion proteins (D). The adsorbates were immunoblotted with anti-His.

Figure 3. MUC1 stabilizes Bcr-Abl. A. Lysates from the indicated K562/CsiRNA and K562/MUC1siRNA cells were immunoblotted with anti-MUC1-C, anti-Bcr and anti-β-actin (left). Cytosolic and nuclear fractions from the indicated cells were immunoblotted with anti-Bcr (right). Purity and equal loading of the fractions was monitored by immunoblot analysis with antibodies against the cytoplasmic IκBα and nuclear lamin B proteins. **B.** Whole cell lysates (left) and cytosolic or nuclear fractions (right) from the indicated KU812 cells were immunoblotted with the indicated antibodies. **C and D.** The indicated K562 (C) or KU812 (D) cells were pulsed with [^{35}S]-methionine and chased for the indicated times. Anti-Bcr precipitates were subjected to SDS-PAGE and autoradiography (left, upper panel) or immunoblotting with anti-Bcr (left, lower panel). Intensity of the Bcr-Abl signals was determined by scanning densitometry and is expressed as the percentage of Bcr-Abl remaining compared to that obtained at 0 h (right).

Figure 4. Silencing MUC1 decreases self-renewal capacity. A. The indicated cells grown for 28 days in methylcellulose supplemented with 10% (upper) or 2% (lower) FBS. **B and C.** Colony number was determined for the indicated K562 cells cultured in 10% (B) or 2% (C) FBS and expressed as the mean±SD of three determinations. Statistical significance was determined by the Student's t-test. **D.** Colony number was determined for the indicated KU812 cells after incubation for 28 days in methylcellulose supplemented with 10% FBS.

Figure 5. Silencing MUC1 is associated with a differentiated erythroid phenotype. **A.** Photomicrographs of the indicated K562 cells stained with benzidine. **B.** The results are expressed as the percentage benzidine positive cells obtained from three separate experiments (mean±SD). **C.** K562 cells were infected with adenoviruses expressing the control CsiRNA, MUC1siRNA#1 or MUC1siRNA#2. Lysates were immunoblotted with the indicated antibodies. **D.** The infected K562 cells were stained with benzidine. The results are expressed as the percentage benzidine positive cells obtained from three separate experiments (mean±SD).

Figure 6. MUC1 blocks differentiation of primary CML cells. **A.** Mononuclear cells isolated from the bone marrow of patient 1 with CML in blast crisis were stained with anti-MUC1-N (upper panels) and analyzed by FISH with probes for Bcr (green) and Abl (red) (lower panels). The Bcr-Abl fusion gene was detectable in MUC1 positive cells. **B.** Mononuclear cells isolated from patient 1 as above and from the bone marrow of patient 2 with CML in blast crisis were cultured for 7 d. The samples contained over 80% blasts as determined by May-Giemsa staining (not shown). The primary CML blasts were infected with adenoviruses expressing CsiRNA, MUC1siRNA#1 or MUC1siRNA#2. At 120 h after infection, the cells were stained with Hoechst dye (upper panels) or anti-MUC1-C (lower panels). **C.** Photomicrographs of the indicated primary CML blasts stained with benzidine. **D.** The results are expressed as

the percentage of benzidine positive cells (mean±SD) obtained from three separate experiments.

Supplemental Figure Legends.

Supplemental Figure S1. MUC1 has no apparent effect on Bcr-Abl mRNA levels. Bcr-Abl, MUC1-C and β-actin mRNA levels were determined for the indicated cells by RT-PCR.

Supplemental Figure S2. Effects of MUC1 on proliferation of K562 and KU812 cells. A. Growth of K562/CsiRNA (●,▲) and K562/MUC1siRNA (○,△) cells in 10% FBS (left) and 2% FBS (right) was determined by trypan blue staining and counting at the indicated times after seeding. **B.** Growth of KU812/CsiRNA (●) and KU812/MUC1siRNA (○,△) cells in 10% FBS (left) and 2% FBS (right) at the indicated times after seeding.

Supplemental Figure S3. Silencing MUC1 is associated with erythroid differentiation of KU812 cells. Photomicrographs of the KU812 cells stained with benzidine.

Supplemental Figure S4. Silencing MUC1 increases sensitivity to imatinib. A and B. The indicated K562 (A) and KU812 (B) cells were treated with imatinib for 48 h, stained with propidium iodide and monitored for sub-G1 content by FACS analysis. **C.** The results are expressed as the percentage apoptosis (mean±SD for three independent experiments).

Supplemental Figure S5. MUC1 blocks imatinib-induced apoptosis of primary CML cells. A. Primary CML blasts infected with the indicated adenoviruses were left untreated or

treated with 50 nM imatinib for 48. The cells were stained with Hoechst dye. **B.** The percentage apoptosis as determined by scoring cells with condensed and fragmented nuclei is expressed as the mean$\pm$SD of three experiments.

Fig. 1AB

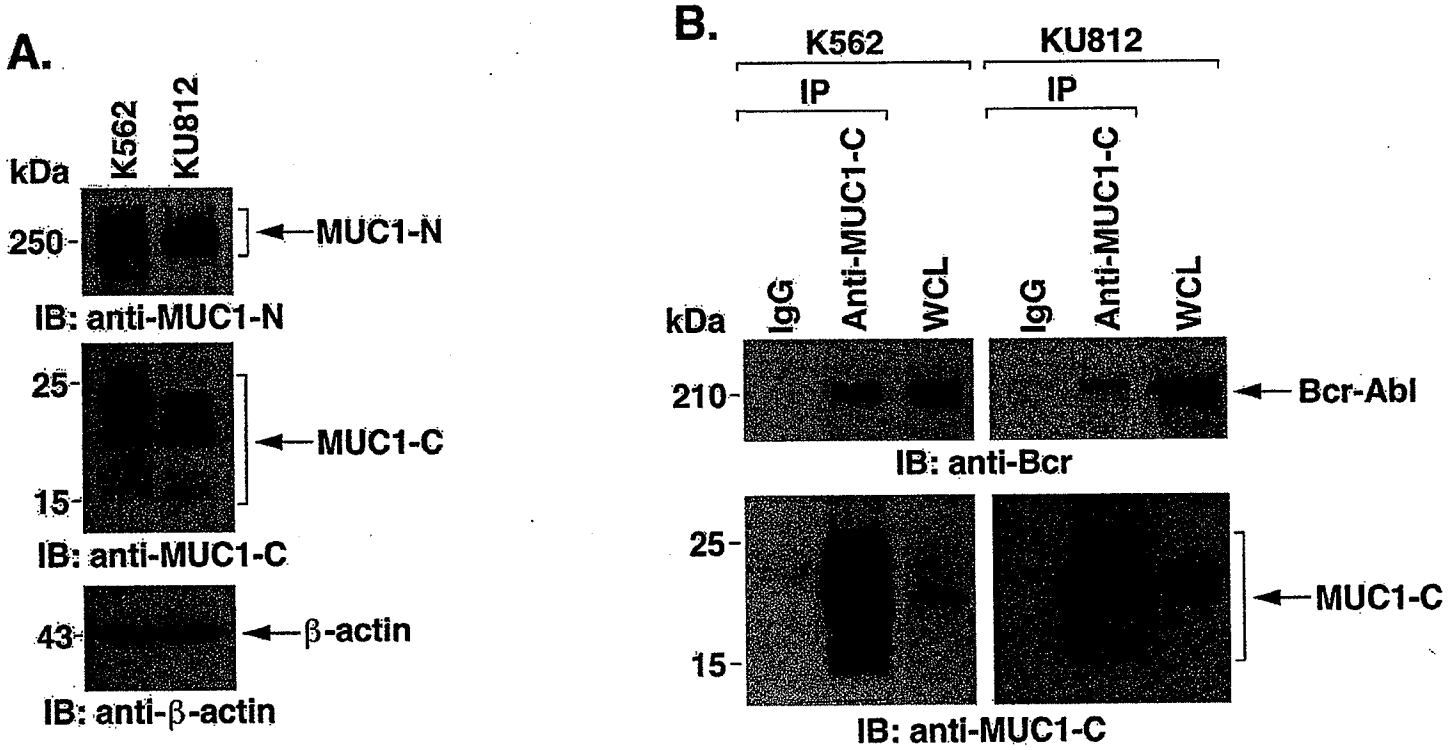
A.
K562
KU812
kDa
250
MUC1-N
IB: anti-MUC1-N
25
15
MUC1-C
IB: anti-MUC1-C
43
β-actin
IB: anti-β-actin
B.
K562
KU812
IP
IP
Anti-MUC1-C
Anti-MUC1-C
IgG
WCL
IgG
WCL
kDa
210
Bcr-Abl
IB: anti-Bcr
25
15
MUC1-C
IB: anti-MUC1-C

Fig. 1C

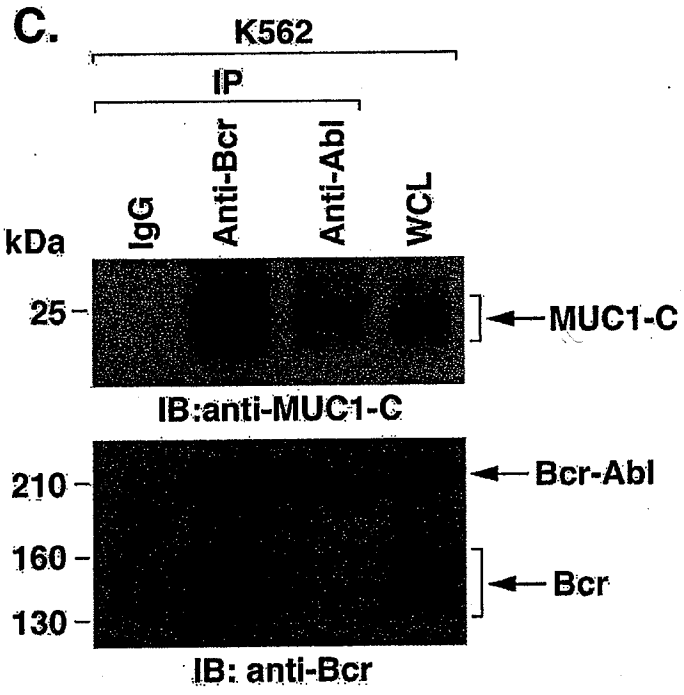
C.
K562
IP
IgG
Anti-Bcr
Anti-Abl
WCL
kDa
25
MUC1-C
IB:anti-MUC1-C
210
160
130
Bcr-Abl
Bcr
IB: anti-Bcr

Fig. 1D

D.

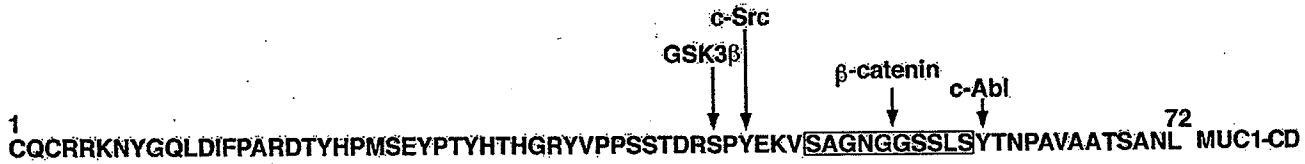
c-Src
GSK3β
β-catenin
c-Abl
1
CQCRRKNYGQLDIFPARDTYHPMSEYPTYHTHGRYVPPSSTDRSPYEKVSAGNGGSSLSYTNPAVAATSANL
72
MUC1-CD

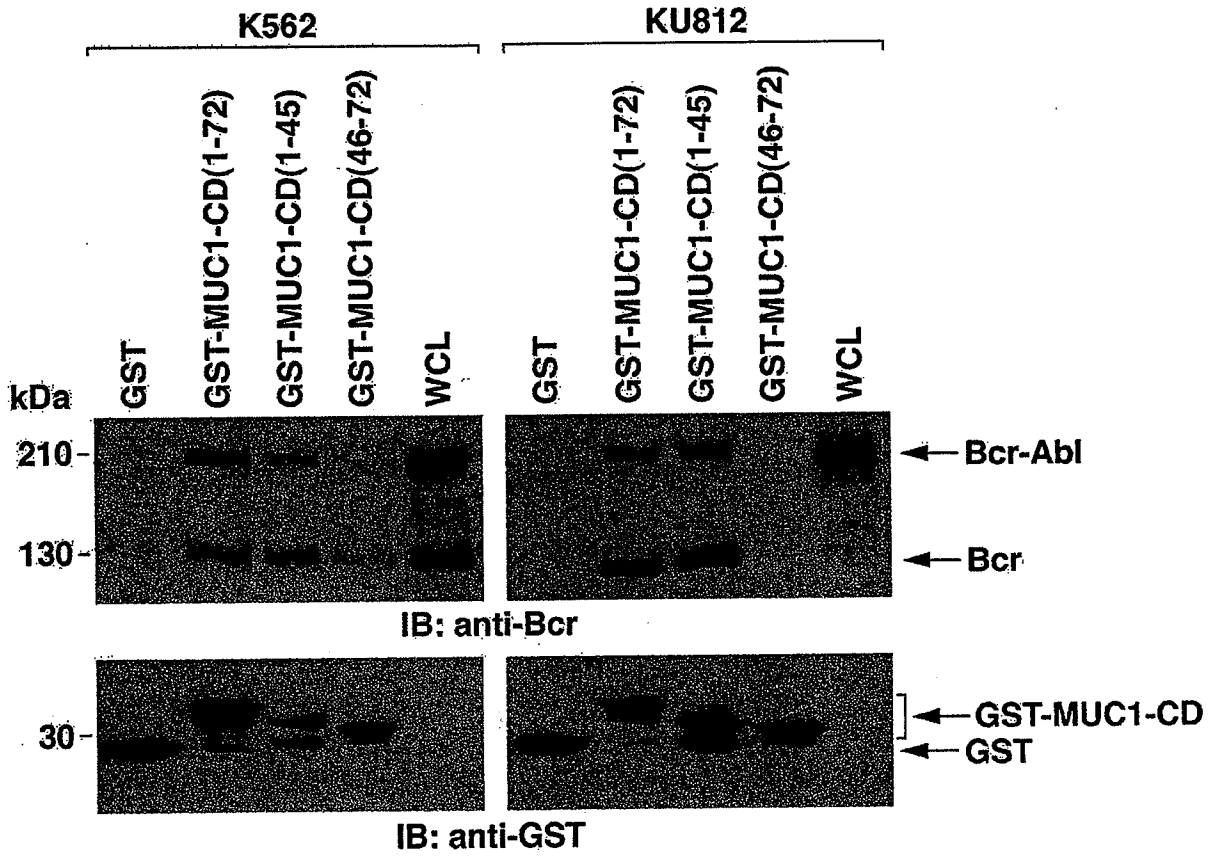
K562
KU812
GST
GST-MUC1-CD(1-72)
GST-MUC1-CD(1-45)
GST-MUC1-CD(46-72)
WCL
kDa
210
130
Bcr-Abl
Bcr
IB: anti-Bcr
30
GST-MUC1-CD
GST
IB: anti-GST

Fig. 2AB

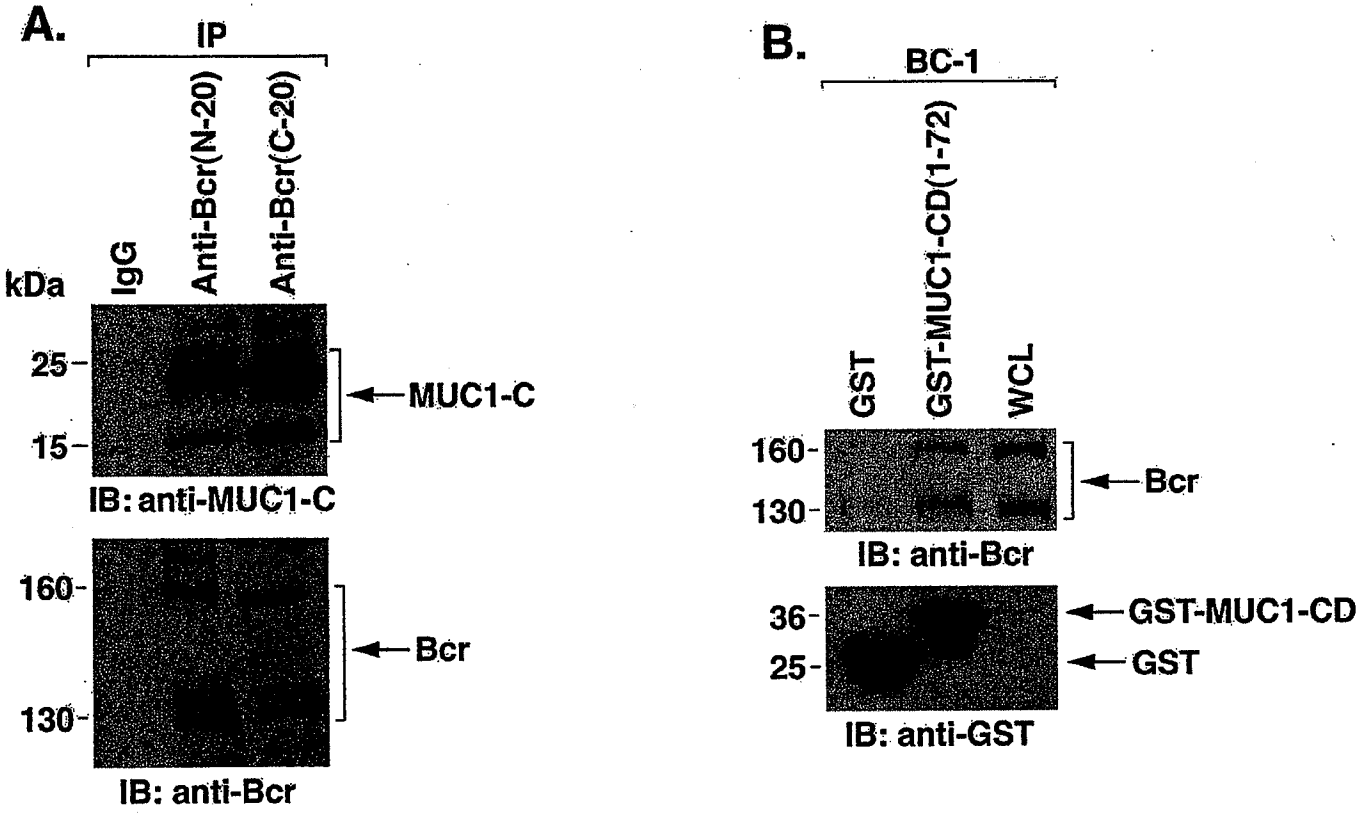
A.
IP
Anti-Bcr(N-20)
Anti-Bcr(C-20)
IgG
kDa
25
15
MUC1-C
IB: anti-MUC1-C
160
130
Bcr
IB: anti-Bcr
B.
BC-1
GST-MUC1-CD(1-72)
GST
WCL
160
130
Bcr
IB: anti-Bcr
36
25
GST-MUC1-CD
GST
IB: anti-GST

Fig. 2CD

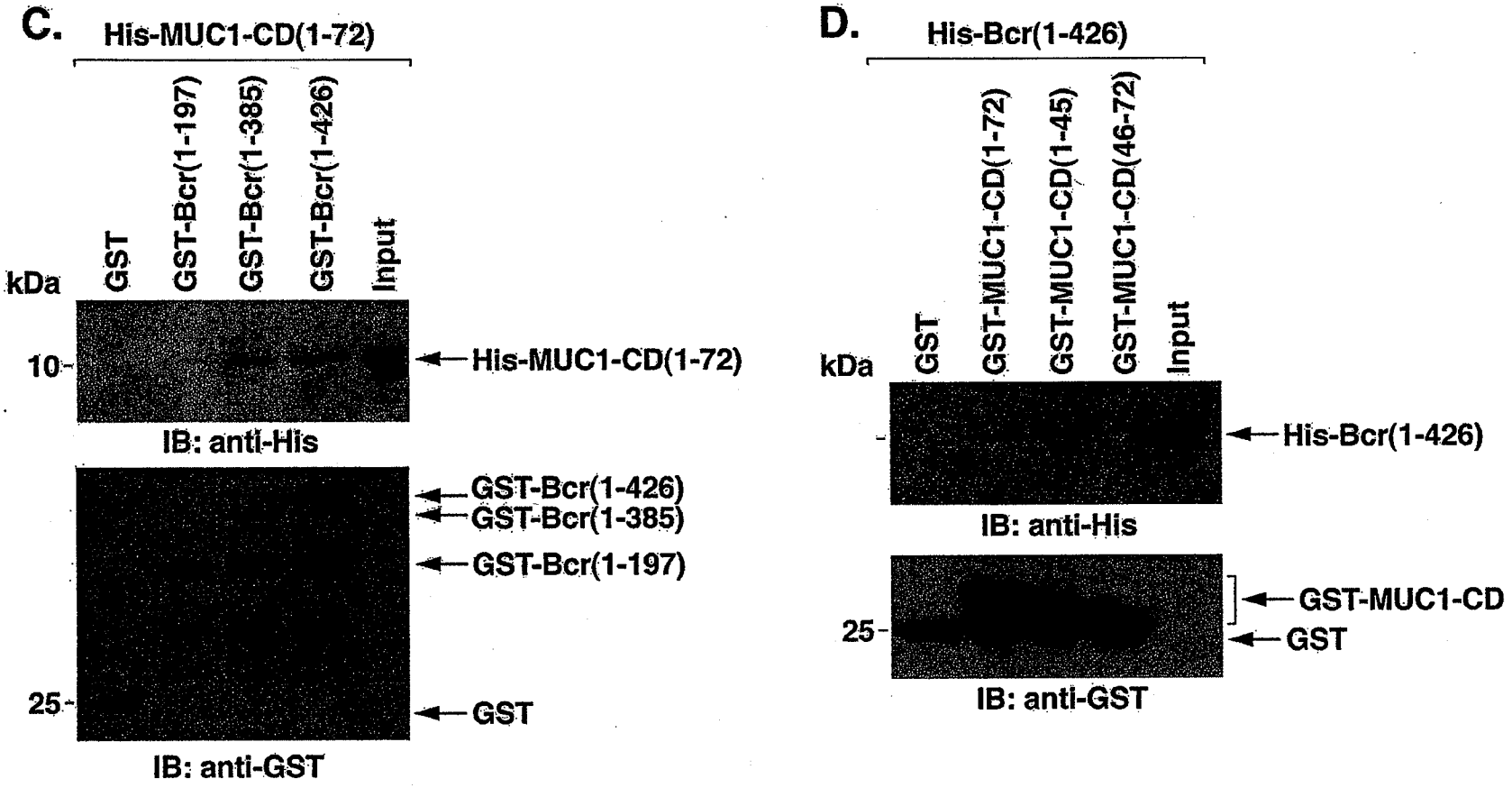
C.
His-MUC1-CD(1-72)
GST
GST-Bcr(1-197)
GST-Bcr(1-385)
GST-Bcr(1-426)
Input
kDa
10
His-MUC1-CD(1-72)
IB: anti-His
GST-Bcr(1-426)
GST-Bcr(1-385)
GST-Bcr(1-197)
25
GST
IB: anti-GST
D.
His-Bcr(1-426)
GST
GST-MUC1-CD(1-72)
GST-MUC1-CD(1-45)
GST-MUC1-CD(46-72)
Input
kDa
His-Bcr(1-426)
IB: anti-His
GST-MUC1-CD
25
GST
IB: anti-GST

Fig. 3A

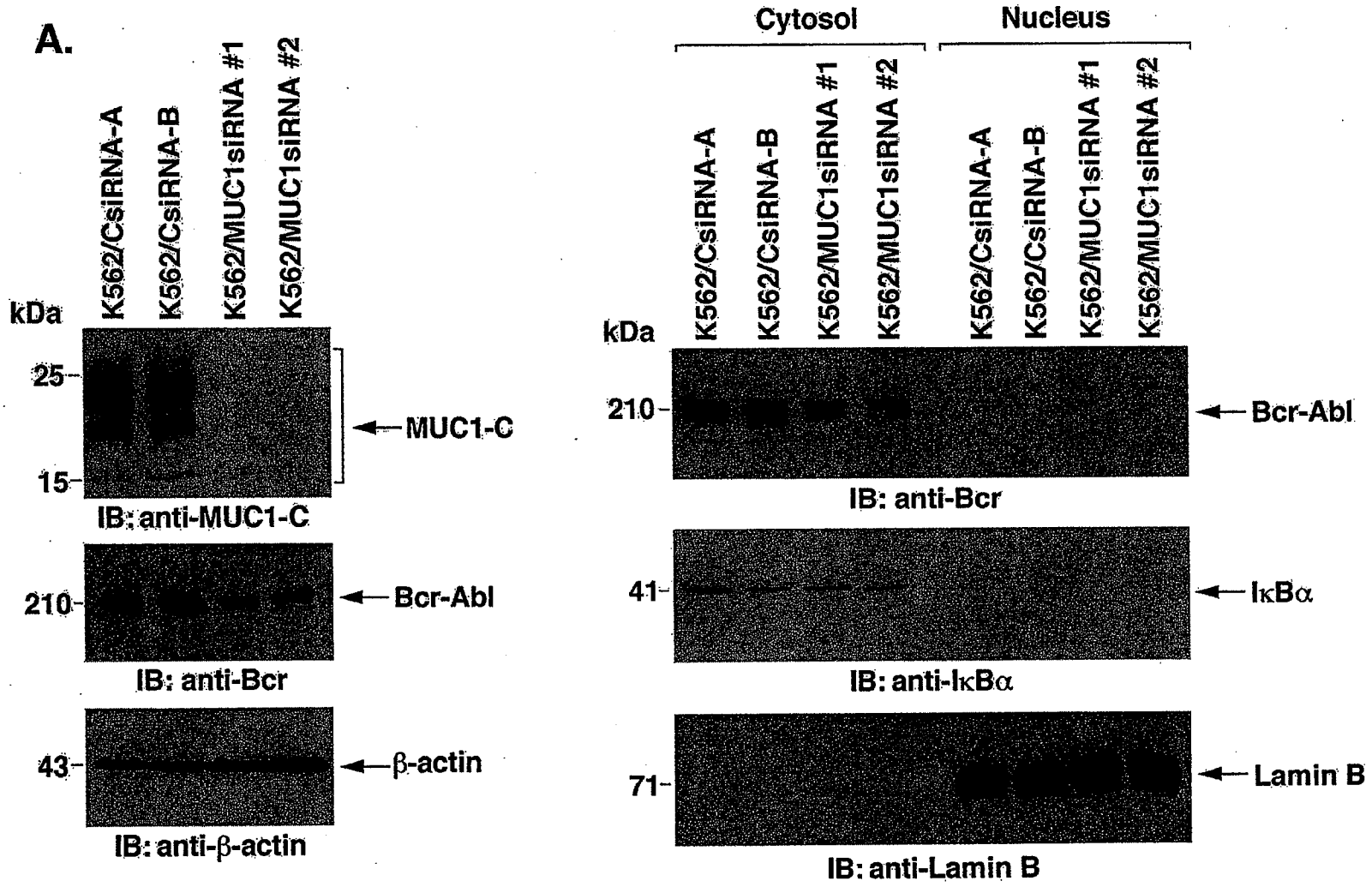
A.
K562/CsiRNA-A
K562/CsiRNA-B
K562/MUC1siRNA #1
K562/MUC1siRNA #2
kDa
25
15
MUC1-C
IB: anti-MUC1-C
210
Bcr-Abl
IB: anti-Bcr
43
β-actin
IB: anti-β-actin
Cytosol
Nucleus
K562/CsiRNA-A
K562/CsiRNA-B
K562/MUC1siRNA #1
K562/MUC1siRNA #2
K562/CsiRNA-A
K562/CsiRNA-B
K562/MUC1siRNA #1
K562/MUC1siRNA #2
kDa
210
Bcr-Abl
IB: anti-Bcr
41
IκBα
IB: anti-IκBα
71
Lamin B
IB: anti-Lamin B

Fig. 3B

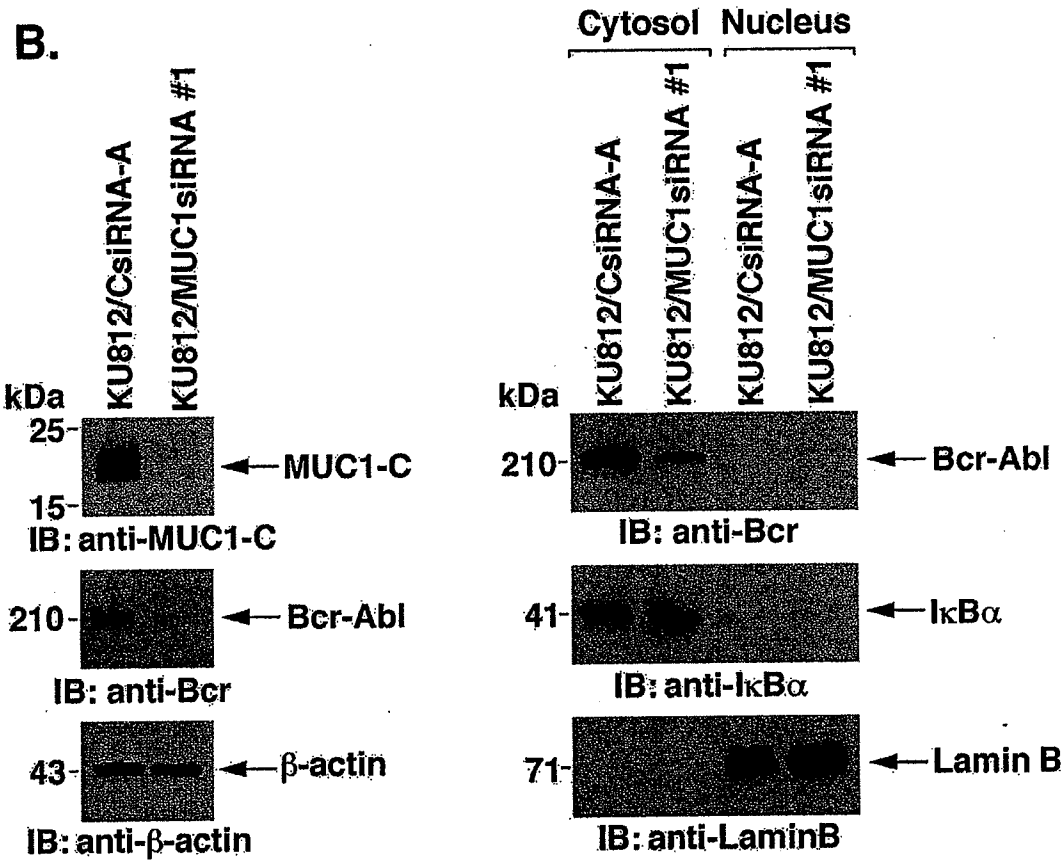
B.
KU812/CsiRNA-A
KU812/MUC1siRNA #1
kDa
25-
15-
MUC1-C
IB: anti-MUC1-C
210-
Bcr-Abl
IB: anti-Bcr
43-
β-actin
IB: anti-β-actin
Cytosol
Nucleus
KU812/CsiRNA-A
KU812/MUC1siRNA #1
KU812/CsiRNA-A
KU812/MUC1siRNA #1
kDa
210-
Bcr-Abl
IB: anti-Bcr
41-
IκBα
IB: anti-IκBα
71-
Lamin B
IB: anti-LaminB

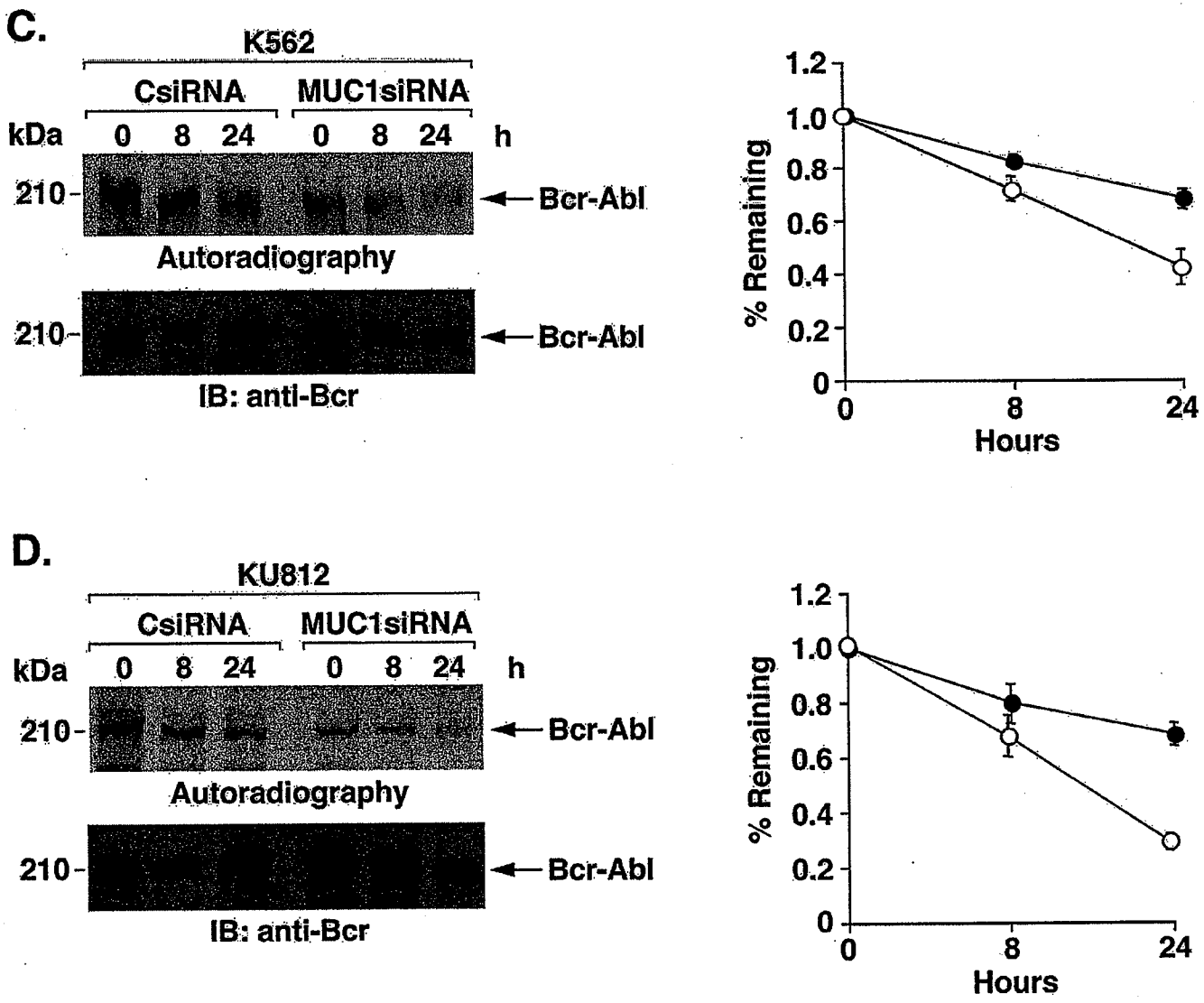
C.
K562
CsiRNA
MUC1siRNA
kDa
0 8 24 0 8 24 h
210
Bcr-Abl
Autoradiography
210
Bcr-Abl
IB: anti-Bcr
% Remaining
1.2
1.0
0.8
0.6
0.4
0.2
0
0 8 24
Hours
D.
KU812
CsiRNA
MUC1siRNA
kDa
0 8 24 0 8 24 h
210
Bcr-Abl
Autoradiography
210
Bcr-Abl
IB: anti-Bcr
% Remaining
1.2
1.0
0.8
0.6
0.4
0.2
0
0 8 24
Hours

Fig. 4A

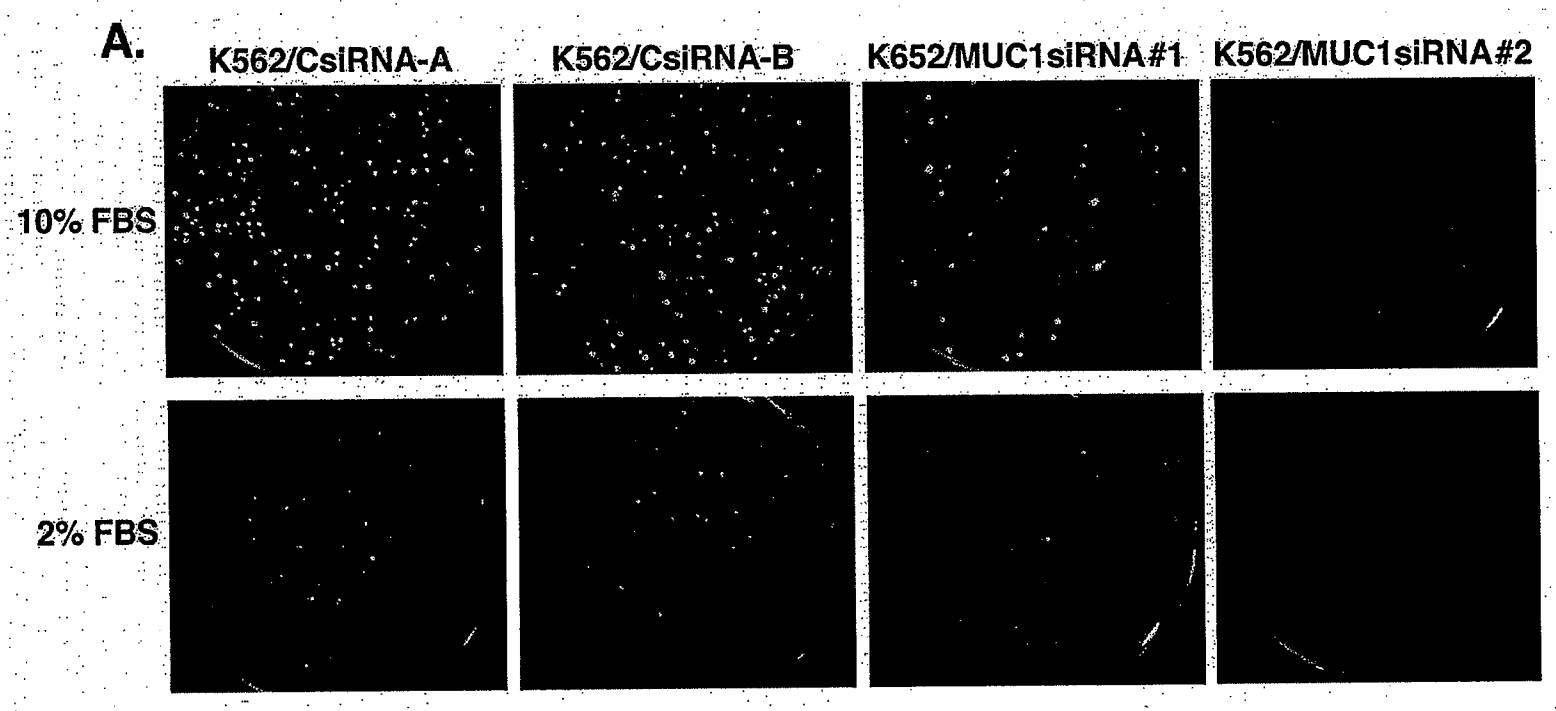
A.
K562/CsiRNA-A
K562/CsiRNA-B
K652/MUC1siRNA#1
K562/MUC1siRNA#2
10% FBS
2% FBS

Fig. 4BC

B. K562

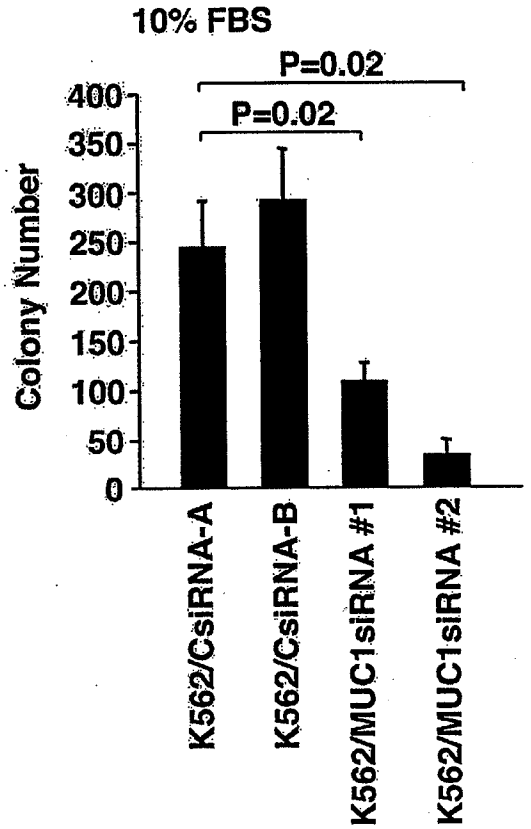

C. K562

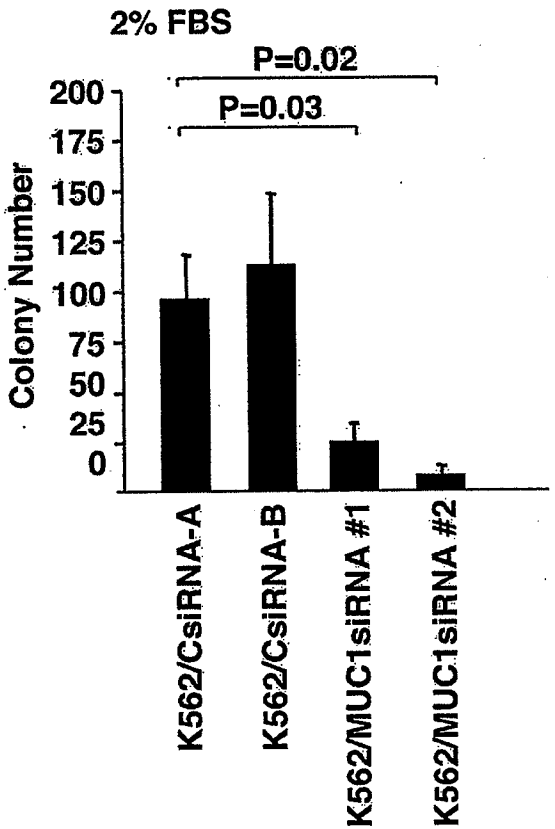

Fig. 4D

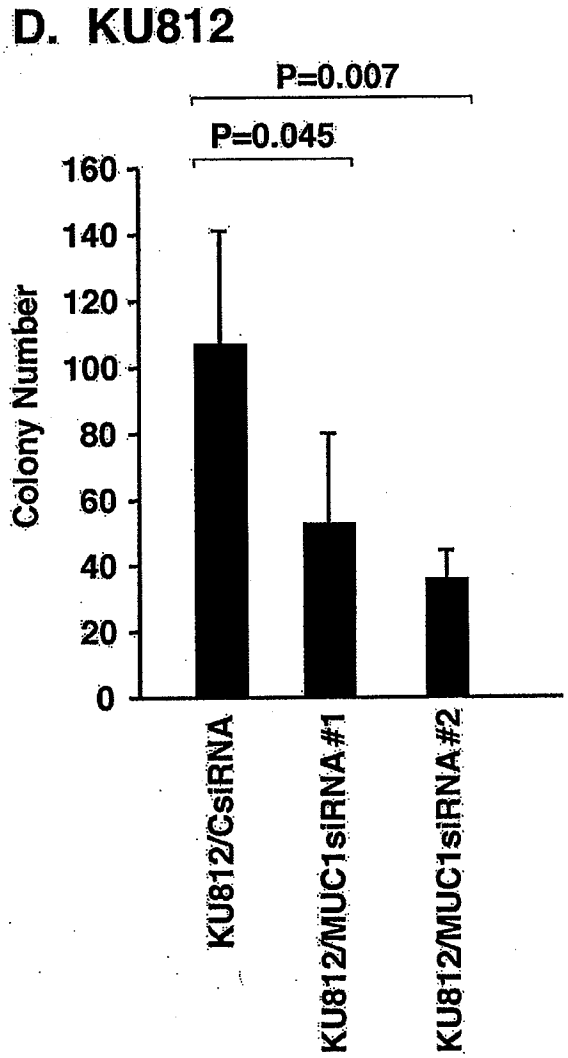
D. KU812
P=0.007
P=0.045
Colony Number
160
140
120
100
80
60
40
20
0
KU812/CsiRNA
KU812/MUC1siRNA#1
KU812/MUC1siRNA#2

Fig. 5A

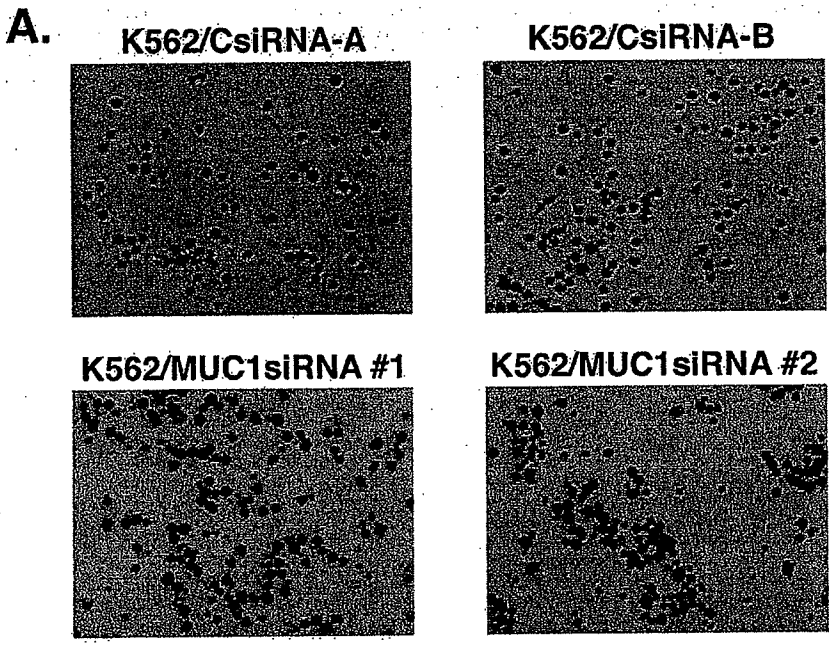
A.
K562/CsiRNA-A
K562/CsiRNA-B
K562/MUC1siRNA #1
K562/MUC1siRNA #2

Fig. 5BC

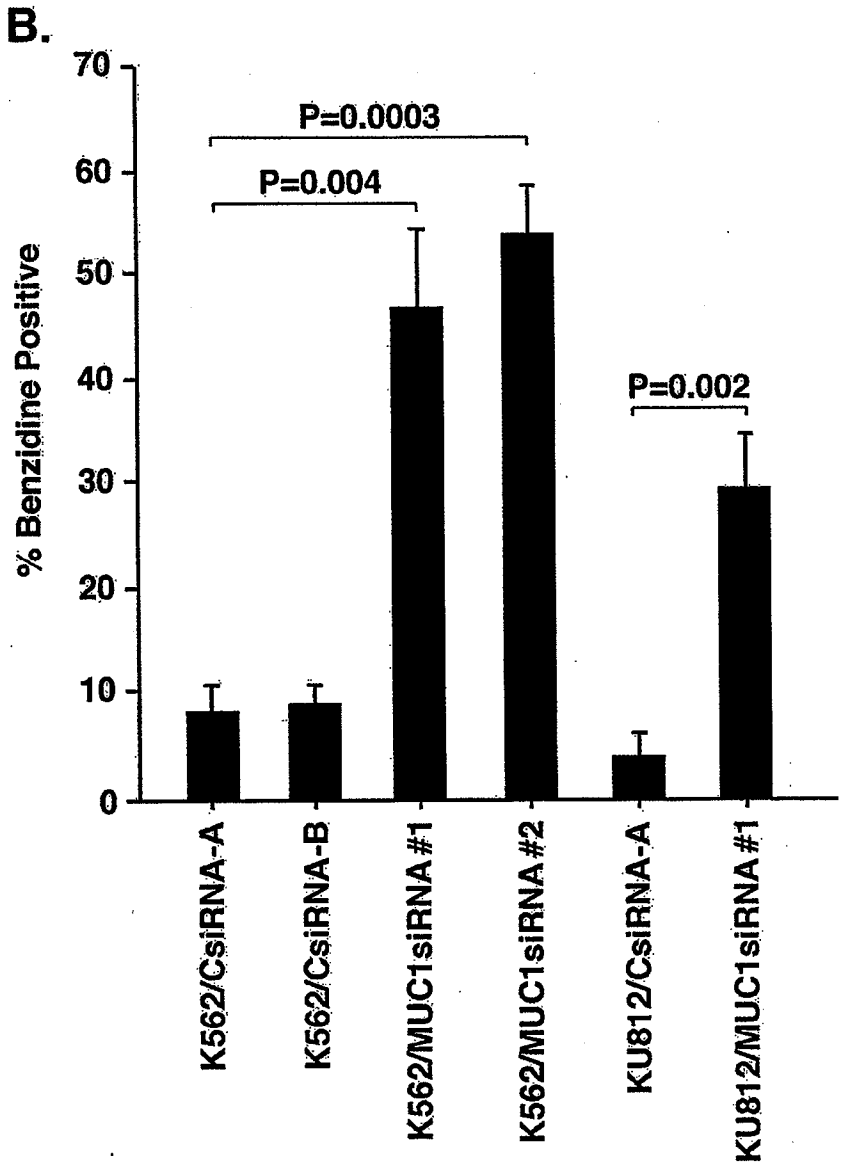
B.
% Benzidine Positive
70
60
50
40
30
20
10
0
P=0.0003
P=0.004
P=0.002
K562/CsiRNA-A
K562/CsiRNA-B
K562/MUC1siRNA #1
K562/MUC1siRNA #2
KU812/CsiRNA-A
KU812/MUC1siRNA #1

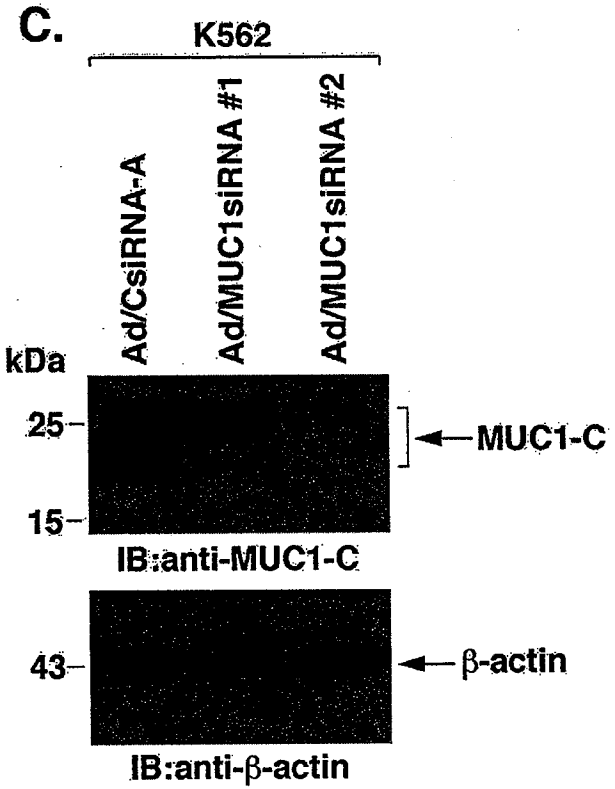
C.
K562
Ad/CsiRNA-A
Ad/MUC1siRNA #1
Ad/MUC1siRNA #2
kDa
25
15
MUC1-C
IB:anti-MUC1-C
43
β-actin
IB:anti-β-actin

Fig. 5D

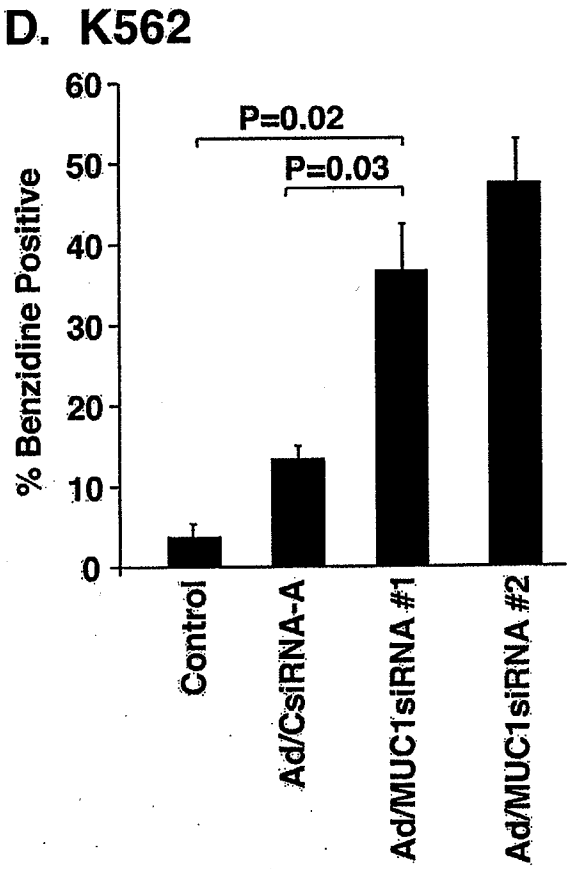
D. K562
% Benzidine Positive
60
50
40
30
20
10
0
P=0.02
P=0.03
Control
Ad/CsiRNA-A
Ad/MUC1siRNA #1
Ad/MUC1siRNA #2

Fig. 6A

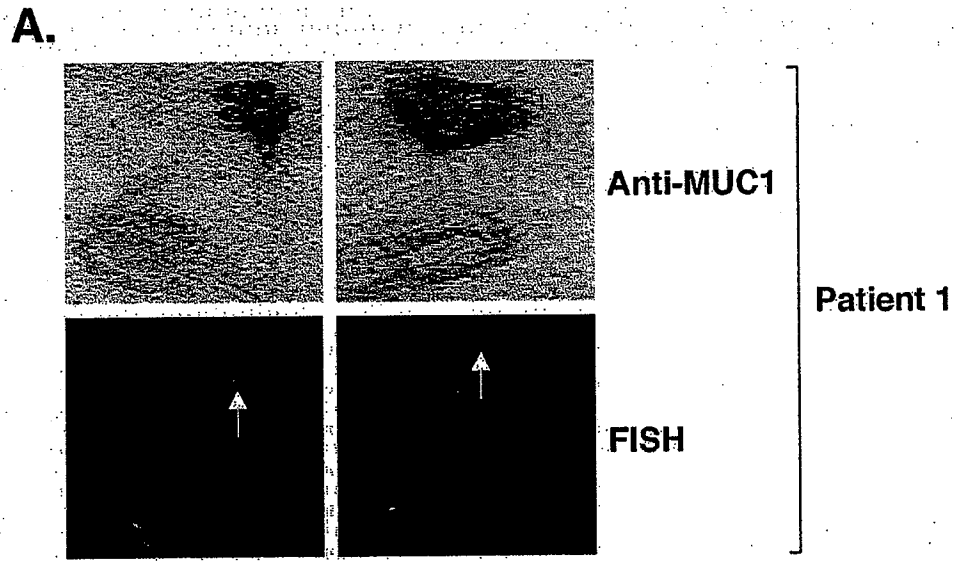

Fig. 6B

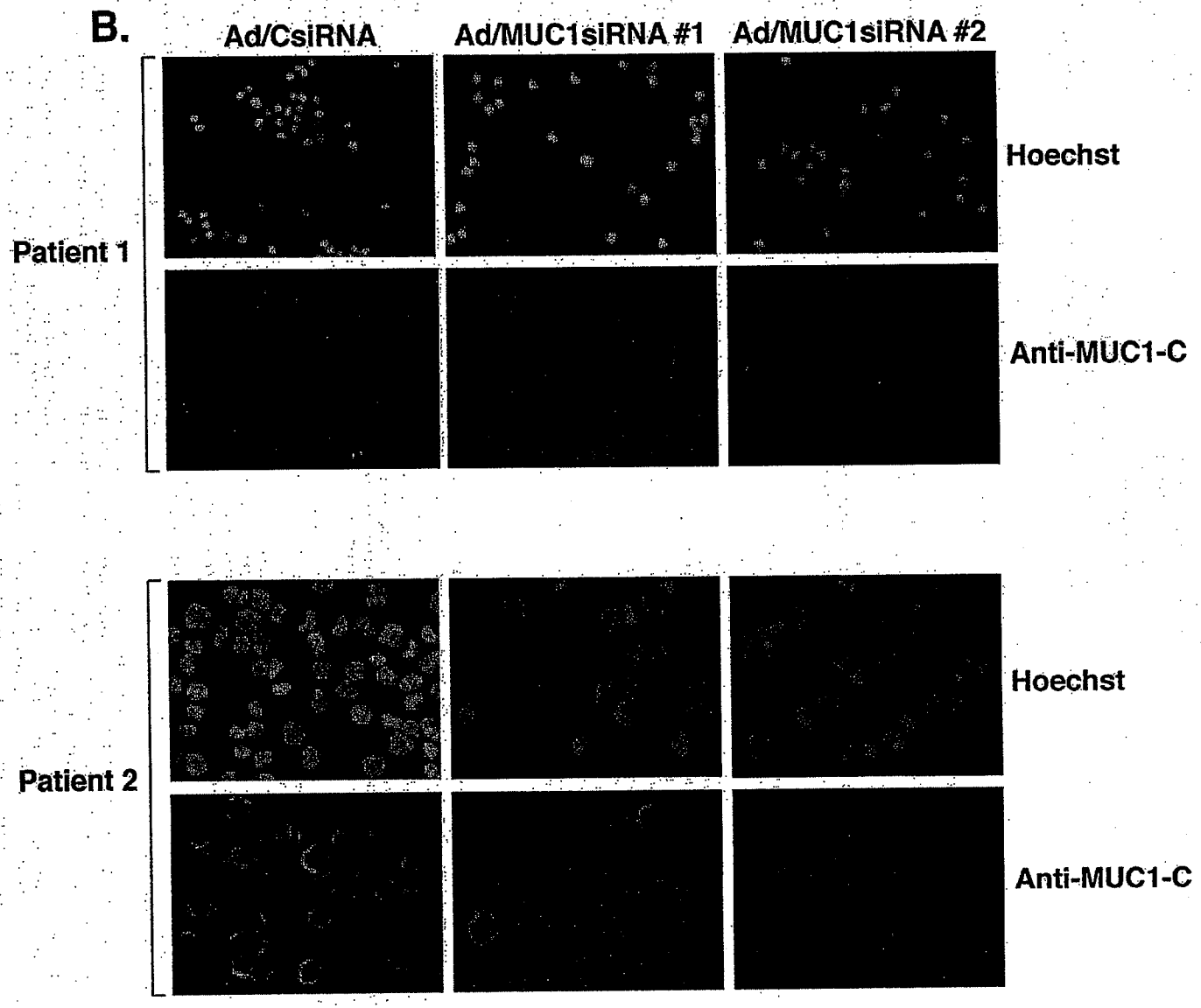
B.
Ad/CsiRNA
Ad/MUC1siRNA #1
Ad/MUC1siRNA #2
Patient 1
Hoechst
Anti-MUC1-C
Patient 2
Hoechst
Anti-MUC1-C

Fig. 6CD

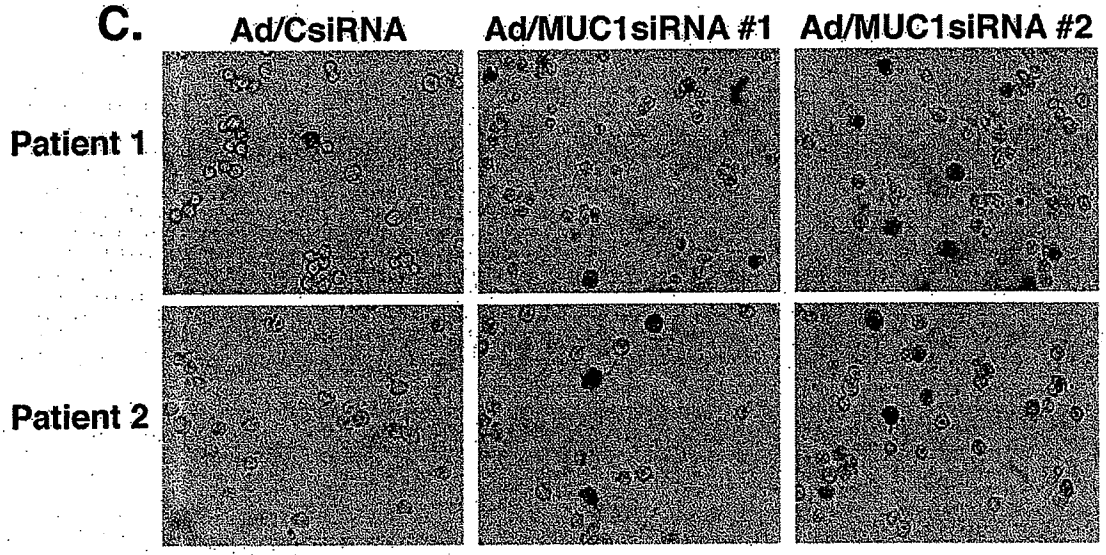
C.
Ad/CsiRNA
Ad/MUC1siRNA #1
Ad/MUC1siRNA #2
Patient 1
Patient 2

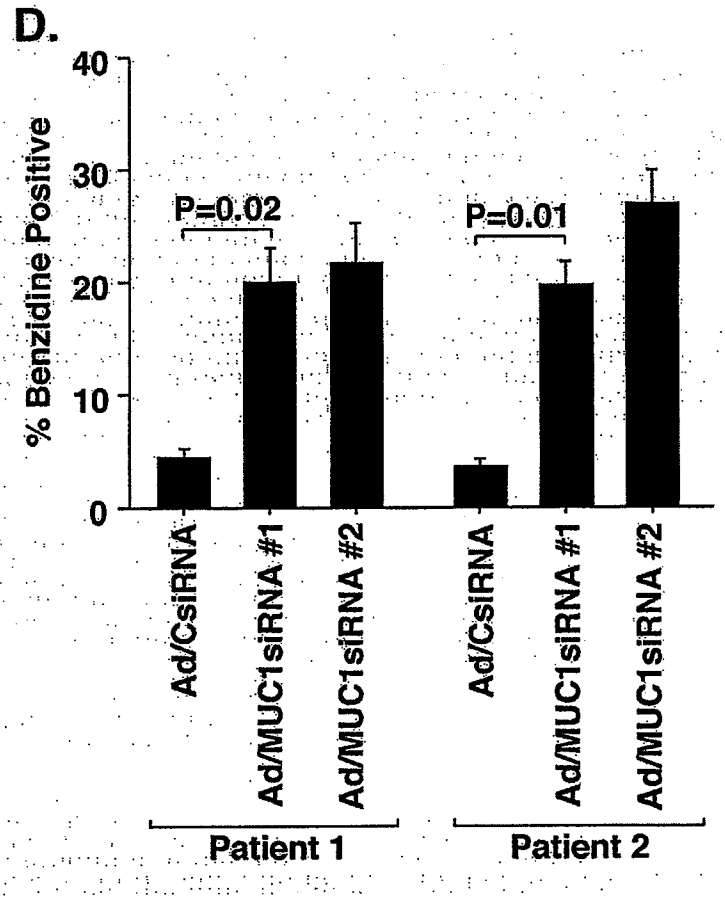
D.
% Benzidine Positive
40
30
20
10
0
P=0.02
P=0.01
Ad/CsiRNA
Ad/MUC1siRNA #1
Ad/MUC1siRNA #2
Ad/CsiRNA
Ad/MUC1siRNA #1
Ad/MUC1siRNA #2
Patient 1
Patient 2

Fig. S1

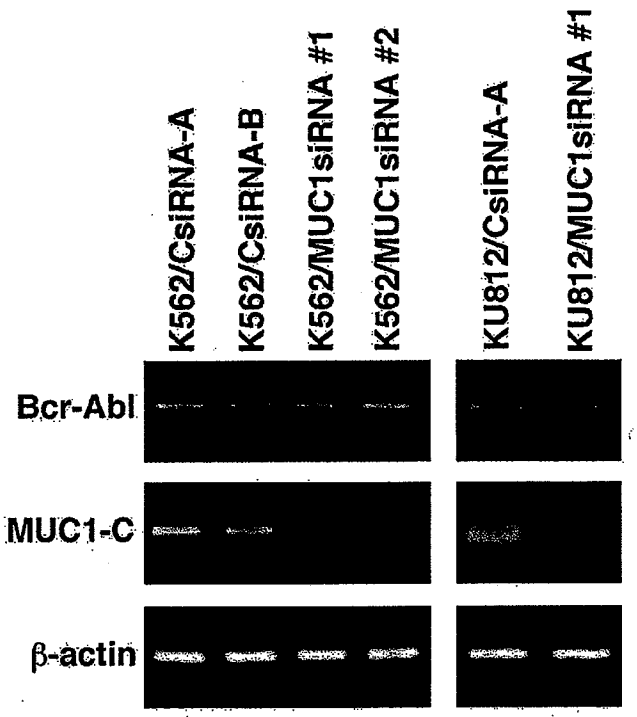
K562/CsiRNA-A
K562/CsiRNA-B
K562/MUC1siRNA #1
K562/MUC1siRNA #2
KU812/CsiRNA-A
KU812/MUC1siRNA #1
Bcr-Abl
MUC1-C
β-actin

Fig. S2A

A. K562

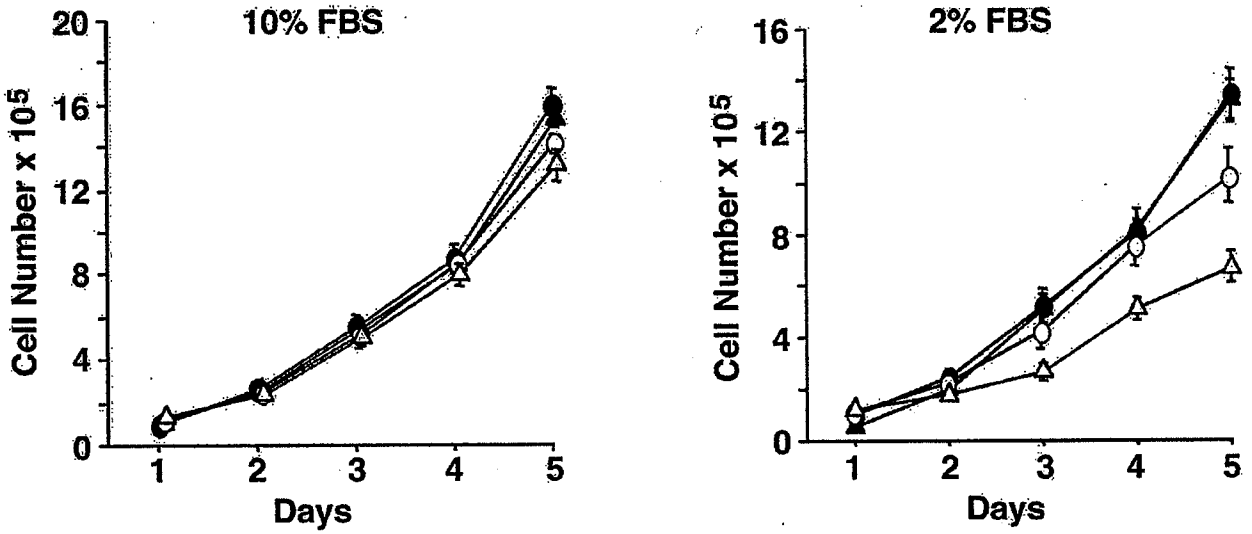

Fig. S2B

B. KU812

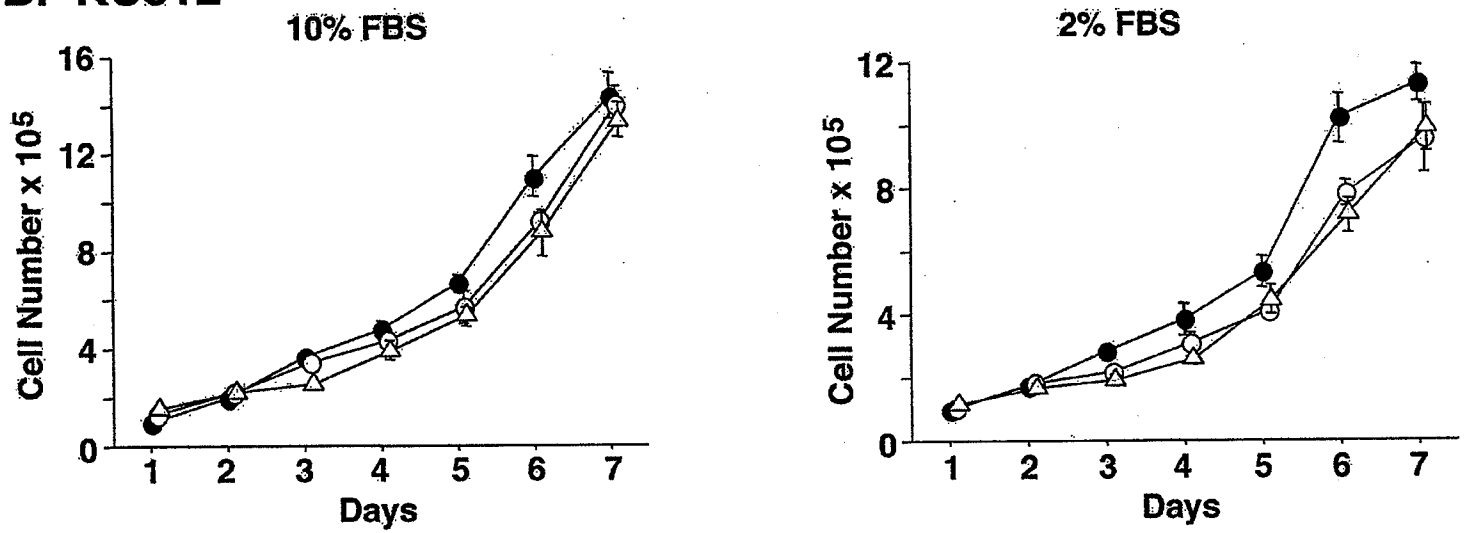

Fig. S3

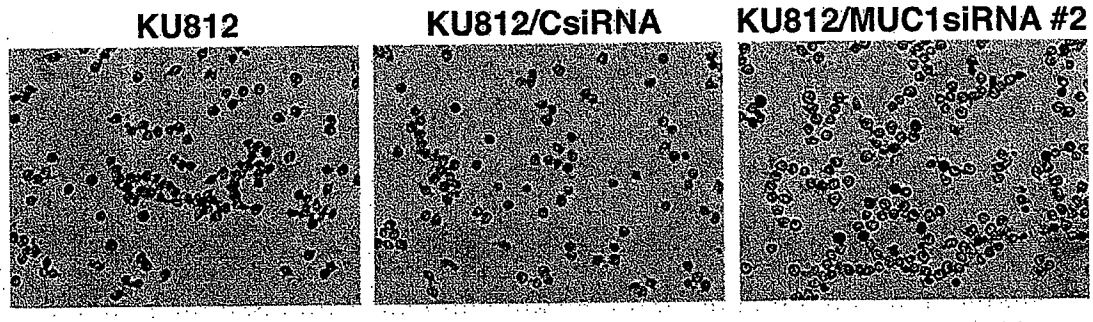

Fig. S4A

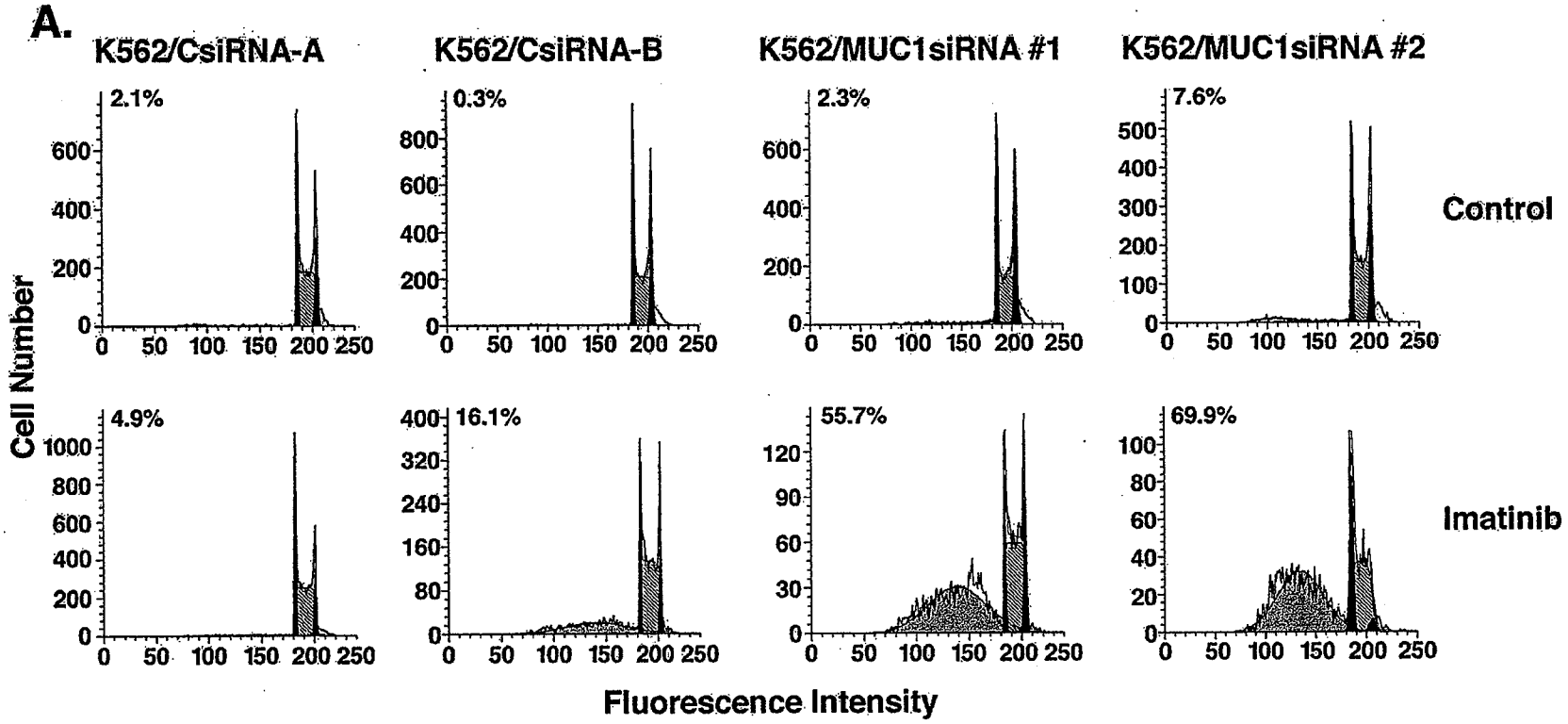
A.
K562/CsiRNA-A
K562/CsiRNA-B
K562/MUC1siRNA #1
K562/MUC1siRNA #2
2.1%
0.3%
2.3%
7.6%
4.9%
16.1%
55.7%
69.9%
Control
Imatinib
Cell Number
Fluorescence Intensity

Fig. S4B

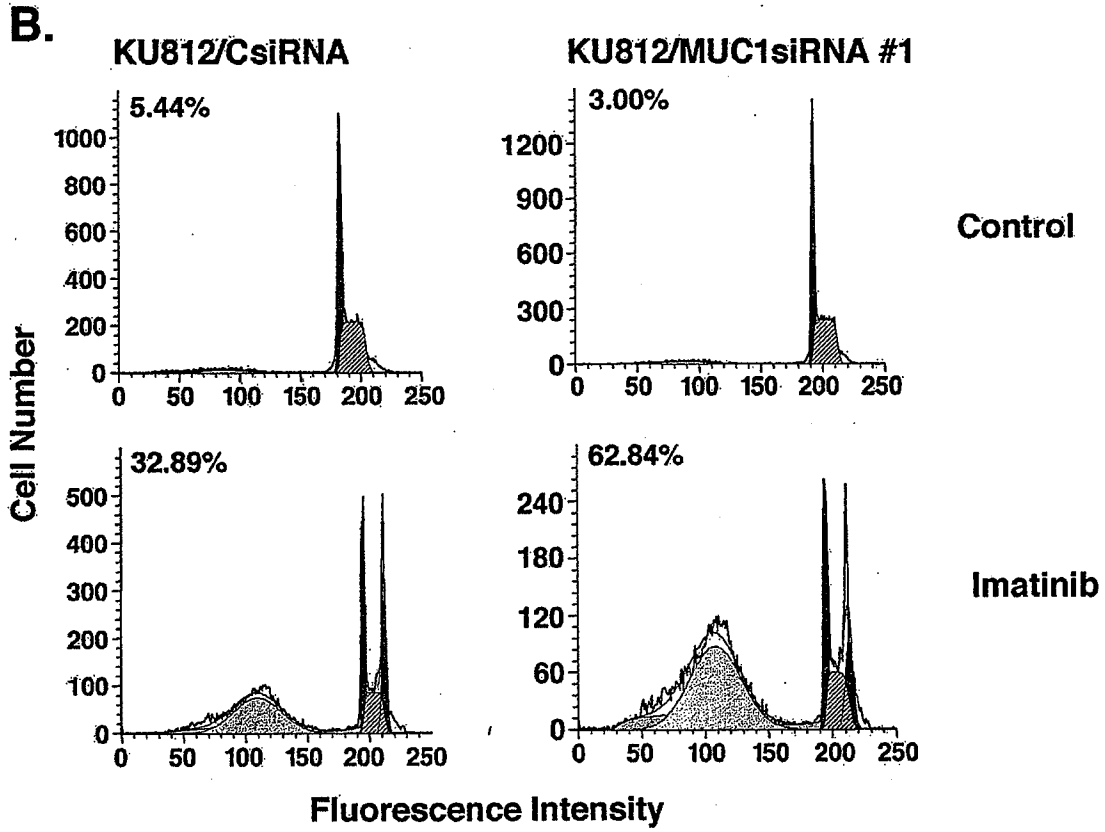
B.
KU812/CsiRNA
KU812/MUC1siRNA #1
5.44%
3.00%
32.89%
62.84%
Control
Imatinib
Cell Number
Fluorescence Intensity

Fig. S4C

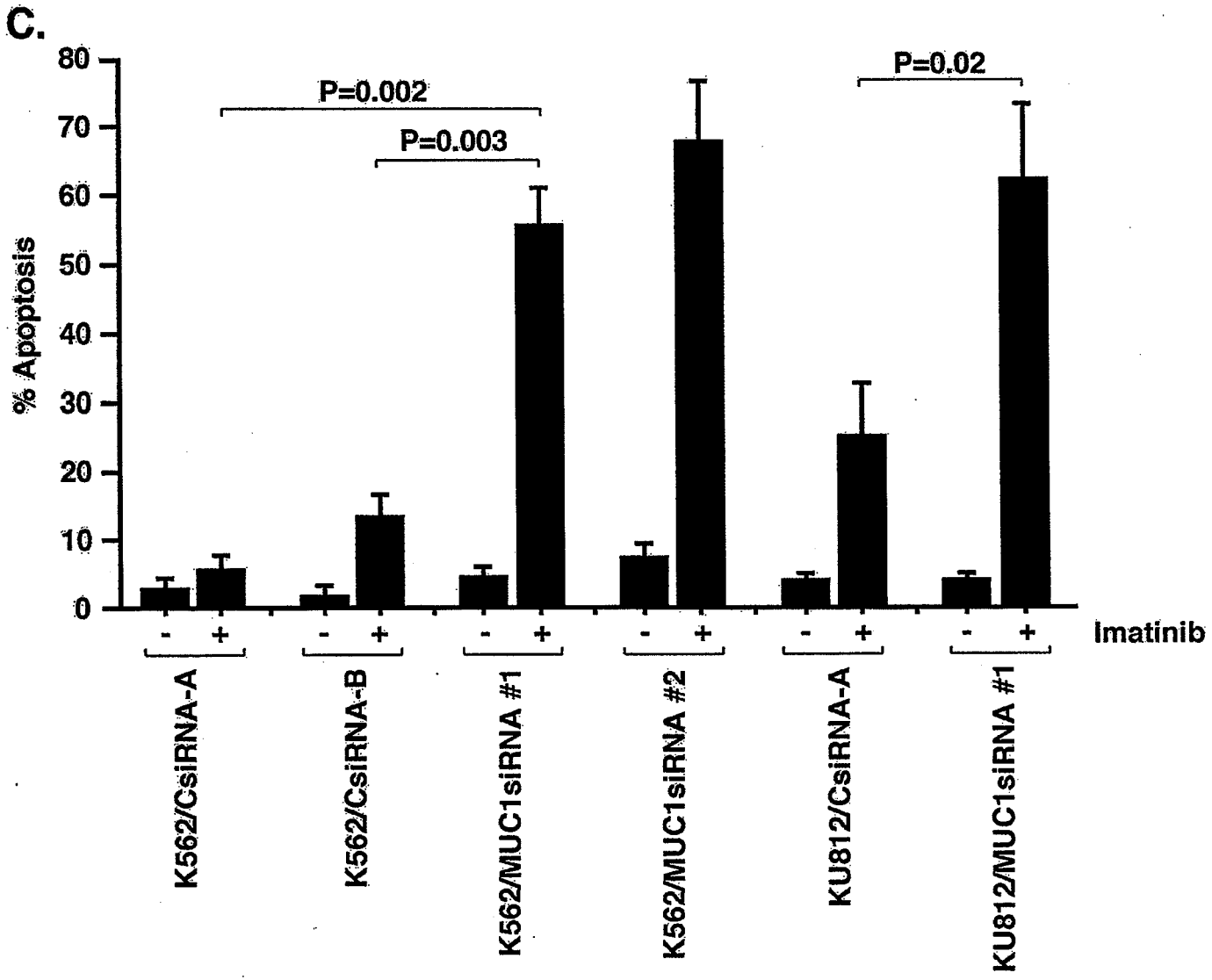
C.
% Apoptosis
80
70
60
50
40
30
20
10
0
P=0.002
P=0.003
P=0.02
- + - + - + - + - + - +
Imatinib
K562/CsiRNA-A
K562/CsiRNA-B
K562/MUC1siRNA #1
K562/MUC1siRNA #2
KU812/CsiRNA-A
KU812/MUC1siRNA #1

Fig. S5A

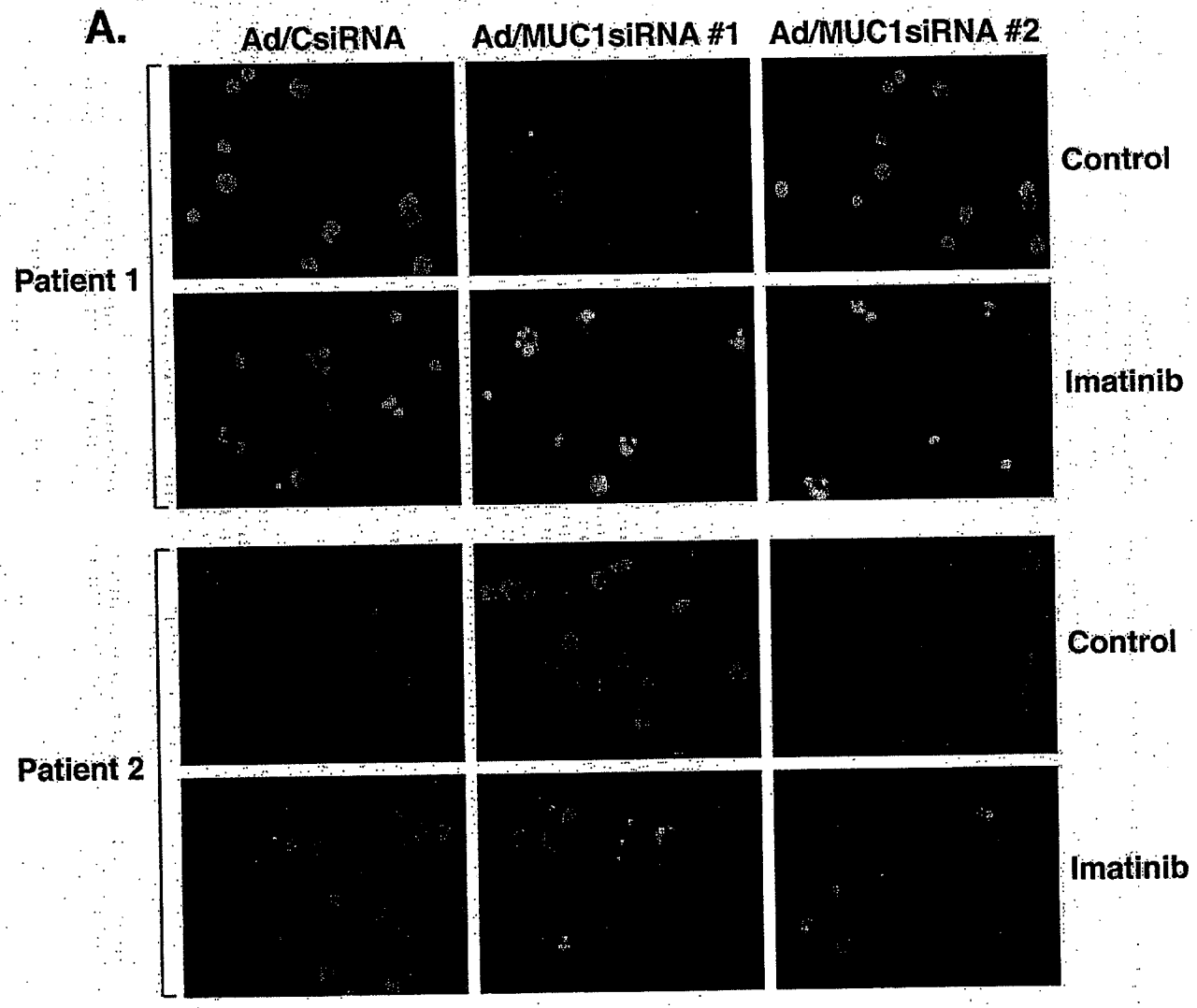
A.
Ad/CsiRNA
Ad/MUC1siRNA #1
Ad/MUC1siRNA #2
Patient 1
Control
Imatinib
Patient 2
Control
Imatinib

Fig. S5B

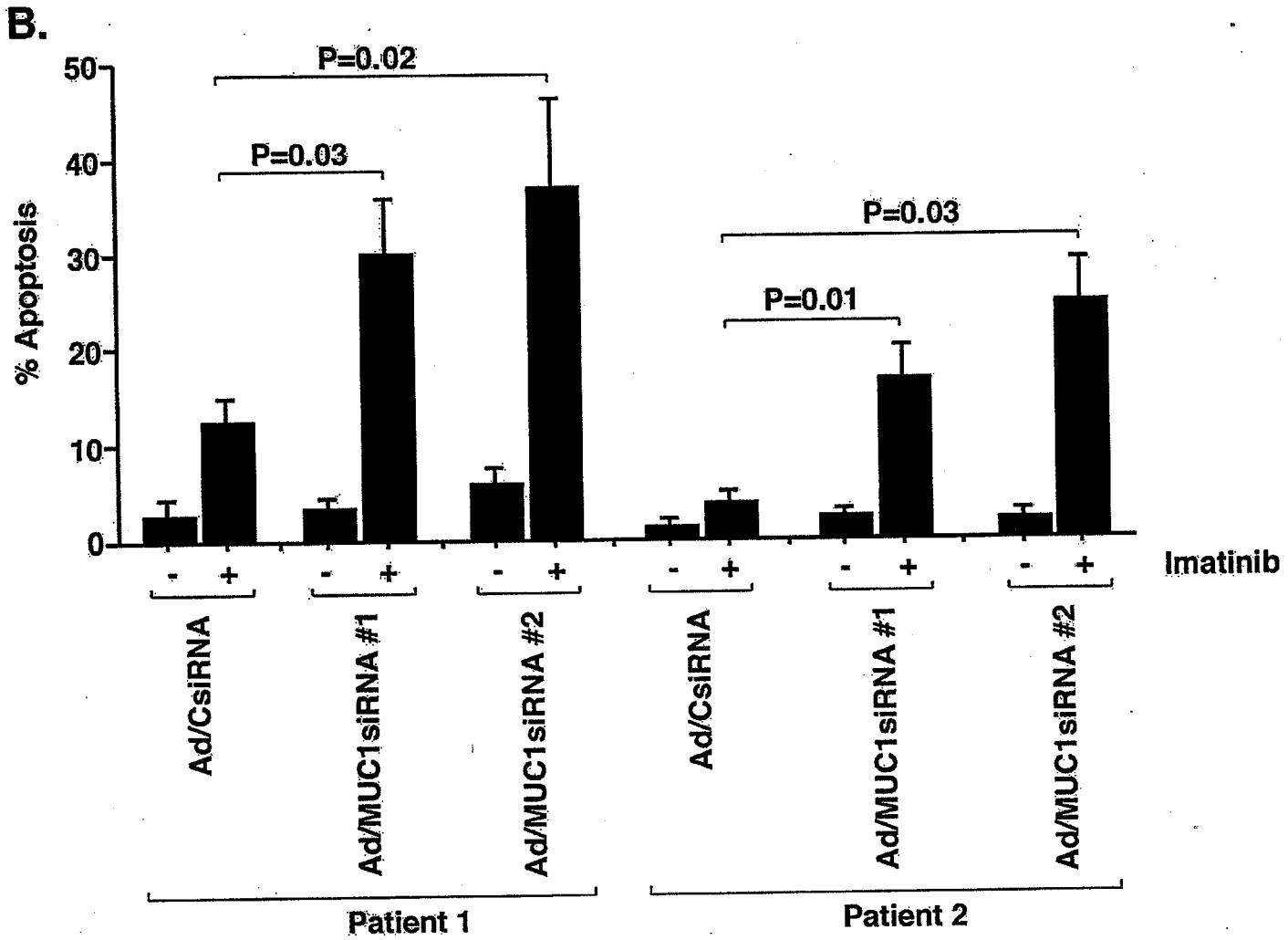
B.
% Apoptosis
50
40
30
20
10
0
P=0.02
P=0.03
P=0.03
P=0.01
- + - + - + - + - + - +
Imatinib
Ad/CsiRNA
Ad/MUC1siRNA #1
Ad/MUC1siRNA #2
Ad/CsiRNA
Ad/MUC1siRNA #1
Ad/MUC1siRNA #2
Patient 1
Patient 2